# Complexity and Quantum Chaos in Krylov Subspace*

Hugo A. Camargo

Gwangju Institute of Science and Technology (GIST)

Quantum Gravity of Open Systems, IFT (UAM-CSIC)

February 5-6, 2025

*Talk based on 2212.14702 , 2306.11632, 2405.11254 and 2412.16472 in collaboration with Yichao **Fu**, Kyoung-Bum **Huh,** Viktor **Jahnke** , Hyun-Sik **Jeong,** Keun-Young **Kim,** Kuntal **Pal,** and Mitsuhiro **Nishida**.

# Background and Motivation



Recently, there has been a renewed interest in studying state and operator dynamics in **Krylov space.** This has been a fruitful pursuit, leading to novel probes of state and operator complexity and new avenues to study quantum chaos in many-body systems and holography.

# Background and Motivation



Recently, there has been a renewed interest in studying state and operator dynamics in **Krylov space.** This has been a fruitful pursuit, leading to novel probes of state and operator complexity and new avenues to study quantum chaos in many-body systems and holography.

- Relation to OTOCs and a new conjectured universal chaos bound (universal operator growth hypothesis [Parker, Cao, Avdoshkin, Scaffidi, Altman (2019)]).
- Connections with holographic complexity in the context of DSSYK/JT gravity ([Rabinovici, Sánchez-Garrido, Shir, Sonner (2023)], [Balasubramanian, Magan Nandi, Wu (2024)]) and momentum-complexity growth rate correspondence ([Caputa, Chen, McDonald, Simón, Strittmatter (2024),…]).
- New tools to study long-time quantum chaos and encoding of RMT behavior (e.g. spectral rigidity) ([Balasubramanian, Magan, Wu (2022, 2023)], [Erdmenger, Jian, Xian (2023)], [Alishahiha, Banerjee, Javad Vasli (2024)]).
- New connections between quantum chaos and quantum computation ([Craps, Evnin and Pascuzzi (2023)]).
- New approaches to study operator growth in **open** quantum systems ([Bhattacharya, Nandy, Nath, Sahu (2022, 2023), Nandy, Pathak, Tezuka (2024),…])

# This Talk



As measures of operator growth and complexity of states, **Krylov complexity** [Parker, et al. (2019)] and **spread complexity** [Balasubramanian, Caputa, Magan, Wu (2022)] respectively, have played a central role in the previous developments.

- In this talk, I will discuss some of their properties as probes of quantum chaos in quantum systems with finite and infinite dimensional Hilbert spaces:

# This Talk



As measures of operator growth and complexity of states, **Krylov complexity** [Parker, et al. (2019)] and **spread complexity** [Balasubramanian, Caputa, Magan, Wu (2022)] respectively, have played a central role in the previous developments.

- In this talk, I will discuss some of their properties as probes of quantum chaos in quantum systems with finite and infinite dimensional Hilbert spaces:

Krylov complexity

A. Infinite dimensional Hilbert spaces:
   - (1) Continuous Energy Spectrum: QFTs in flat space
   - (2) Discrete Energy Spectrum: Quantum Billiards

B. Finite dimensional Hilbert spaces:
   - (3) Quantum spin chains
   - (4) Random Matrix Theory

Spread complexity

# The Lanczos Algorithm 

- Basic idea: study the time evolution of states or operators in dynamical quantum systems. For a time-independent Hamiltonian $H$:

$$(\mathscr{L} := [H, \cdot\,])$$

$$|\psi(t)\rangle = e^{-iHt}|\psi_0\rangle = \sum_{n\geq 0} \frac{(-it)^n}{n!} H^n |\psi_0\rangle = \sum_{n\geq 0} \frac{(-it)^n}{n!} |\psi_n\rangle \qquad \Bigg| \qquad \mathcal{O}(t) = e^{iHt}\mathcal{O}_0\, e^{-iHt} = \sum_{n\geq 0} \frac{(it)^n}{n!} \mathscr{L}^n \mathcal{O}_0 = \sum_{n\geq 0} \frac{(it)^n}{n!} \mathcal{O}_n := e^{i\mathscr{L}t}\mathcal{O}_0$$

- The states $|\psi_n\rangle$ ( and operators $|\mathcal{O}_n)$) span a subspace of the full Hilbert space (or the GNS one): the **Krylov subspace** $\mathscr{K}$ , but are in general not orthogonal or even normalized.

# The Lanczos Algorithm 

- Basic idea: study the time evolution of states or operators in dynamical quantum systems. For a time-independent Hamiltonian $H$:

$$|\psi(t)\rangle = e^{-iHt}|\psi_0\rangle = \sum_{n\geq 0}\frac{(-it)^n}{n!}H^n|\psi_0\rangle = \sum_{n\geq 0}\frac{(-it)^n}{n!}|\psi_n\rangle$$

$(\mathscr{L} := [H, \cdot\,])$

$$\mathcal{O}(t) = e^{iHt}\mathcal{O}_0\, e^{-iHt} = \sum_{n\geq 0}\frac{(it)^n}{n!}\mathscr{L}^n\mathcal{O}_0 = \sum_{n\geq 0}\frac{(it)^n}{n!}\mathcal{O}_n := e^{i\mathscr{L}t}\mathcal{O}_0$$

- The states $|\psi_n\rangle$ ( and operators $|\mathcal{O}_n)$) span a subspace of the full Hilbert space (or the GNS one): the **Krylov subspace** $\mathscr{K}$ , but are in general not orthogonal or even normalized.

- Using the **Lanczos algorithm**, it is possible to construct an orthonormal basis (**Krylov basis**) in Krylov subspace $\mathscr{K}$ which brings the Hamiltonian $H$ or Liouvillian $\mathscr{L}$ to a Hessenberg (or <u>tridiagonal</u>) form ([Viswanath & Müller (1994)]).

| <u>Initial state/operator + dynamics</u> | → | <u>Unnormalized Basis in Krylov space $\mathscr{K}$</u> | → | <u>Lanczos algorithm</u> | → | **<u>Krylov basis</u>** |
|---|---|---|---|---|---|---|
| $\{\,|\psi_0\rangle\,, H\}$ | | $|\psi_n\rangle := H^n|\psi_0\rangle$ | | Gramm-Schmidt procedure | | $\{\,|K_n\rangle\,\}\quad \langle K_m|K_n\rangle = \delta_{mn}$ |
| $\{\mathcal{O}_0\,, \mathscr{L} = [H, \cdot\,]\,,$ +operator inner product} (e.g. $(A|B) :=$ Tr$(A^\dagger B)$ ) | | $|\mathcal{O}_n) := \mathscr{L}^n|\mathcal{O}_0)$ (promoted to states in the GNS construction) | | | | $\{\,|\tilde{\mathcal{O}}_n)\,\}\quad (\tilde{\mathcal{O}}_m|\tilde{\mathcal{O}}_n) = \delta_{mn}$ (with $|K_0\rangle = |\psi_0\rangle$ and $|\tilde{\mathcal{O}}_0) = |\mathcal{O}_0)$) |

# Krylov and Spread Complexity

- The Lanczos algorithm also yields the **Lanczos coefficients** $\{a_n, b_n\}$

( usually $(\tilde{\mathcal{O}}_n|\mathcal{L}|\tilde{\mathcal{O}}_n) := a_n \equiv 0$ )

$$\begin{array}{c}\langle\psi_m|H|\psi_n\rangle \\ (\mathcal{O}_m|\mathcal{L}|\mathcal{O}_n)\end{array} \sim \begin{pmatrix} *_{11} & *_{12} & *_{13} & *_{14} & \cdots \\ *_{21} & *_{22} & *_{23} & *_{24} & \cdots \\ *_{31} & *_{32} & *_{33} & *_{34} & \cdots \\ *_{41} & *_{42} & *_{43} & *_{44} & \cdots \\ \vdots & \vdots & \vdots & \vdots & \ddots \end{pmatrix} \xrightarrow{\text{Lanczos algorithm}} \begin{array}{c}\langle K_m|H|K_n\rangle \\ (\tilde{\mathcal{O}}_m|\mathcal{L}|\tilde{\mathcal{O}}_n)\end{array} \sim \begin{pmatrix} a_0 & b_1 & 0 & 0 & \cdots \\ b_1 & a_1 & b_2 & 0 & \cdots \\ 0 & b_2 & a_2 & b_3 & \cdots \\ 0 & 0 & b_3 & a_3 & \ddots \\ \vdots & \vdots & \vdots & \ddots & \ddots \end{pmatrix}$$

(in general not orthonormal bases)

(orthonormal bases)

# Krylov and Spread Complexity

- The Lanczos algorithm also yields the **Lanczos coefficients** $\{a_n, b_n\}$

( usually $(\tilde{\mathcal{O}}_n|\mathcal{L}|\tilde{\mathcal{O}}_n) := a_n \equiv 0$ )

$$\begin{matrix}\langle\psi_m|H|\psi_n\rangle \\ (\mathcal{O}_m|\mathcal{L}|\mathcal{O}_n)\end{matrix} \sim \begin{pmatrix} *_{11} & *_{12} & *_{13} & *_{14} & \cdots \\ *_{21} & *_{22} & *_{23} & *_{24} & \cdots \\ *_{31} & *_{32} & *_{33} & *_{34} & \cdots \\ *_{41} & *_{42} & *_{43} & *_{44} & \cdots \\ \vdots & \vdots & \vdots & \vdots & \ddots \end{pmatrix} \xrightarrow{\text{Lanczos algorithm}} \begin{matrix}\langle K_m|H|K_n\rangle \\ (\tilde{\mathcal{O}}_m|\mathcal{L}|\tilde{\mathcal{O}}_n)\end{matrix} \sim \begin{pmatrix} a_0 & b_1 & 0 & 0 & \cdots \\ b_1 & a_1 & b_2 & 0 & \cdots \\ 0 & b_2 & a_2 & b_3 & \cdots \\ 0 & 0 & b_3 & a_3 & \ddots \\ \vdots & \vdots & \vdots & \ddots & \ddots \end{pmatrix}$$

(in general not orthonormal bases) (orthonormal bases)

- In the Krylov basis, the coefficients of the time-evolved state/operator $\{\phi_n(t)\}, \{\varphi_n(t)\}$ have the interpretation of **probability amplitudes**:

$$|\mathcal{O}(t)) = \sum_{n\geq 0} i^n \varphi_n(t)|\tilde{\mathcal{O}}_n) \quad \begin{cases} \varphi_n(t) := i^{-n}(\tilde{\mathcal{O}}_n|\mathcal{O}(t)) \\ \sum_{n\geq 0} |\varphi_n(t)|^2 = 1 \quad \forall t \end{cases}$$

$$|\psi(t)\rangle = \sum_{n\geq 0} \phi_n(t)|K_n\rangle \quad \begin{cases} \phi_n(t) := \langle K_n|\psi(t)\rangle \\ \sum_{n\geq 0} |\phi_n(t)|^2 = 1 \quad \forall t \end{cases}$$

- The Krylov complexity of **operators**, and the spread complexity of **states** are defined by:

Krylov Complexity

$$\boxed{K_{\mathcal{O}}(t) := \sum_{n\geq 0} n|(\tilde{\mathcal{O}}_n|\mathcal{O}(t))|^2 = \sum_{n\geq 0} n|\varphi_n(t)|^2}$$

$$\boxed{C_\psi(t) := \sum_{n\geq 0} n|\langle K_n|\psi(t)\rangle|^2 = \sum_{n\geq 0} n|\phi_n(t)|^2}$$

Spread Complexity

Krylov complexity measures how operators grow in Krylov subspace. It is an example of a "*quelconque-complexity*" [Parker, et al. (2019)], a class of operator growth measures arising from positive semi-definite super-operators that can be defined in algebras of operators (GNS Hilbert spaces).

Defining the super-operator: $\hat{n}_{\mathcal{O}} = \sum_{n\geq 0} n\,|\,\tilde{\mathcal{O}}_n)(\tilde{\mathcal{O}}_n\,|$, its expectation value in the time-evolved GNS state $|\,\mathcal{O}(t))$ yields

$$(\hat{n}_{\mathcal{O}})_t := (\mathcal{O}(t)\,|\,\hat{n}_{\mathcal{O}}\,|\,\mathcal{O}(t)) = \sum_{n\geq 0} n\,|\,\varphi_n(t)\,|^2 \equiv K_{\mathcal{O}}(t)$$

Krylov complexity measures how operators grow in Krylov subspace. It is an example of a "*quelconque*-complexity" [Parker, et al. (2019)], a class of operator growth measures arising from positive semi-definite super-operators that can be defined in algebras of operators (GNS Hilbert spaces).

Defining the super-operator: $\hat{n}_{\mathcal{O}} = \sum_{n\geq 0} n\,|\tilde{\mathcal{O}}_n)(\tilde{\mathcal{O}}_n|$, its expectation value in the time-evolved GNS state $|\mathcal{O}(t))$ yields

$$(\hat{n}_{\mathcal{O}})_t := (\mathcal{O}(t)|\hat{n}_{\mathcal{O}}|\mathcal{O}(t)) = \sum_{n\geq 0} n\,|\varphi_n(t)|^2 \equiv K_{\mathcal{O}}(t)$$

The Krylov complexity $K_{\mathcal{O}}(t)$ gives the average position of the operator $\mathcal{O}(t)$ in the **Krylov chain**.

$$\partial_t \varphi_n(t) = i a_n \varphi_n(t) - b_{n+1}\varphi_{n+1}(t) + b_n \varphi_{n-1}(t)$$

$\boxed{\text{Key: } \varphi_0(t) := (\mathcal{O}_0|\mathcal{O}(t))}$

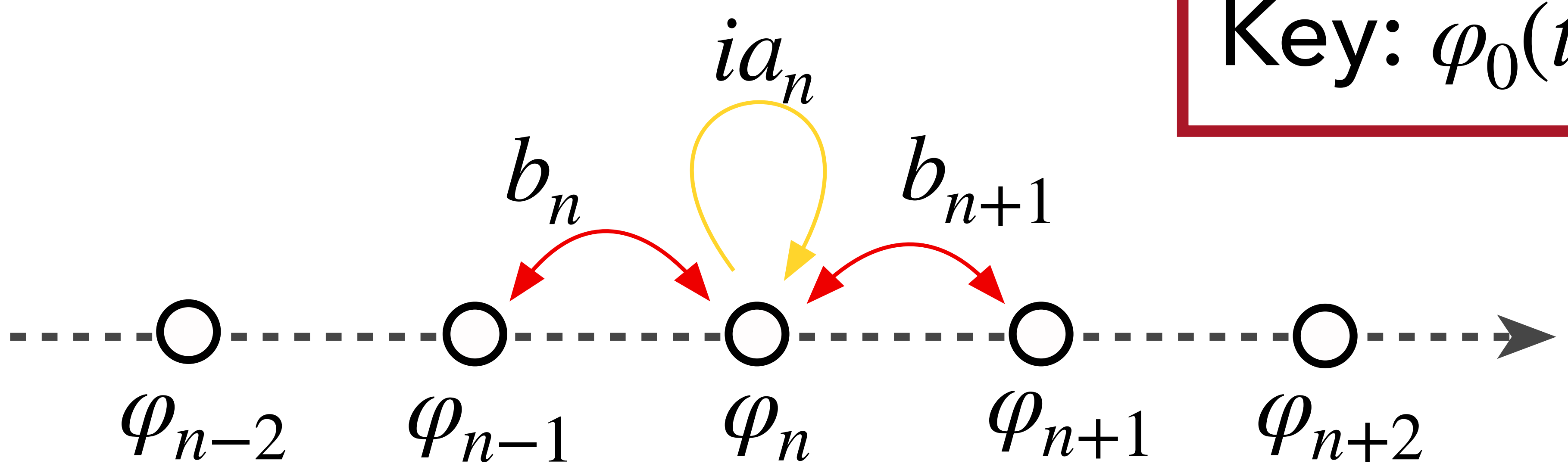


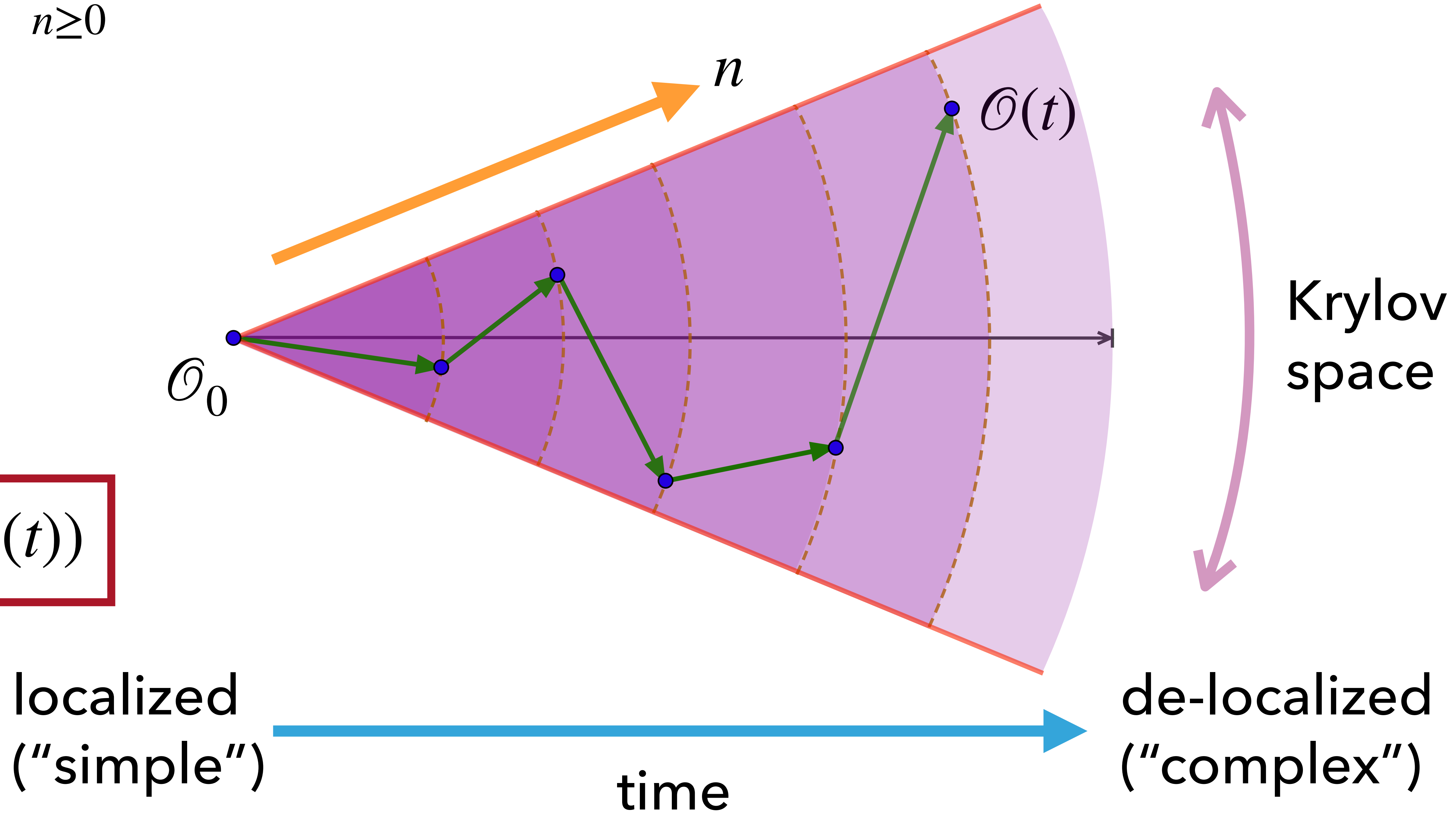

# Interpretation of Krylov and Spread Complexity



Similarly, spread complexity tells us how an initial state spreads in Krylov space. One can also view it as arising from as the expectation value of the spreading operator $\hat{n}_\psi = \sum_{n\geq 0} n\,|K_n\rangle\langle K_n|$ in the time-evolved state $|\psi(t)\rangle$

$$\langle \hat{n}_\psi \rangle_t := \langle \psi(t)|\hat{n}_\psi|\psi(t)\rangle = \sum_{n\geq 0} n\,|\phi_n(t)|^2 \equiv C_\psi(t)$$

$\boxed{\text{Key: } \phi_0(t) := \langle \psi_0|\psi(t)\rangle}$

Similarly, spread complexity tells us how an initial state spreads in Krylov space. One can also view it as arising from as the expectation value of the spreading operator $\hat{n}_\psi = \sum_{n\geq 0} n\,|K_n\rangle\langle K_n|$ in the time-evolved state $|\psi(t)\rangle$

$$\langle \hat{n}_\psi \rangle_t := \langle \psi(t)|\hat{n}_\psi|\psi(t)\rangle = \sum_{n\geq 0} n\,|\phi_n(t)|^2 \equiv C_\psi(t)$$

Key: $\phi_0(t) := \langle \psi_0|\psi(t)\rangle$

In [Balasubramanian, Caputa, Magan, Wu (2022)] it was argued that (for a finite time and in continuous time evolution) the Krylov basis $\{|K_n\rangle\}_{n\geq 0}$, generated by applying the Lanczos algorithm to $\{|\psi_n\rangle = H^n|\psi_0\rangle\}_{n\geq 0}$ , minimizes the complexity **cost functional**

$$C_{\mathbb{B}}(t) = \sum_{n\geq 0} n\,|\langle B_n|\psi(t)\rangle|^2 = \sum_{n\geq 0} n\, p_{\mathbb{B}}(n,t)$$

where $\mathbb{B} = \{|B_n\rangle\}_{n\geq 0}$ is a complete, orthonormal, ordered basis in Hilbert space: $C_\psi(t) = \min_{\mathbb{B}}\{C_{\mathbb{B}}(t)\}$.

This was shown to hold near $t = 0$ and for a finite time using arguments related to the Taylor series coefficients of $C_{\mathbb{B}}(t)$ as well as for all times in discrete time evolution implemented by sequences of unitaries.

# I. Krylov Complexity and

# “Semiclassical” signatures of Chaos

# Universal Operator Growth Hypothesis

"In the thermodynamic limit, the Lanczos coefficients $b_n$ of generic non-integrable quantum many-body systems with local interactions should grow as fast as possible, i.e. $b_n \sim \alpha n + \gamma$ for $n \to \infty$" [Parker, et al. (2019)]

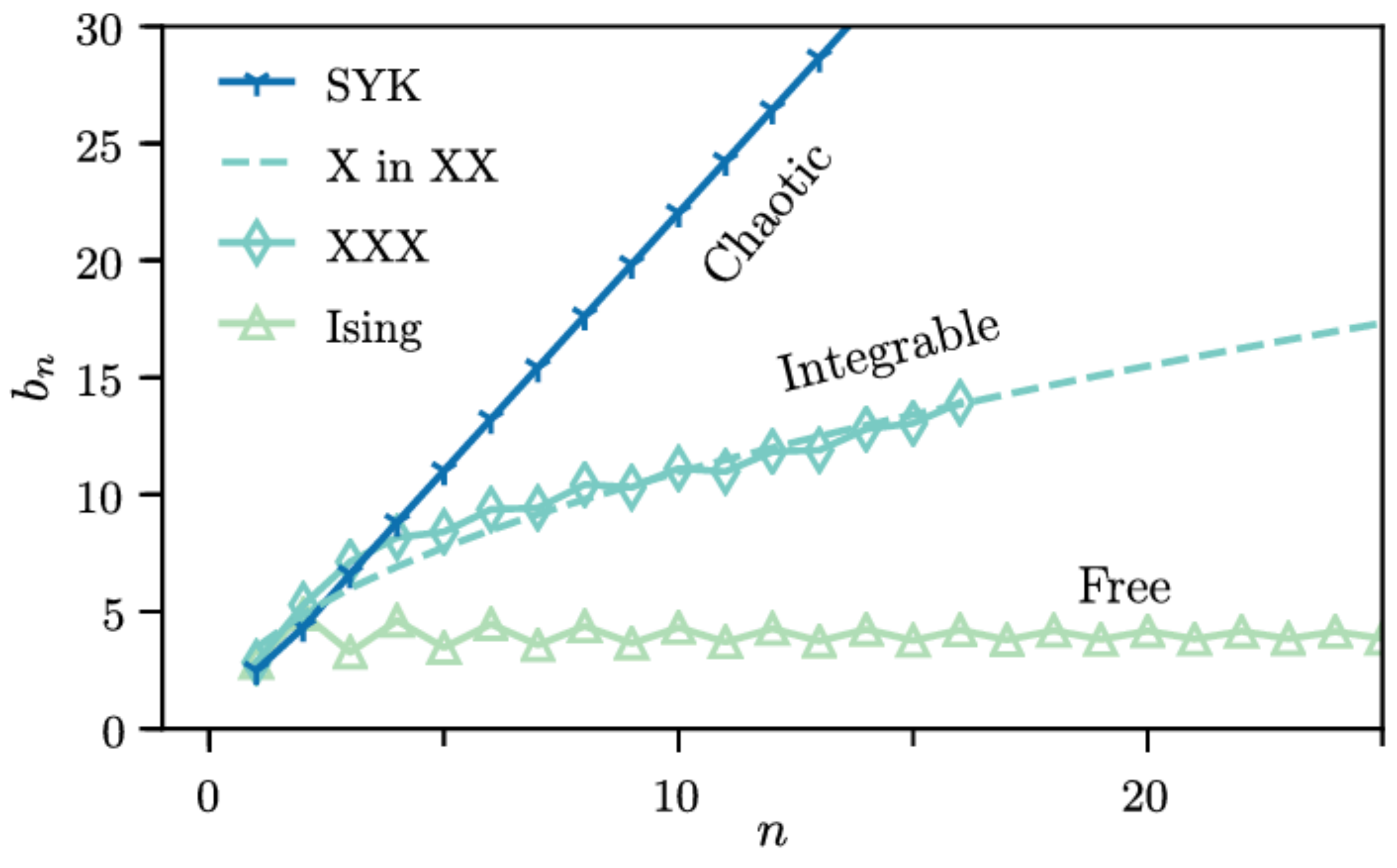


e.g. in the large-$N$ limit of SYK$_q$ at $\beta \to 0$ for $\mathcal{O}_0 = \sqrt{2}\gamma_1$

$$b_n^{(q)} = \begin{cases} \mathcal{J}\sqrt{2/q} + O(1/q) & , \; n = 1 \\ \mathcal{J}\sqrt{n(n-1)} + O(1/q) & , \; n > 1 \end{cases}$$

$$(\alpha = \mathcal{J})$$

# Universal Operator Growth Hypothesis

"In the thermodynamic limit, the Lanczos coefficients $b_n$ of generic non-integrable quantum many-body systems with local interactions should grow as fast as possible, i.e. $b_n \sim \alpha n + \gamma$ for $n \to \infty$" [Parker, et al. (2019)]

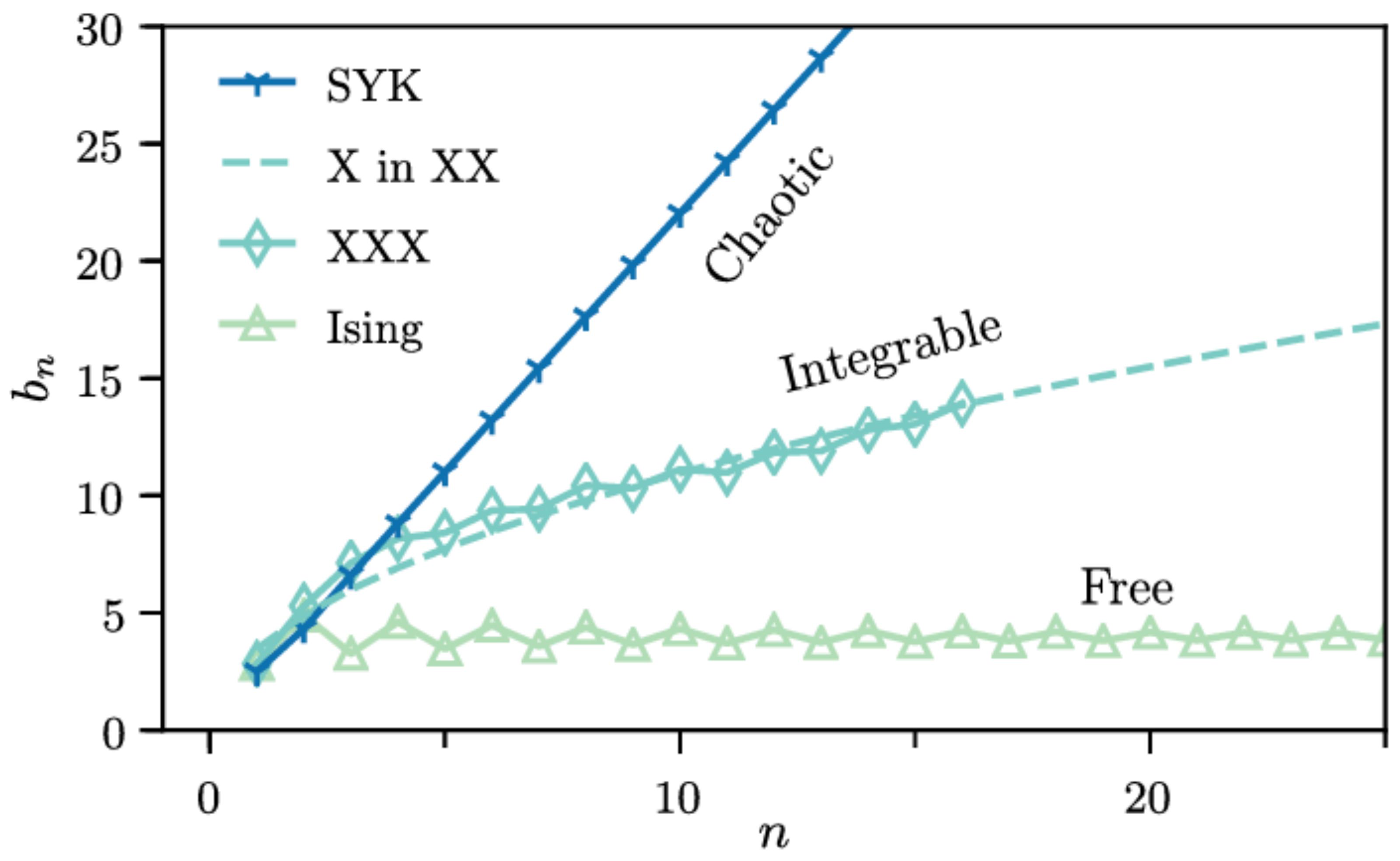


e.g. in the large-$N$ limit of SYK$_q$ at $\beta \to 0$ for $\mathcal{O}_0 = \sqrt{2}\gamma_1$

$$b_n^{(q)} = \begin{cases} \mathcal{J}\sqrt{2/q} + O(1/q) & , \; n = 1 \\ \mathcal{J}\sqrt{n(n-1)} + O(1/q) & , \; n > 1 \end{cases}$$

$$(\alpha = \mathcal{J})$$

Whenever the Lanczos coefficients have a **smooth** linear behavior, the Krylov complexity is expected to grow exponentially $K_{\mathcal{O}}(t) \sim e^{\lambda_K t}$ where $\lambda_K = 2\alpha$. The growth rate of Krylov complexity $\lambda_K$ should also bound the growth rates of other notions of operator growth, such as OTOCs ( [Parker, et al. (2019)] ).

(At $\beta \to 0$ assuming smooth $b_n$ )

$$\lambda_L \leq \lambda_K = 2\alpha$$

Shown in [Parker, et al. (2019)]

$$([V, \mathcal{O}(t)] \,|\, [V, \mathcal{O}(t)]) \sim e^{\lambda_L t}$$

(Finite $1/\beta$)

$$\lambda_L \leq 2\alpha \leq 2\pi/\beta$$

Conjecture

# Krylov Complexity in scalar QFTs



The previous statements were formulated in the context of quantum many-body systems. What happens in QFTs? If we consider a free QFT, do we recover the behavior expected for an integrable theory?

- Consider a free (real) massive scalar field in $d$-spacetime dimensions: $L_E = \frac{1}{2}(\partial\phi)^2 + \frac{1}{2}m^2\phi^2$ .

# Krylov Complexity in scalar QFTs



The previous statements were formulated in the context of quantum many-body systems. What happens in QFTs? If we consider a free QFT, do we recover the behavior expected for an integrable theory?

- Consider a free (real) massive scalar field in $d$-spacetime dimensions: $L_E = \frac{1}{2}(\partial\phi)^2 + \frac{1}{2}m^2\phi^2$ .

We want to study finite temperature $\beta^{-1}$ effects. The starting point, and key object, is the thermal (Wightman) 2-point function $\Pi^W(t,\mathbf{x}) = \langle \phi(t - i\beta/2,\mathbf{x})\phi(0,\mathbf{0})\rangle_\beta$ , which is related to the spectral density $\rho(\omega,\mathbf{k})$ and associated (Wightman) power spectrum $f^W(\omega)$ via:

$$\int \mathrm{d}t\, \Pi^W(t,\mathbf{0})e^{i\omega t} = f^W(\omega) = \frac{1}{|\sinh(\beta\omega/2)|}\int \frac{\mathrm{d}^{d-1}\mathbf{k}}{(2\pi)^{d-1}}\rho(\omega,\mathbf{k}) \longleftarrow \rho(\omega,\mathbf{k}) = \frac{\mathcal{N}}{\epsilon_\mathbf{k}}\big(\delta(\omega-\epsilon_\mathbf{k}) - \delta(\omega+\epsilon_\mathbf{k})\big)$$

$$\epsilon_\mathbf{k} = \sqrt{|\mathbf{k}|^2 + m^2}$$

In this case we do not explicitly construct the Krylov basis starting from $|\mathcal{O}_0) = |\phi(0,\mathbf{0}))$ , so to find the Lanczos coefficients we compute them from the **moments** $\mu_{2n}$ ([Viswanath & Müller (1994)]):

$(\mu_{i+j})$ = Hankel matrix

$$\frac{1}{2\pi}\int_{-\infty}^{+\infty} \mathrm{d}\omega\, \omega^{2n} f^W(\omega) = \mu_{2n} = \frac{1}{i^{2n}}\left(\frac{\mathrm{d}^{2n}\Pi^W(t,\mathbf{0})}{\mathrm{d}t^{2n}}\right)\Bigg|_{t=0} \longrightarrow \begin{cases} b_1^{2n}\cdots b_n^2 = \det(\mu_{i+j})_{0\le i,j\le n} \\ a_n \equiv 0 \qquad (\phi(t,\mathbf{x}) \text{ is Hermitian}) \end{cases}$$

# Krylov Complexity in scalar QFTs



The Wightman power spectrum $f^W(\omega)$ can be evaluated explicitly for any $d \geq 3$:

$$f^W(\omega) = N(m, \beta, d)\frac{(\omega^2 - m^2)^{(d-3)/2}}{|\sinh(\beta\omega/2)|}\Theta(|\omega| - m)$$

$\left( N \text{ is fixed by } \int_{-\infty}^{+\infty} \frac{\mathrm{d}\omega}{2\pi} f^W(\omega) = 1 \right)$

# Krylov Complexity in scalar QFTs



The Wightman power spectrum $f^W(\omega)$ can be evaluated explicitly for any $d \geq 3$:

$$f^W(\omega) = N(m,\beta,d)\frac{(\omega^2 - m^2)^{(d-3)/2}}{|\sinh(\beta\omega/2)|}\Theta(|\omega| - m) \qquad \left( N \text{ is fixed by } \int_{-\infty}^{+\infty} \frac{d\omega}{2\pi} f^W(\omega) = 1 \right)$$

The mass (an IR cutoff in the power spectrum) induces a **staggering** (dimerization) of the Lanczos coefficients $b_n$. However, their asymptotic ($n \gg 1$) behavior is **linear** in $n$ , with fixed growth rate $\pi/\beta$ .

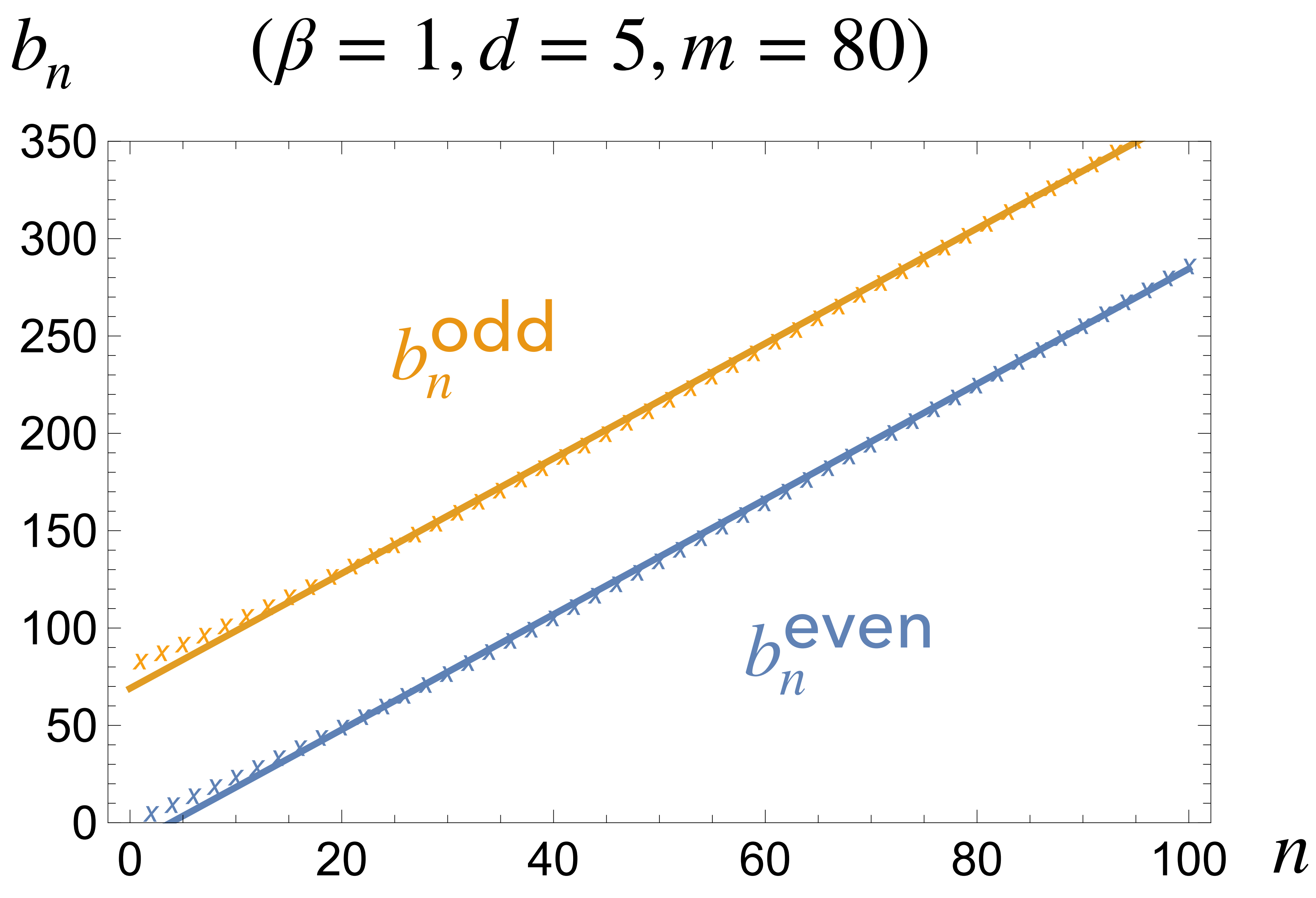


*i)* $n \ll \beta m$

$$\beta^2 b_n^2 = (m\beta)^2 \times \begin{cases} 1 + 4\frac{1+n}{m\beta} + O\left(\frac{1}{(m\beta)^2}\right) & , \ (n \text{ odd}) \\ 4\frac{n(n+2)}{(m\beta)^2} + O\left(\frac{1}{(m\beta)^3}\right) & , \ (n \text{ even}) \end{cases}$$

*ii)* $n \gg \beta m$

(asymptotic)

$$\boxed{b_n \longrightarrow \begin{cases} \frac{\pi}{\beta}n + \gamma_{\text{odd}} & , \ (n \text{ odd}) \\ \frac{\pi}{\beta}n + \gamma_{\text{even}} & , \ (n \text{ even}) \end{cases}}$$

(with $|\gamma_{\text{even}} - \gamma_{\text{odd}}| \propto m$)

# Interlude: Decay of the power spectrum

The decay of the power spectrum, the pole-structure of the two-point function and the growth rate of the Lanczos coefficients are intimately connected:

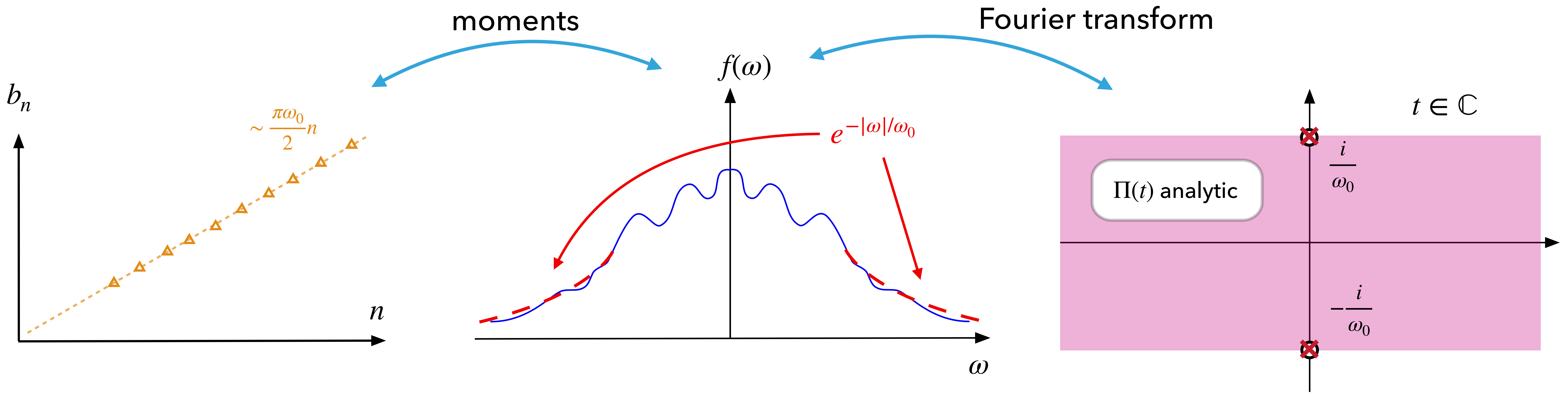


$$b_n \sim \frac{\pi\omega_0}{2}n \quad \longleftrightarrow \quad f(\omega) \sim e^{-|\omega|/\omega_0} \quad \longleftrightarrow \quad \Pi(i\tau) \sim (|\tau| - \omega_0^{-1})^{-1}$$

asymptotic linear growth — exponentially-decaying tail — pole in imaginary time

(e.g. $\Pi^W_\beta(t) = \langle \mathcal{O}^\dagger(0)\mathcal{O}(t+i\beta/2)\rangle_\beta$)

# Krylov Complexity in scalar QFTs



The Krylov complexity $K_\phi(t)$ inherits subtleties derived from the IR cutoff, while still growing exponentially

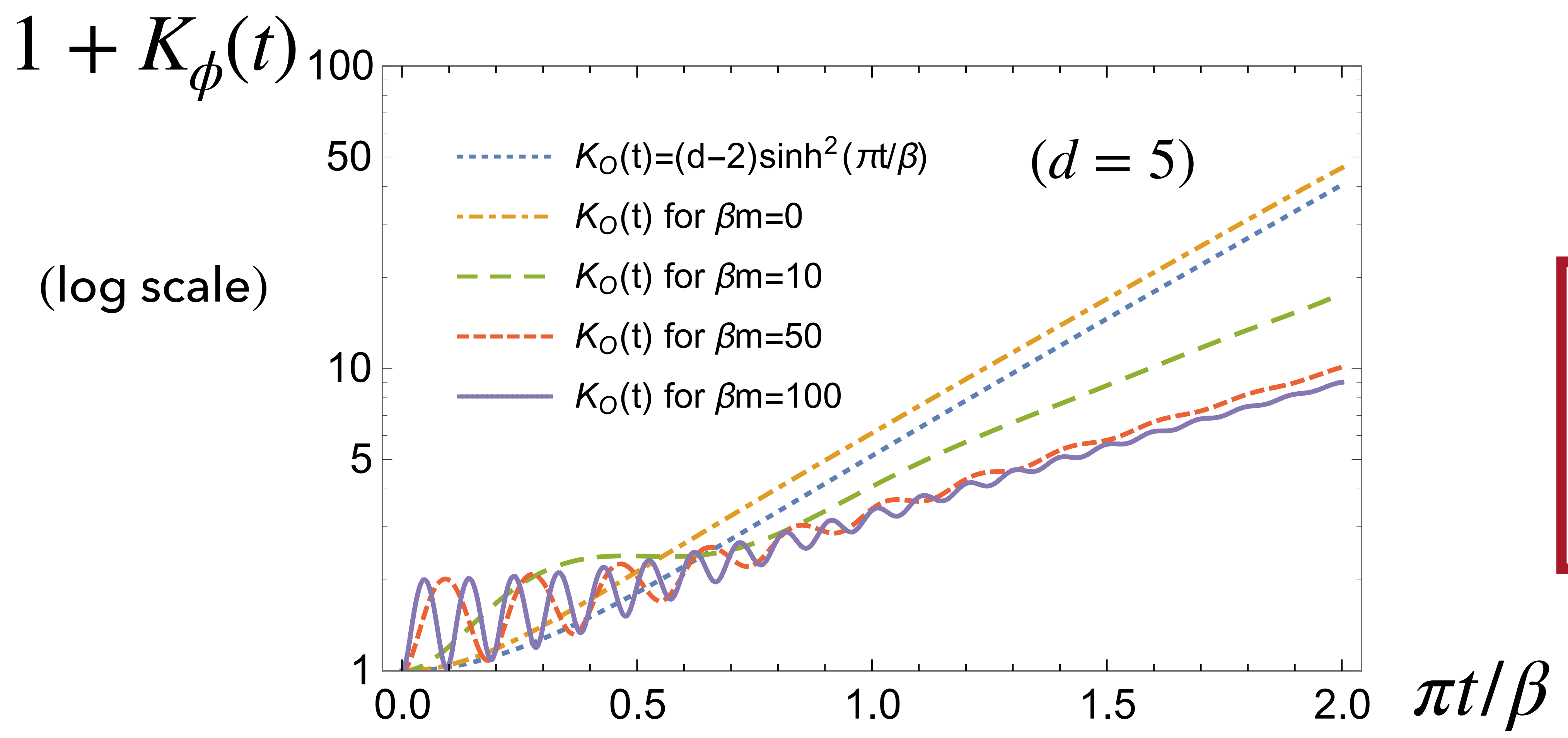


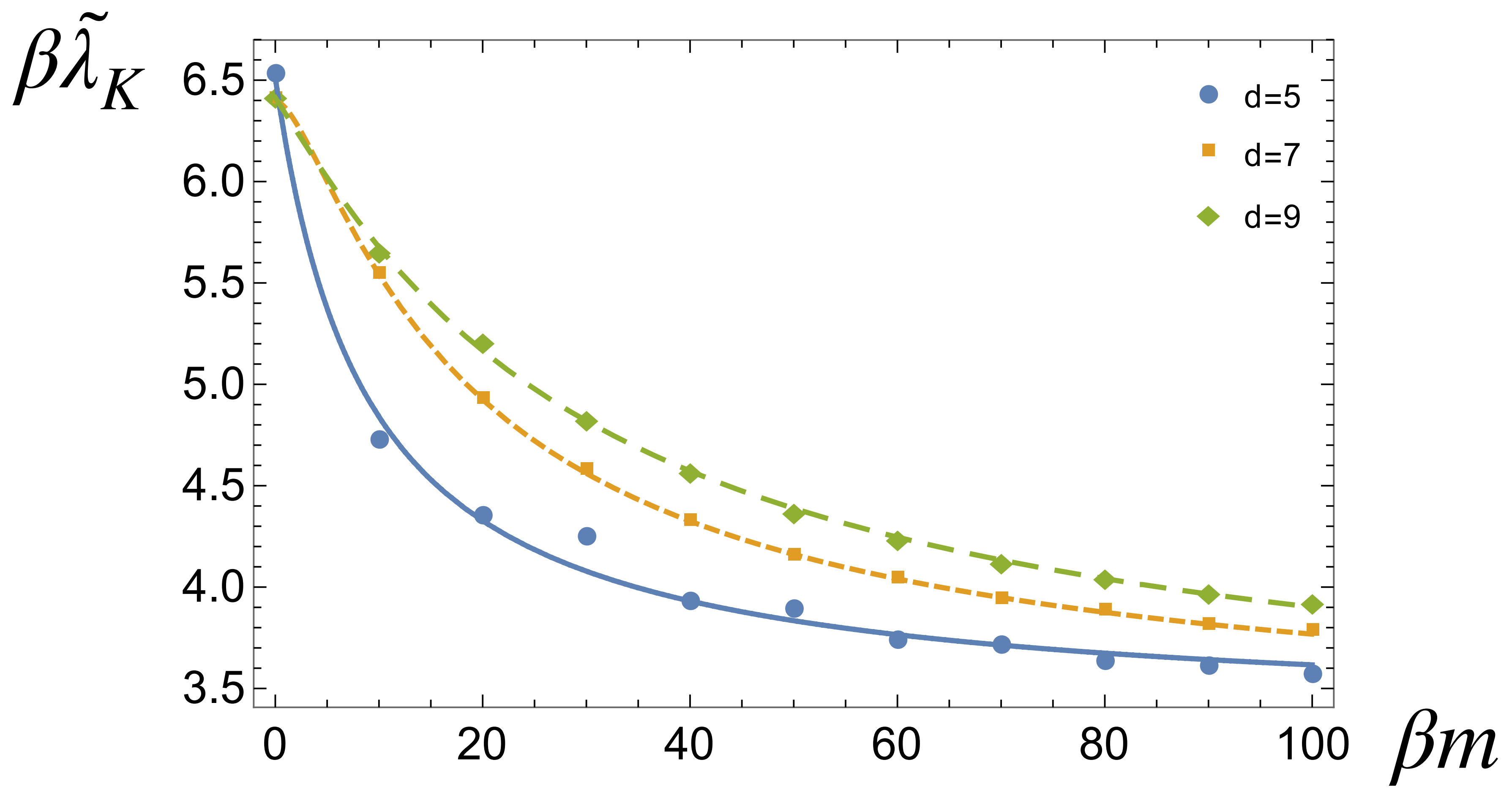


$$K_\phi(t) \sim \exp\left(\tilde{\lambda}_K t\right) \qquad \left(1.5 \leq \frac{\pi t}{\beta} \leq 2.0\right)$$

$$\boxed{\beta\tilde{\lambda}_K \sim 2\pi + k_1\left(\frac{1}{k_2+\beta m} - \frac{1}{k_2}\right) + k_3\left(\frac{1}{(k_2+\beta m)^2} - \frac{1}{(k_2)^2}\right) \leq 2\pi}$$

# Krylov Complexity in scalar QFTs



The Krylov complexity $K_\phi(t)$ inherits subtleties derived from the IR cutoff, while still growing exponentially

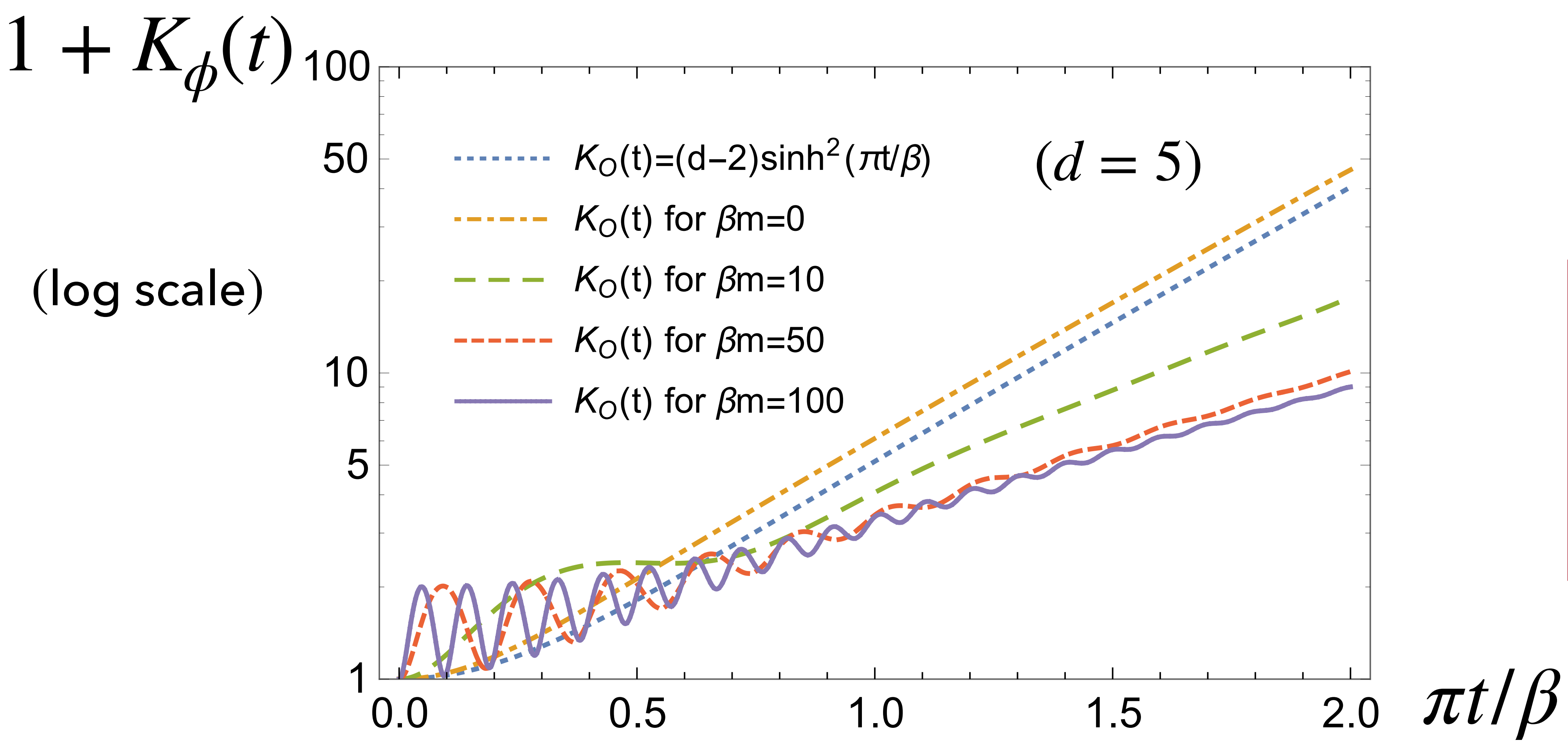


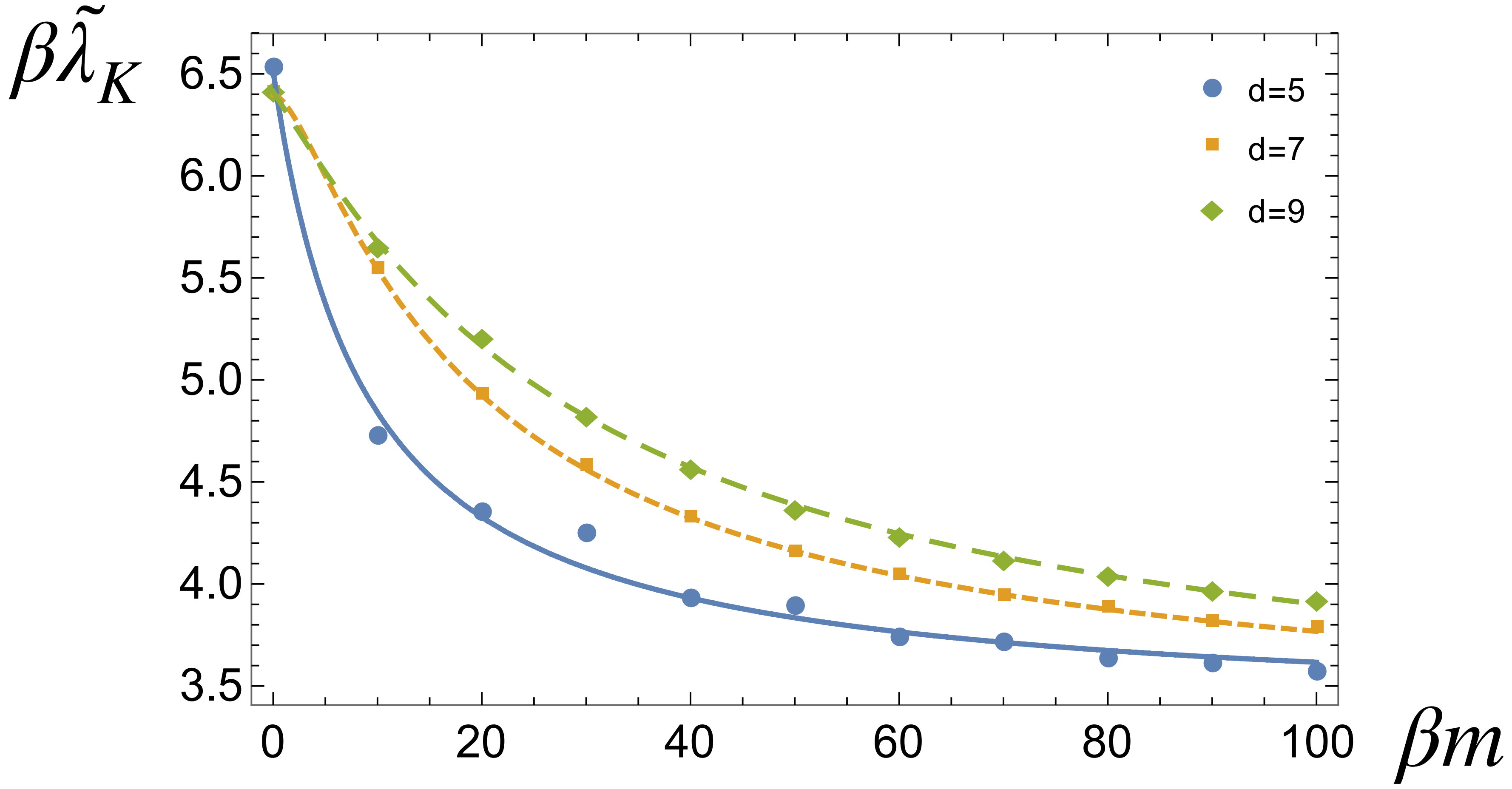


$$K_\phi(t) \sim \exp\left(\tilde{\lambda}_K t\right) \qquad \left(1.5 \leq \frac{\pi t}{\beta} \leq 2.0\right)$$

$$\boxed{\beta\tilde{\lambda}_K \sim 2\pi + k_1\left(\frac{1}{k_2+\beta m} - \frac{1}{k_2}\right) + k_3\left(\frac{1}{(k_2+\beta m)^2} - \frac{1}{(k_2)^2}\right) \leq 2\pi}$$

The mass decreases the growth rate of Krylov complexity (at least in a finite time window)

In the limit $m \to 0$ we recover the CFT result

$$\lim_{m\to 0} \tilde{\lambda}_K = 2\pi/\beta \qquad \text{[Dymarsky, Smolkin (2021)]}$$

This behavior is a consequence of the pole structure of the 2-point function and **does not** imply chaotic behavior.

# Effect of a "hard" UV Cutoff



The late time growth of Krylov complexity and asymptotic behavior of Lanczos coefficients is determined by the UV physics of the theory. What happens if we introduce a UV cutoff $\Lambda$ in the power spectrum? For concreteness, focus on $d = 5$ and $\beta\Lambda > \beta m$ :

$$f^W(\omega) = N(m, \beta, d)\frac{(\omega^2 - m^2)}{|\sinh(\beta\omega/2)|}\Theta(|\omega| - m, \Lambda - |\omega|)$$

# Effect of a "hard" UV Cutoff



The late time growth of Krylov complexity and asymptotic behavior of Lanczos coefficients is determined by the UV physics of the theory. What happens if we introduce a UV cutoff $\Lambda$ in the power spectrum? For concreteness, focus on $d = 5$ and $\beta\Lambda > \beta m$ :

$$f^W(\omega) = N(m, \beta, d)\frac{(\omega^2 - m^2)}{|\sinh(\beta\omega/2)|}\Theta(|\omega| - m, \Lambda - |\omega|)$$

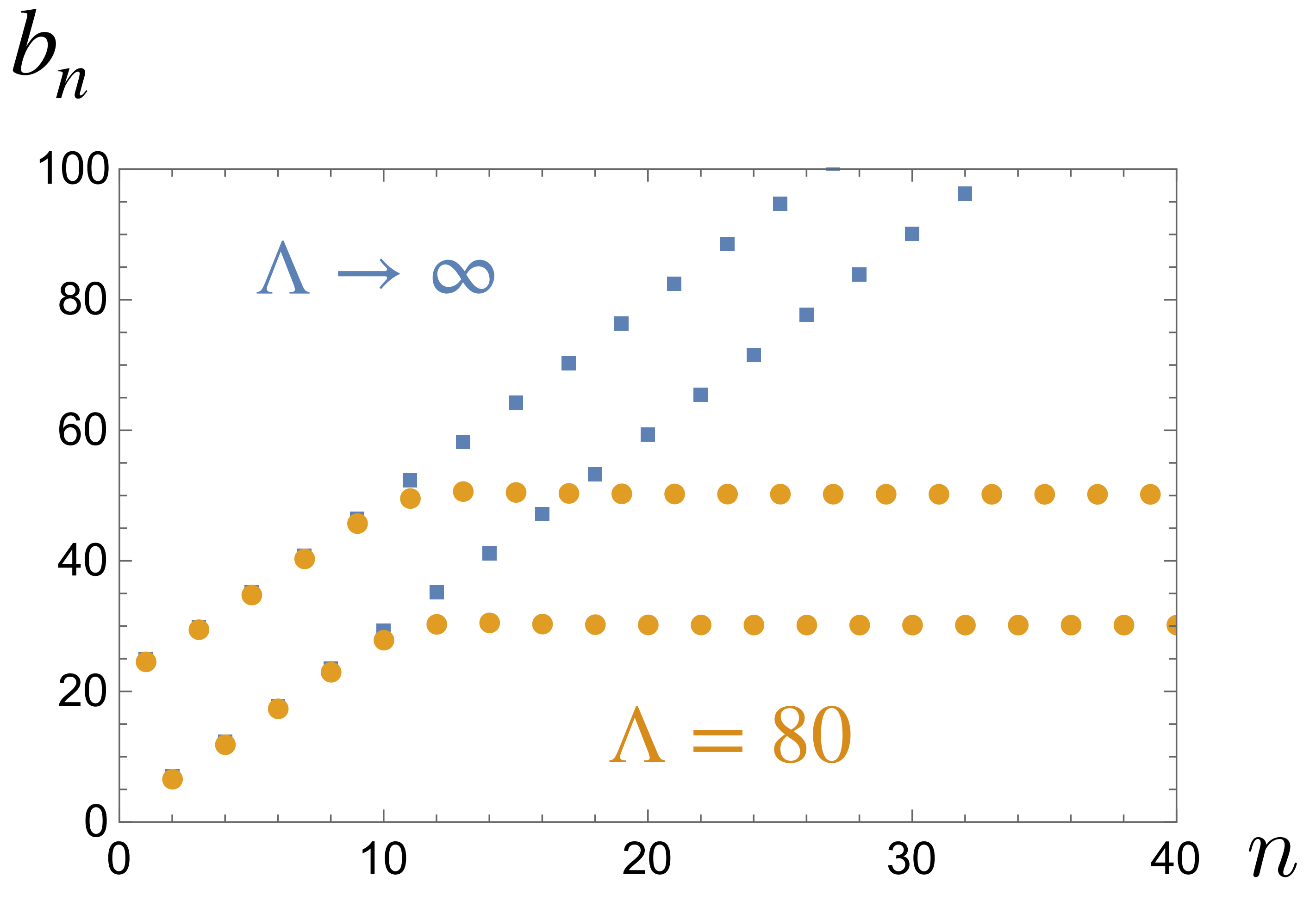


$(m = 20, \beta = 1)$

$$\boxed{b_{\pm}^{\text{sat}} = \frac{(\Lambda \pm m)}{2} \qquad n_{\text{sat}} \propto O(\Lambda)}$$

Early-time **exponential** growth

Late-time **linear** growth consistent with lattice computations ([Avdoshkin, Dymarsky, Smolkin (2023)])

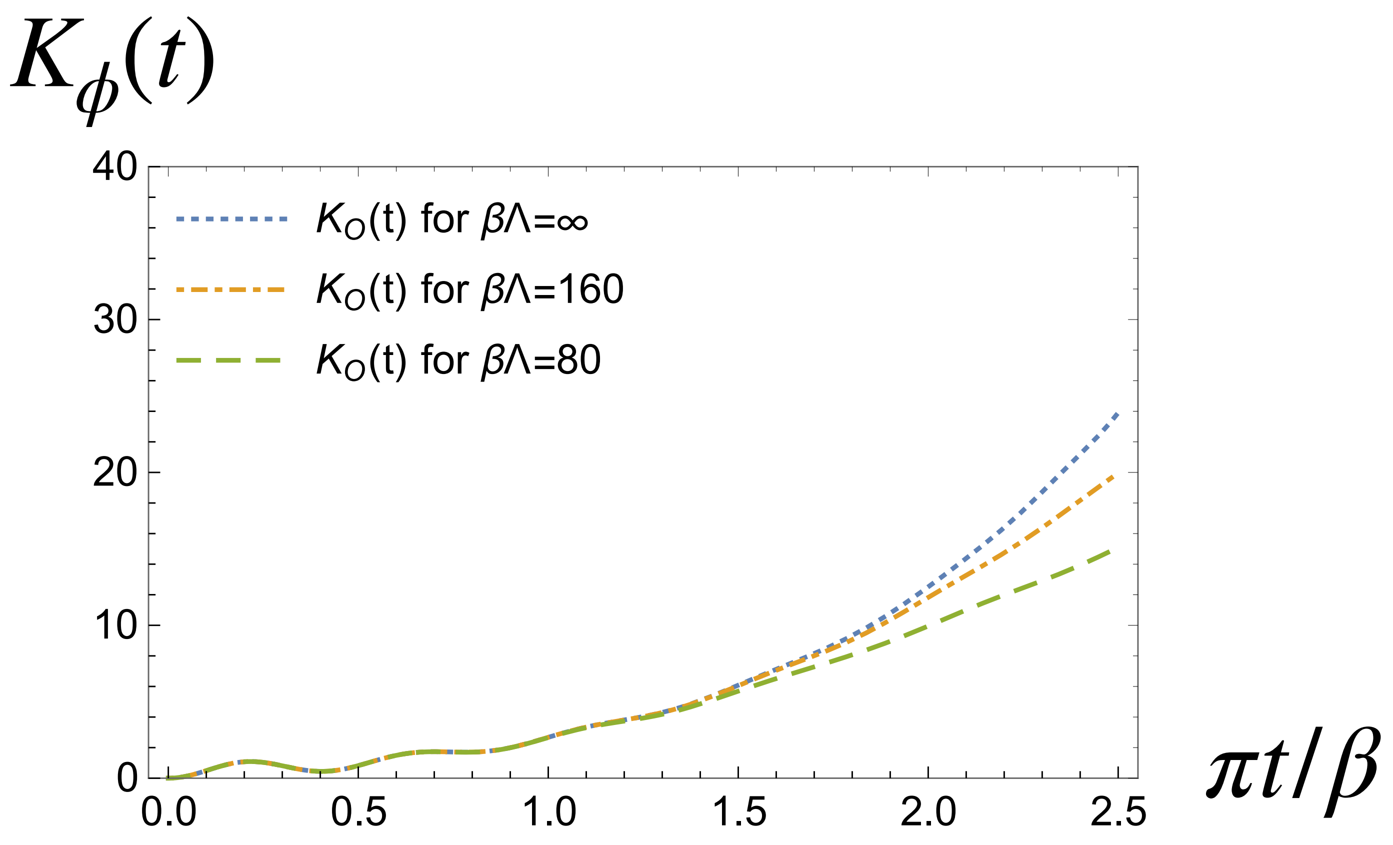


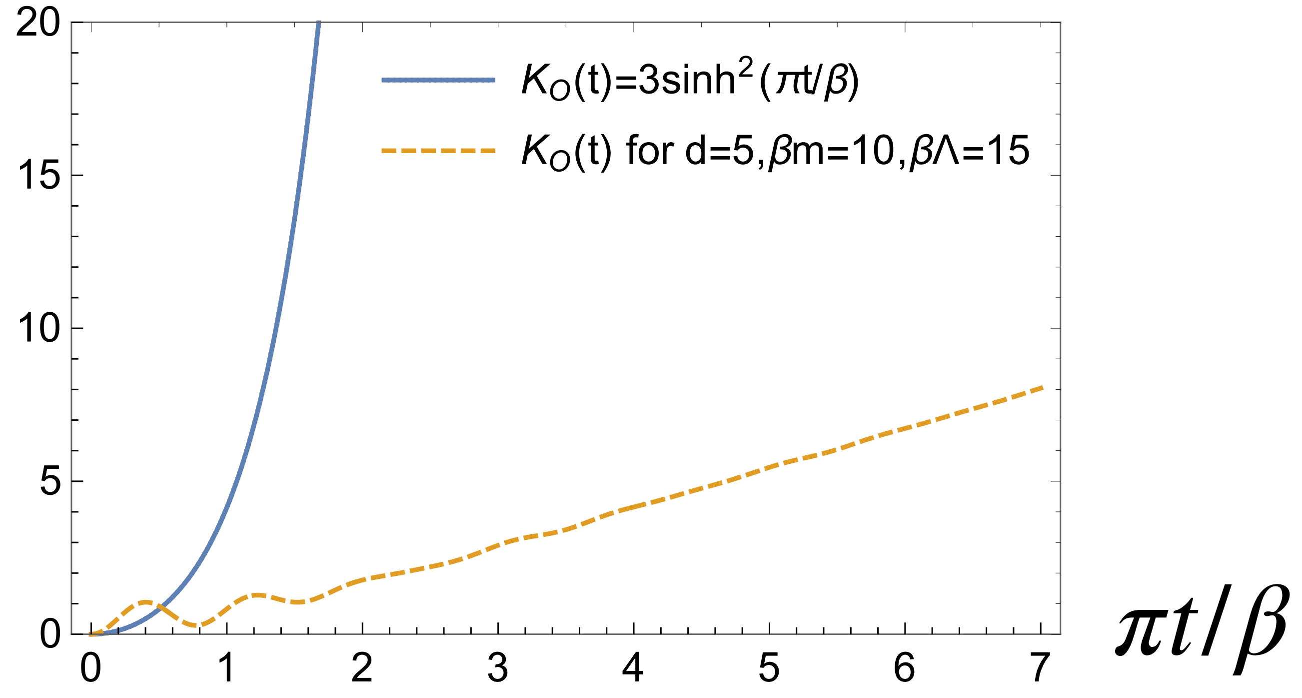

# Krylov Complexity in Interacting Scalar QFTs



Can we alter the behavior of Krylov complexity by adding an interaction term of the form: $L_{\text{int}} = g_\ell \phi^\ell / \ell\,!$ to the free Lagrangian? Focus on $d = 4$ and consider both relevant $\ell = 3$ and marginal $\ell = 4$ deformations at finite temperature $\beta^{-1}$.

# Krylov Complexity in Interacting Scalar QFTs



Can we alter the behavior of Krylov complexity by adding an interaction term of the form: $L_{\text{int}} = g_\ell \phi^\ell/\ell!$ to the free Lagrangian? Focus on $d=4$ and consider both relevant $\ell=3$ and marginal $\ell=4$ deformations at finite temperature $\beta^{-1}$.

- We compute the contributions to the spectral density arising from the one-loop correction through the self-energy

$i)$ $\phi^4$ – theory $\quad \Pi_E(g) =$ 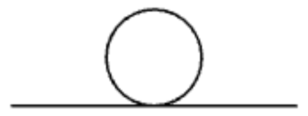

The self-energy $\Pi_E(g)$ induces a thermal mass $m_{\text{th}}(g)$

$$m \to m_{\text{eff}}(g) = \sqrt{m^2 + m_{\text{th}}^2(g)}$$

The effect is similar to the massive case, i.e. staggering in Lanczos coefficients and a decrease in the exponential growth-rate of Krylov complexity: $\boxed{\beta\tilde{\lambda}_K(g) \le 2\pi}$

$ii)$ $\phi^3$ – theory $\quad \Pi_E(g) =$ 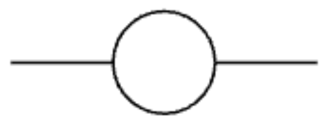

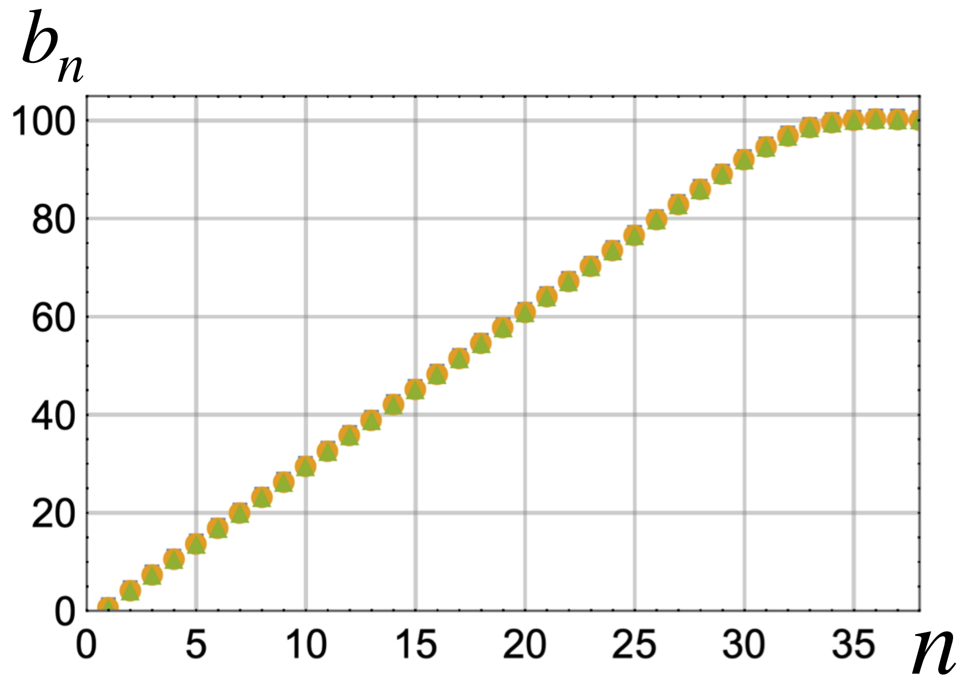


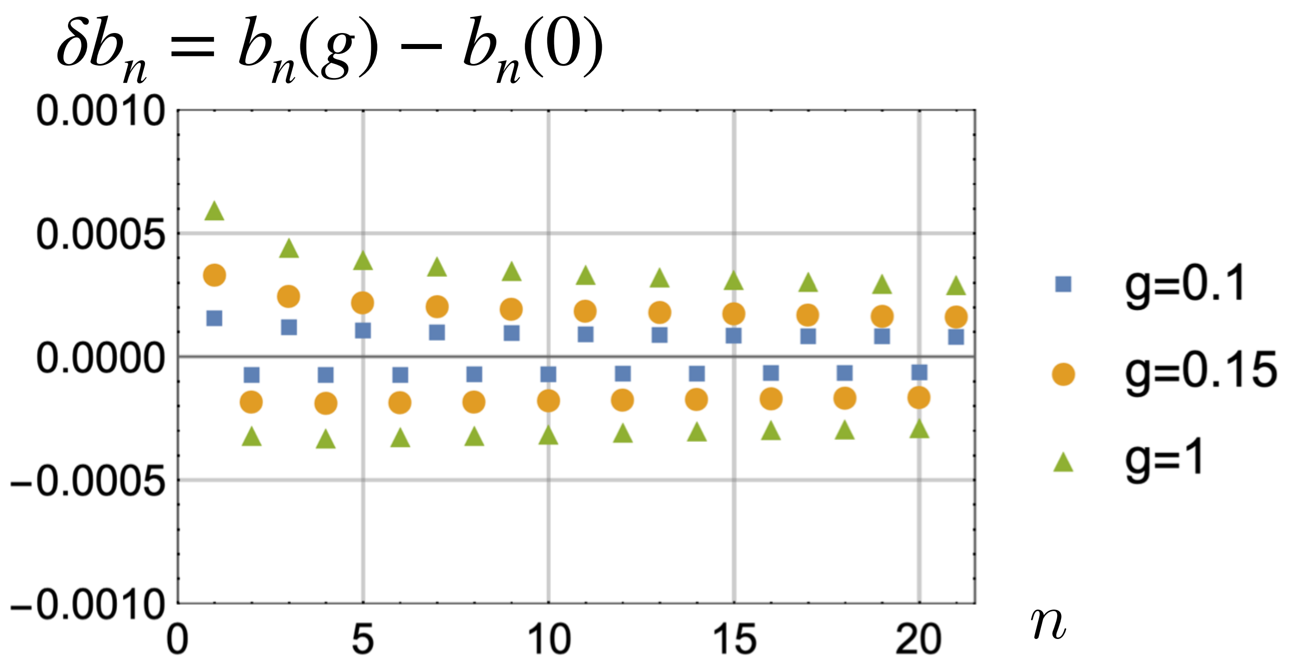


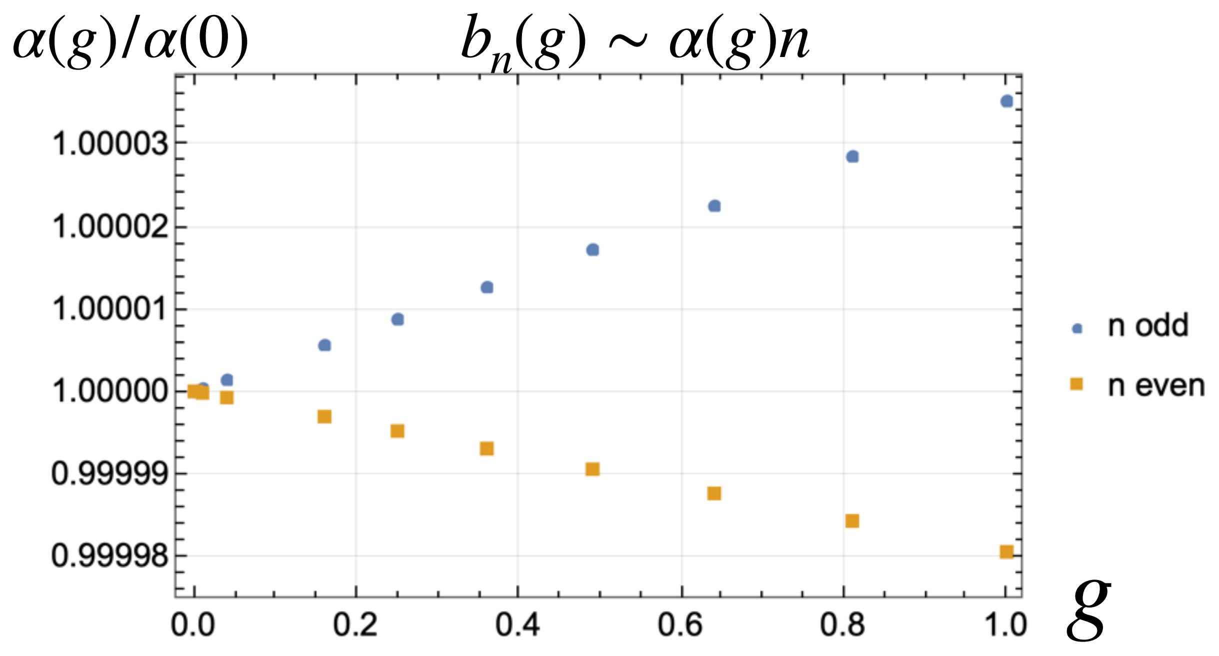


The coupling induces staggering which decreases as n increases.

# Quantum Billiards

Our working definition of quantum chaos is derived from the study of quantum systems that have classically chaotic analogues ([Bohigas, Giannoni, Schmit (1984)]). An example of such systems are quantum billiards.

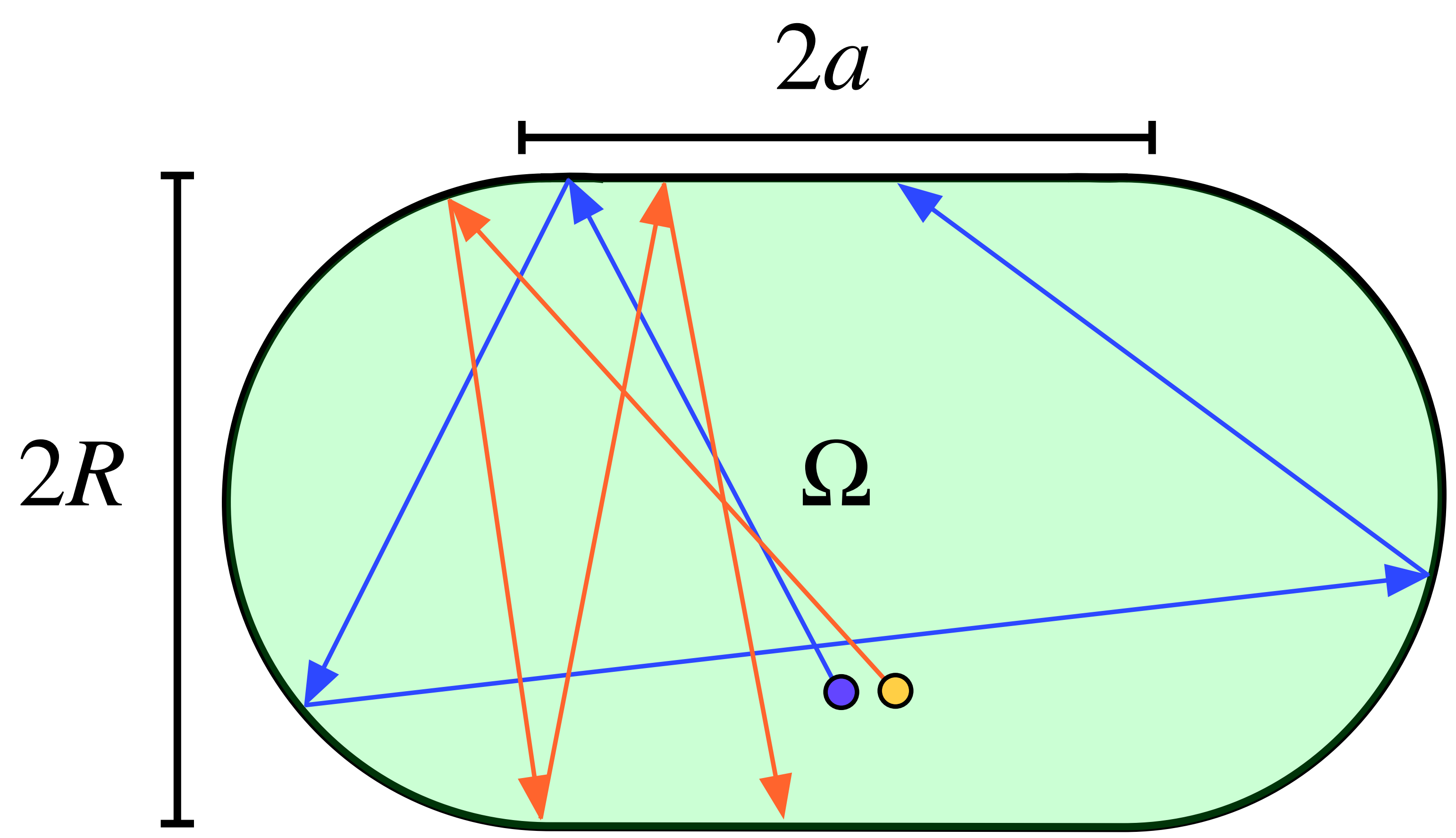

# Quantum Billiards

Our working definition of quantum chaos is derived from the study of quantum systems that have classically chaotic analogues ([Bohigas, Giannoni, Schmit (1984)]). An example of such systems are quantum billiards.

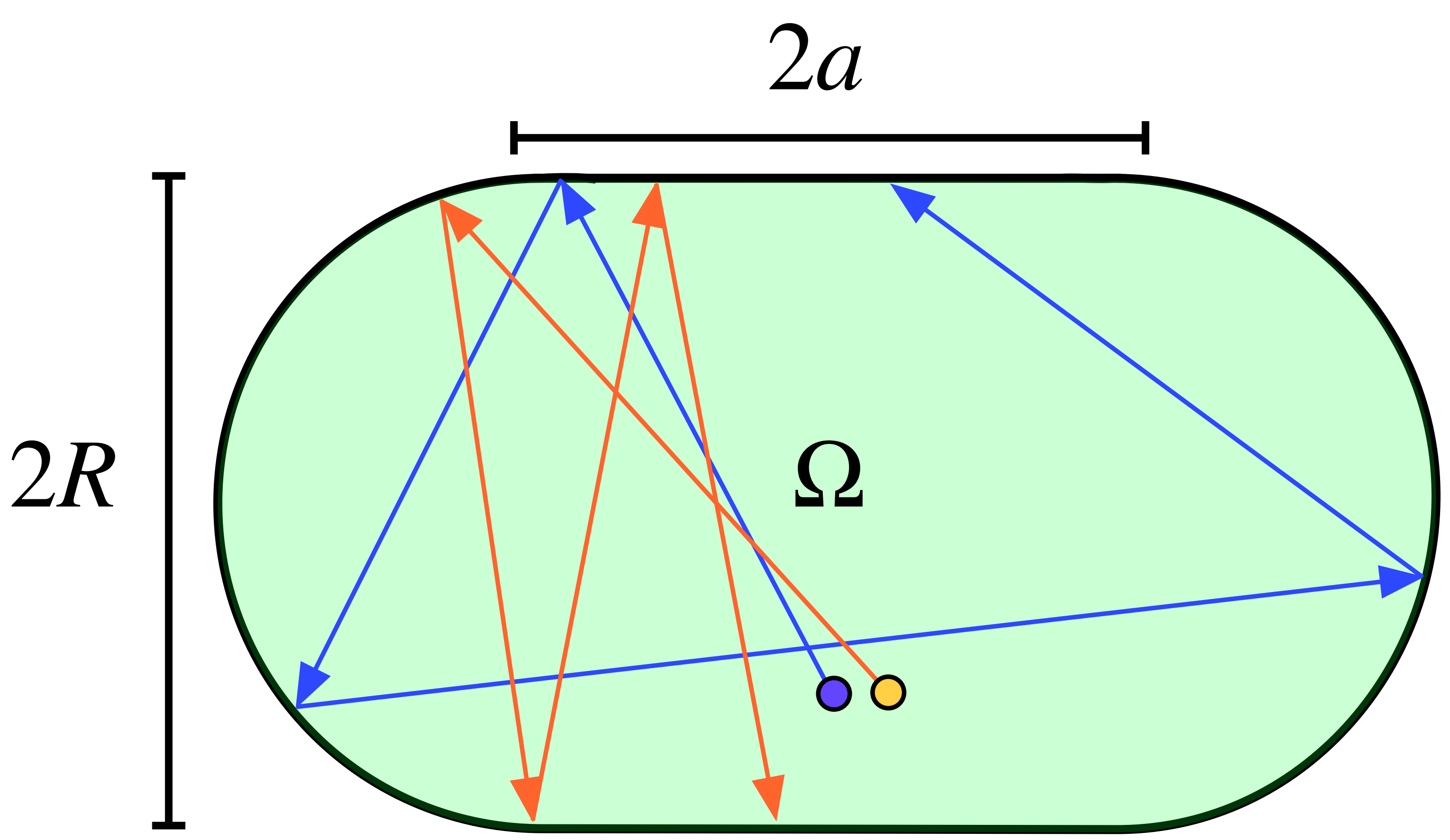


- Bohigas-Giannoni-Schmit (BGS) conjecture: "The spectral statistics of quantum systems, whose classical analogs are chaotic, conform to those predicted by **Random Matrix Theory (RMT)**, specifically the Gaussian Orthogonal Ensemble (GOE) for time-reversal invariant systems."- [BGS (1984)].

(energy-level repulsion and spectral rigidity)

- Berry-Tabor conjecture: "The level spacing of quantum systems whose classical analogs are integrable follow a Poisson distribution."- [Berry, Tabor (1977)].

[BGS (1984)]

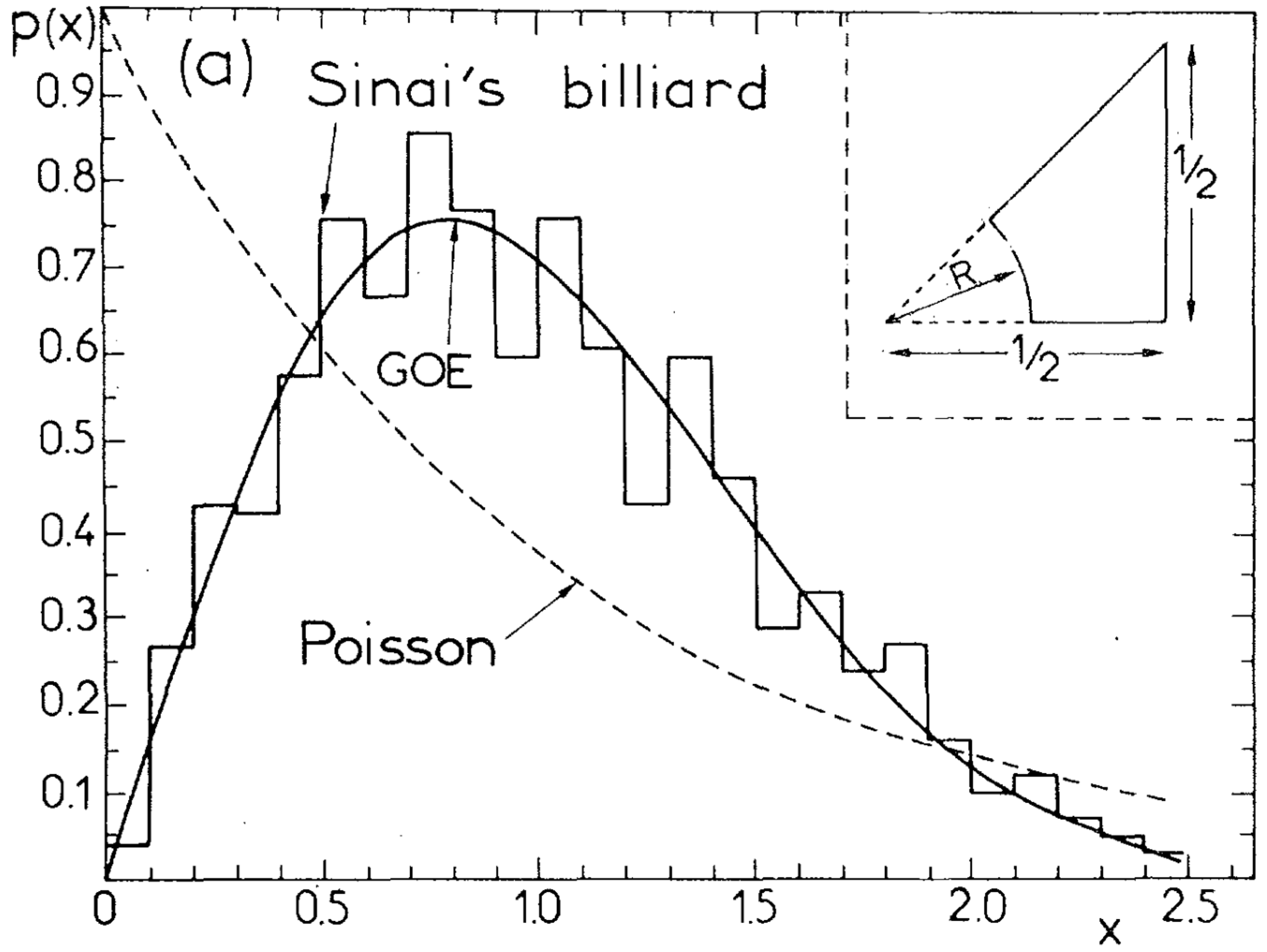


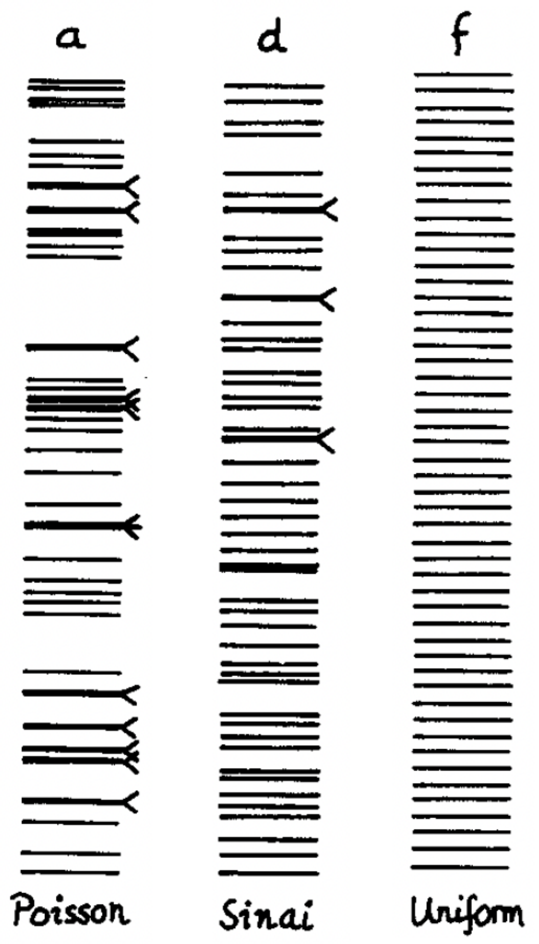


[Bohigas, Giannoni (1984)]

# Quantum Billiards



Can Krylov complexity capture signatures of semiclassical chaos in quantum billiards? Is the growth rate of the Lanczos coefficients bounded at finite temperature?

The idea is to solve numerically the Schrödinger equation $H|E_n\rangle = E_n|E_n\rangle$ with $H = p_x^2 + p_y^2$ and imposing Dirichlet BC at the boundary of the billiard $\Psi_n(x,y)|_{\partial\Omega} = 0$ , where $\Psi_n(x,y) = \langle x, y | E_n\rangle$. The area of the billiard $\Omega A_\Omega = \pi R^2 + 4aR$ is fixed to $1$, with the parameter $a/R$ controlling the transition from a circular (integrable): $a/R = 0$ to a stadium (chaotic) billiard $a/R = 1$.

# Quantum Billiards



Can Krylov complexity capture signatures of semiclassical chaos in quantum billiards? Is the growth rate of the Lanczos coefficients bounded at finite temperature?

The idea is to solve numerically the Schrödinger equation $H|E_n\rangle = E_n|E_n\rangle$ with $H = p_x^2 + p_y^2$ and imposing Dirichlet BC at the boundary of the billiard $\Psi_n(x,y)|_{\partial\Omega} = 0$ , where $\Psi_n(x,y) = \langle x,y|E_n\rangle$. The area of the billiard $\Omega A_\Omega = \pi R^2 + 4aR$ is fixed to $1$, with the parameter $a/R$ controlling the transition from a circular (integrable): $a/R = 0$ to a stadium (chaotic) billiard $a/R = 1$.

(Large variance in $b_n$ , [Hashimoto, et al. (2023)])

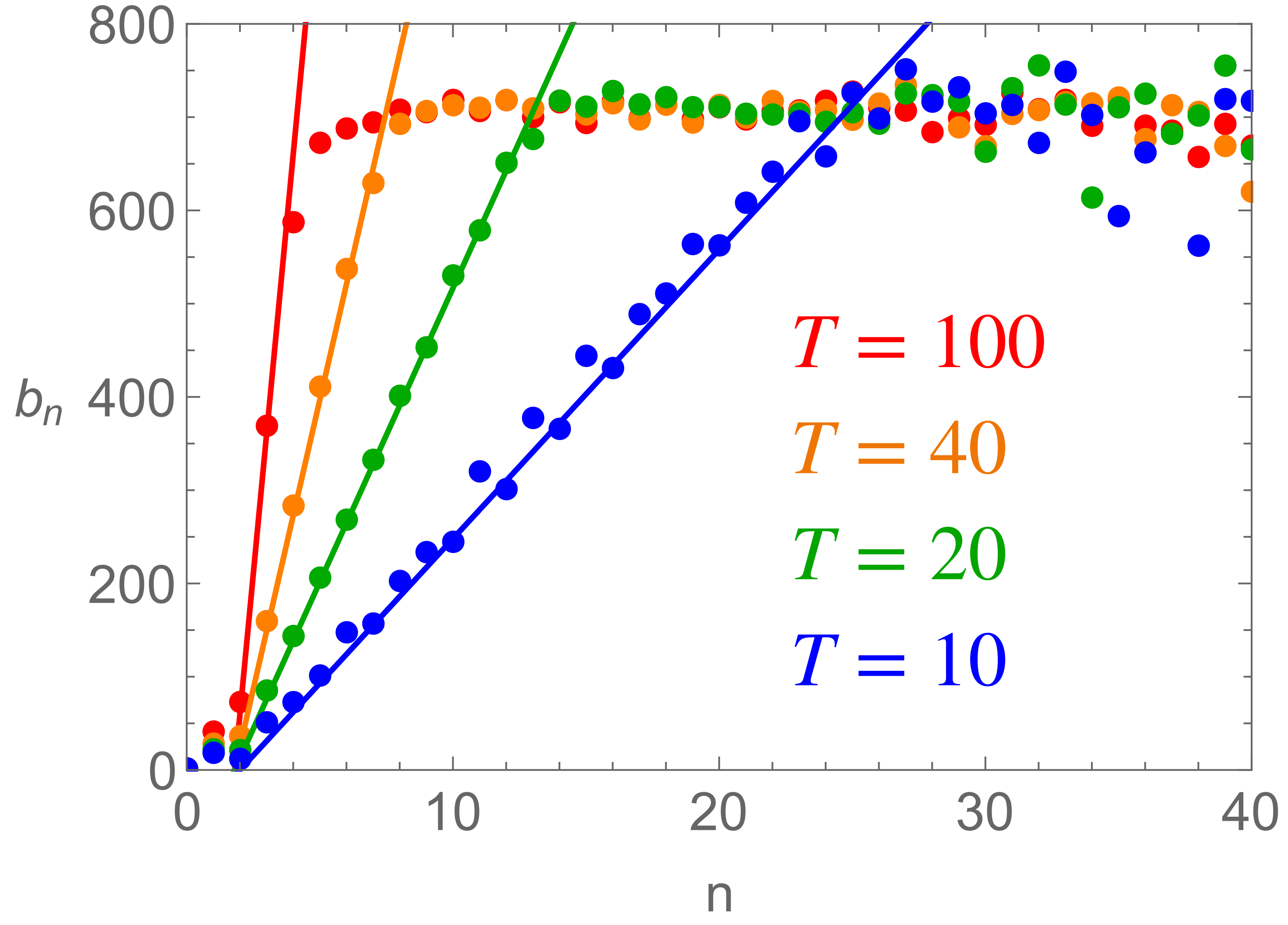


Stadium ($a/R = 1$)
(Chaotic)

**Saturation** in $b_n$ is due to a cutoff $N_{\text{max}} = 100$ in the Hilbert space.

We choose $\mathcal{O}_0 = \hat{x}$ and Wightman inner-product:

$$(A|B)^W := \text{tr}\left(e^{-\beta H/2}A^\dagger e^{-\beta H/2}B\right)/\text{tr}\left(e^{-\beta H}\right)$$

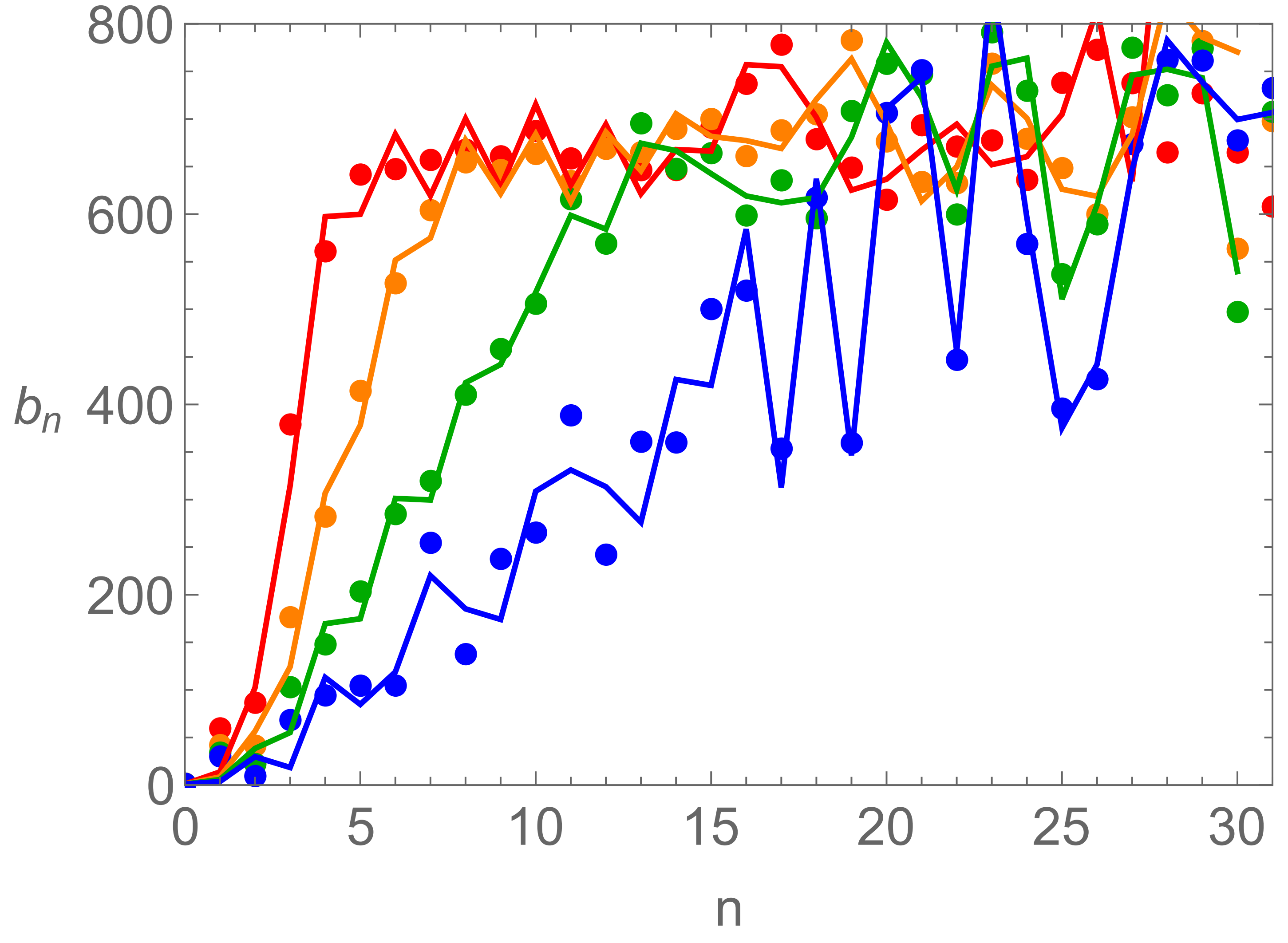


$T = 100$
$T = 40$
$T = 20$
$T = 10$

Circle ($a/R = 0$)
(Integrable)

# Quantum Billiards



In this case, the growth rate of the Lanczos coefficients $\alpha$ for the stadium billiard is bounded by $\pi T$:

$$\boxed{2\alpha \leq 2\pi T}$$

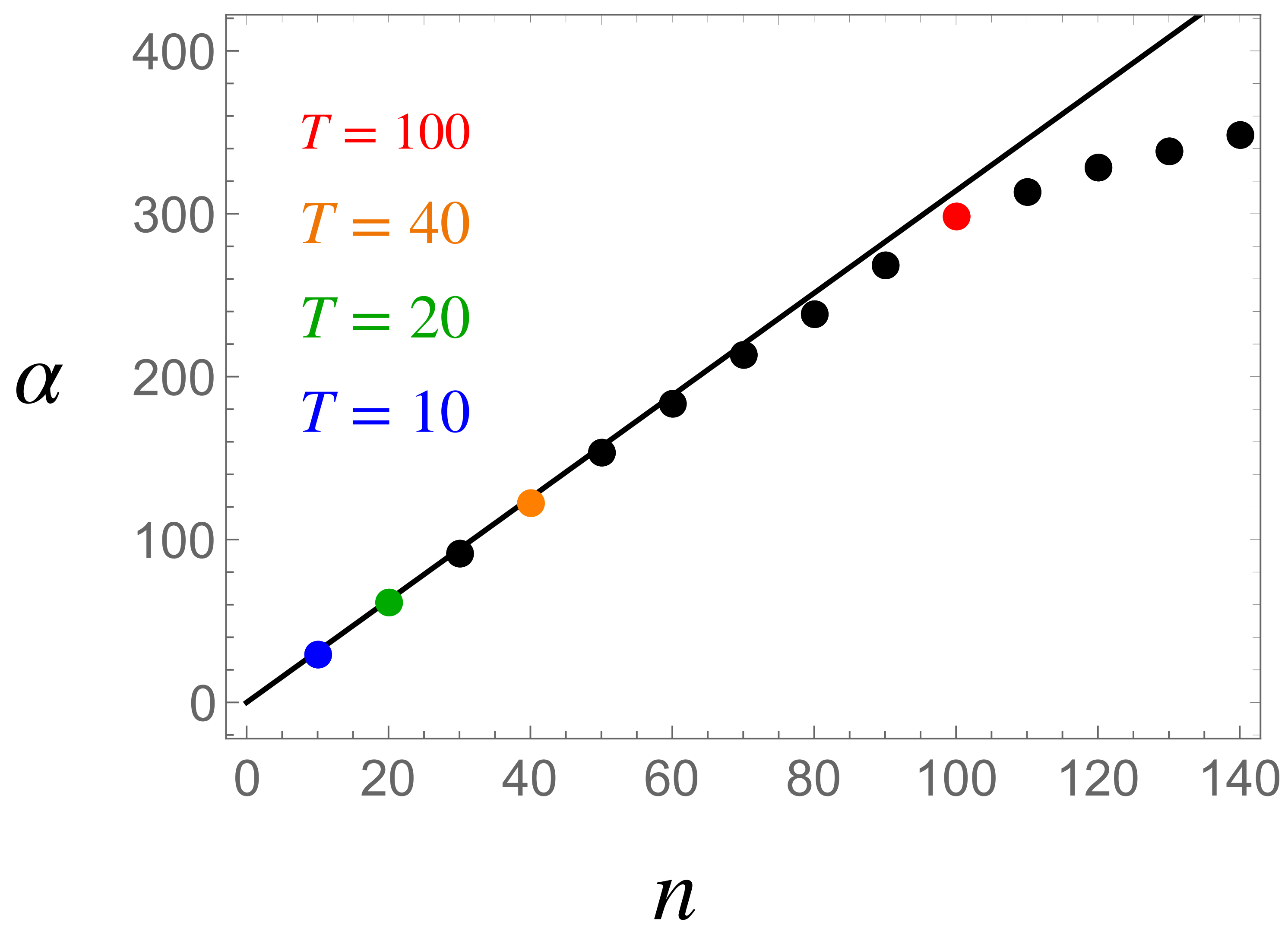


This bound is **saturated** at low $T$.

# Quantum Billiards



In this case, the growth rate of the Lanczos coefficients $\alpha$ for the stadium billiard is bounded by $\pi T$:

$$\boxed{2\alpha \leq 2\pi T}$$

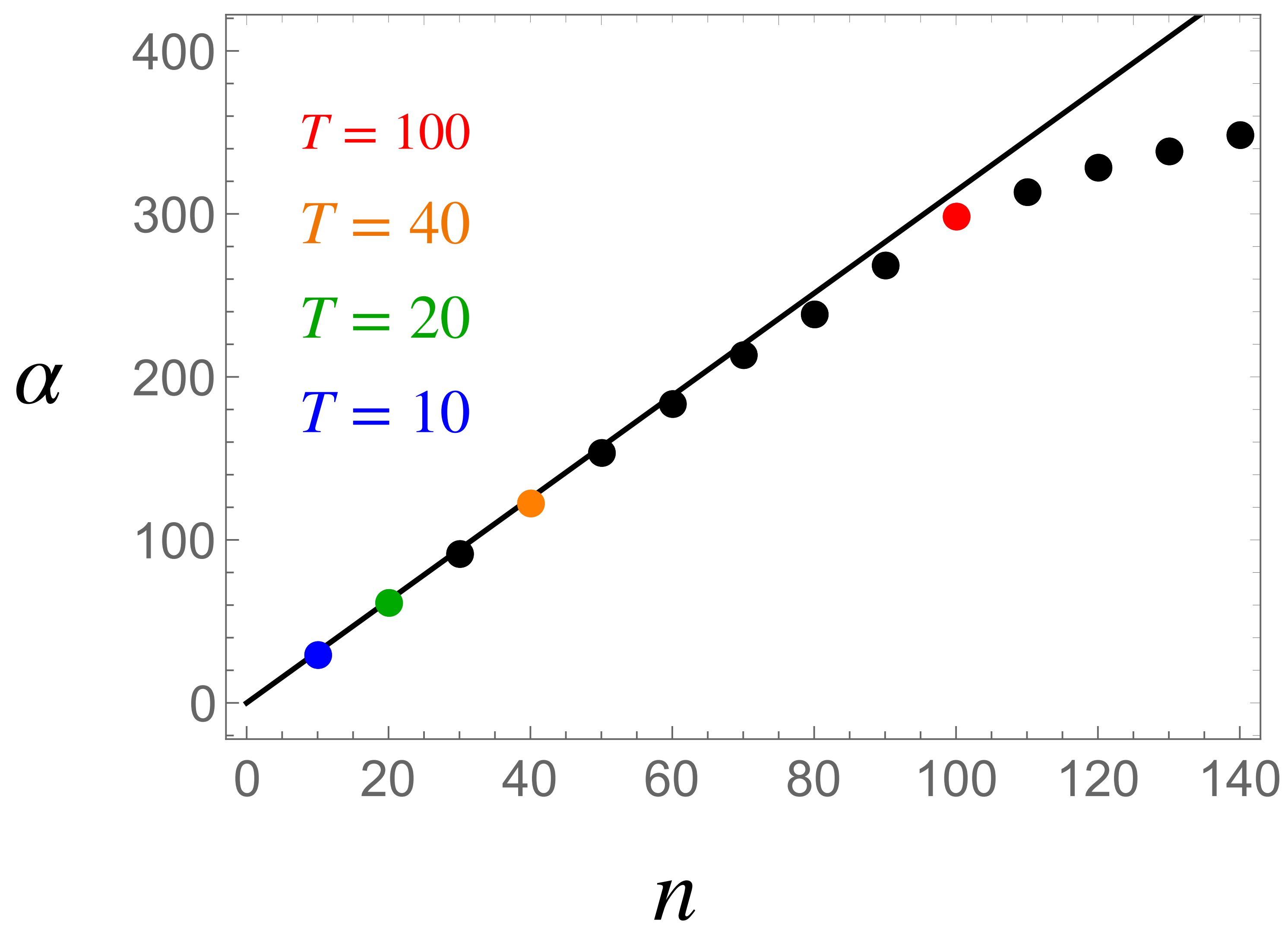


This bound is **saturated** at low $T$.

The early-time growth of Krylov complexity $K_x(t)$ is exponential. Furthermore, $K_x(t)$ can be shown to satisfy an ***Eherenfest theorem*** (EoM for Krylov complexity) ([Erdmenger, Jian, Xian (2023)])

$$\partial_t^2 \langle \hat{n}_x \rangle_t = \partial_t^2 (x(t)\,|\,\hat{n}_x\,|\,x(t)) = -\,(x(t)\,|\,[[\hat{n}_x\,,\mathscr{L}],\mathscr{L}]\,|\,x(t)) = -\,[[\langle \hat{n}_x \rangle_t\,,\mathscr{L}],\mathscr{L}]$$

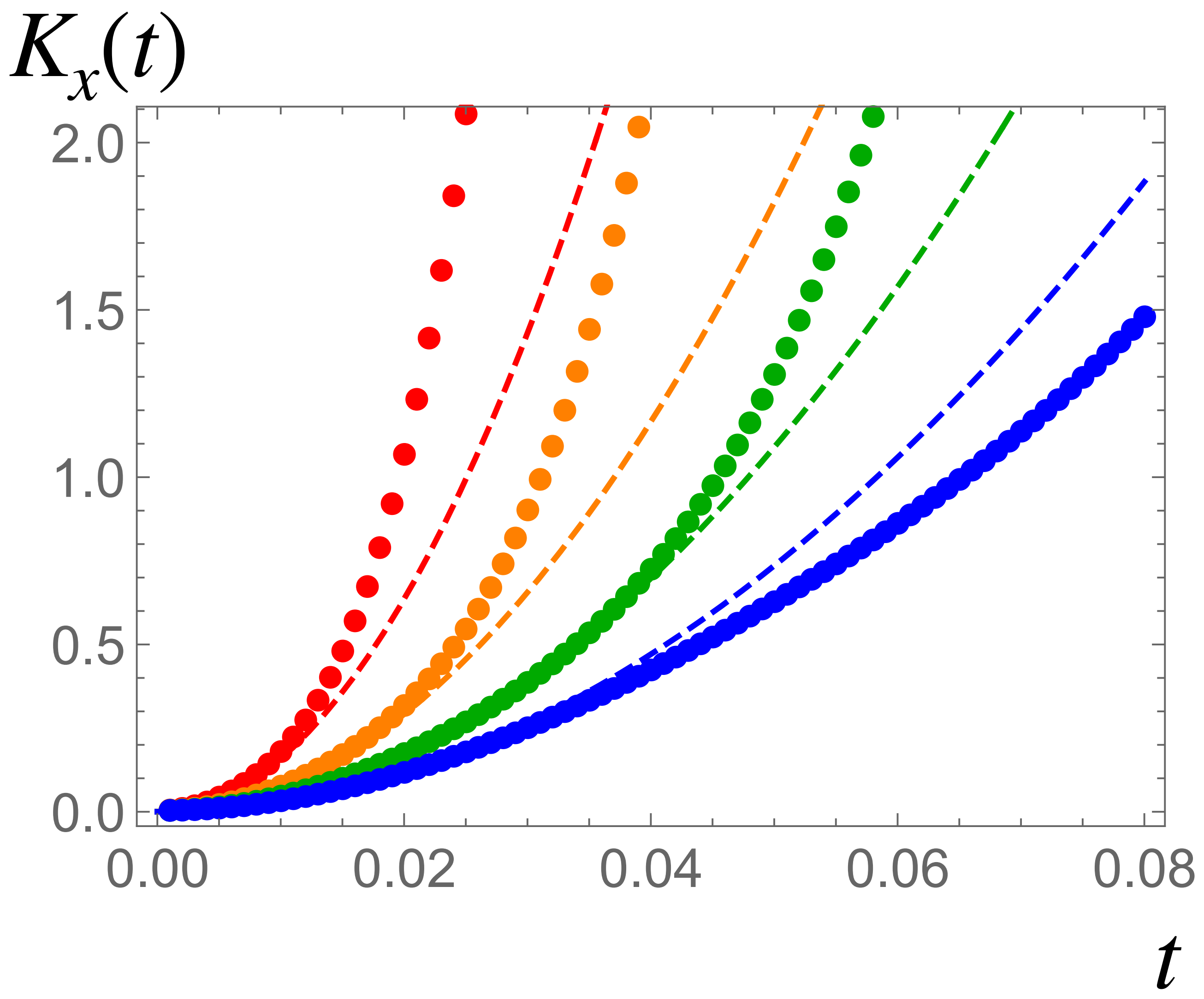


Stadium $(a/R = 1)$
(Chaotic)

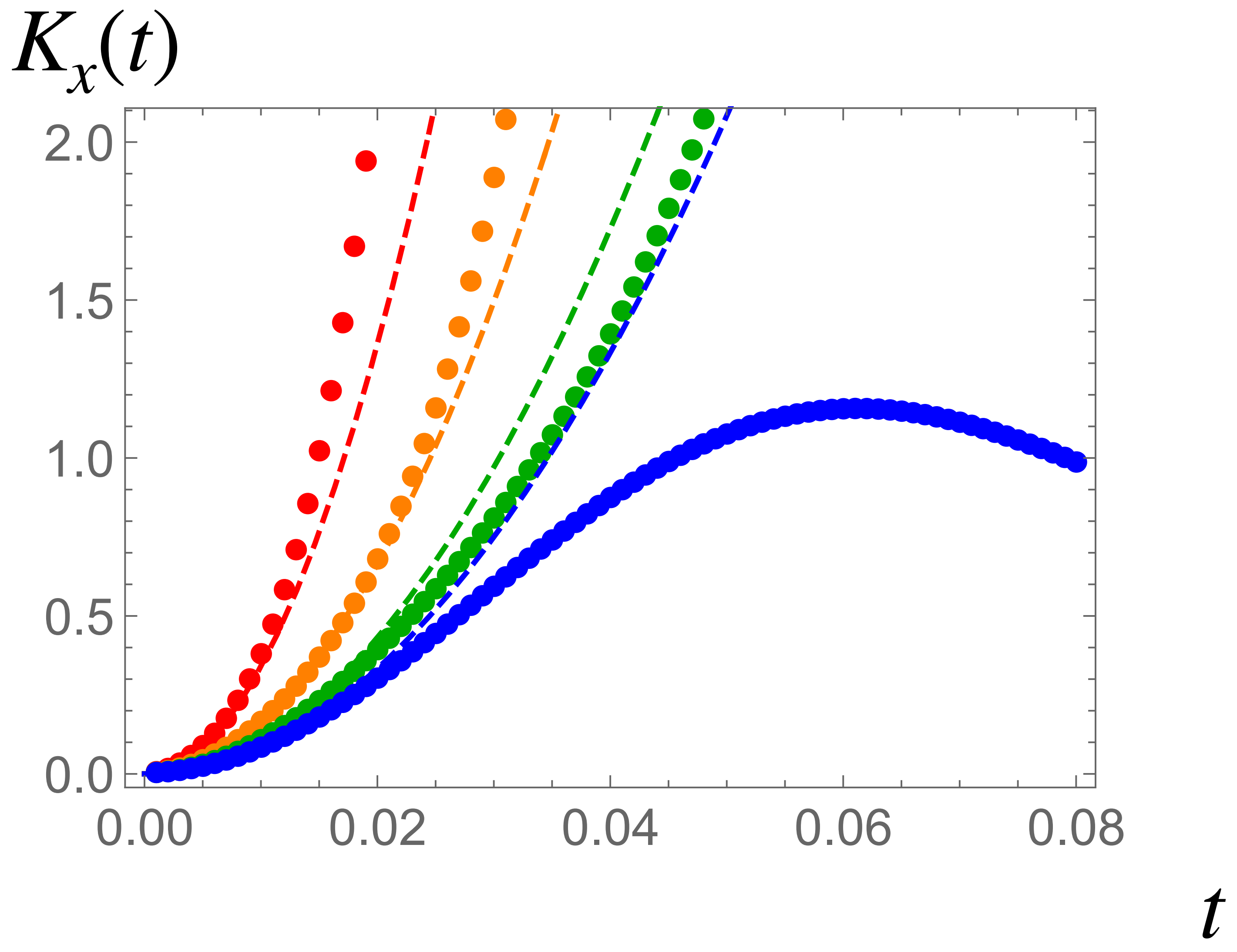


Circle $(a/R = 0)$
(Integrable)

Dots = numerical data.
Dashed lines = analytic early-time results

# II. Spread Complexity and "Long-time" Quantum Chaos

# Spread complexity of the TFD state



Spread complexity can be defined for *any* state $|\psi_0\rangle$. However, we are interested in comparing it with other spectral quantities, such as the spectral form factor (SFF). It is natural to consider the TFD state as the initial state.

$$|\psi_0\rangle = |\mathrm{TFD}_\beta\rangle := \frac{1}{\sqrt{Z_\beta}} \sum_n e^{-\frac{\beta E_n}{2}} |n\rangle \otimes |n\rangle \qquad \left( Z_\beta = \mathrm{tr}\left(e^{-\beta H}\right) = \sum_n e^{-\beta E_n} \right)$$

# Spread complexity of the TFD state

Spread complexity can be defined for *any* state $|\psi_0\rangle$. However, we are interested in comparing it with other spectral quantities, such as the spectral form factor (SFF). It is natural to consider the TFD state as the initial state.

$$|\psi_0\rangle = |\mathrm{TFD}_\beta\rangle := \frac{1}{\sqrt{Z_\beta}} \sum_n e^{-\frac{\beta E_n}{2}} |n\rangle \otimes |n\rangle \qquad \left( Z_\beta = \mathrm{tr}\left(e^{-\beta H}\right) = \sum_n e^{-\beta E_n} \right)$$

In this case, the first probability amplitude $\phi_0(t)$ (given by the return amplitude of the TFD state) is directly related to the SFF:

$$\phi_0(t) := \langle \mathrm{TFD}_\beta | \mathrm{TFD}_{\beta+2it} \rangle = \frac{Z_{\beta+it}}{Z_\beta} \sim \sqrt{\mathrm{SFF}(t)} \qquad \mathrm{SFF}(t) := \frac{|Z_{\beta+it}|^2}{|Z_\beta|^2} = \frac{1}{|Z_\beta|^2} \sum_{n,m} e^{-\beta(E_n+E_m)} e^{it(E_n-E_m)}$$

The spread complexity depends only on the spectrum of the theory $\{E_n, |n\rangle\}$ and $\beta$.

- At early times: $C_\psi(t) \approx b_1^2 t^2$
- Saturation value (at $\beta = 0$): $\lim_{t\to\infty} C_\psi(t) = \dfrac{d-1}{2}$

($d$ = Hilbert space dim.)

# Spin Chains: From Integrability to Chaos



We consider two paradigmatic spin chains: next-to-nearest-neighbour (NNN) deformation of the Heisenberg (XXZ) chain and the mixed-field Ising (MFI):

$$H = H_{XXZ} + H_{NNN}$$

$$\begin{cases} H_{XXZ} = \displaystyle\sum_{i=1}^{N-1} J\,(S_i^x S_{i+1}^x + S_i^y S_{i+1}^y) + J_{zz} S_i^z S_{i+1}^z \\ H_{NNN} = \displaystyle\sum_{i=1}^{N-2} J_c S_i^z S_{i+2}^z \end{cases}$$

$$(J, J_{zz}, J_c) = \begin{cases} (1, 0.5, 1)\,, & \text{(Chaotic case)}, \\ (1, 0.5, 0)\,, & \text{(Integrable case)}\,. \end{cases}$$

$$H_I = \sum_{i=1}^{N-1} S_i^z S_{i+1}^z + \sum_{i=1}^{N} \left(h_x S_i^x + h_z S_i^z\right)$$

$$(h_x, h_z) = \begin{cases} (1.05, \, -0.5)\,, & \text{(Chaotic case)} \\ (1, 0)\,. & \text{(Integrable case)} \end{cases}$$

# Spin Chains: From Integrability to Chaos



We consider two paradigmatic spin chains: next-to-nearest-neighbour (NNN) deformation of the Heisenberg (XXZ) chain and the mixed-field Ising (MFI):

$$H = H_{XXZ} + H_{NNN}$$

$$\begin{cases} H_{XXZ} = \sum_{i=1}^{N-1} J\,(S_i^x S_{i+1}^x + S_i^y S_{i+1}^y) + J_{zz} S_i^z S_{i+1}^z \\ H_{NNN} = \sum_{i=1}^{N-2} J_c\, S_i^z S_{i+2}^z \end{cases}$$

$$(J, J_{zz}, J_c) = \begin{cases} (1, 0.5, 1)\,, & \text{(Chaotic case)}, \\ (1, 0.5, 0)\,, & \text{(Integrable case)}\,. \end{cases}$$

$$H_I = \sum_{i=1}^{N-1} S_i^z S_{i+1}^z + \sum_{i=1}^{N} \left(h_x S_i^x + h_z S_i^z\right)$$

$$(h_x, h_z) = \begin{cases} (1.05, -0.5)\,, & \text{(Chaotic case)} \\ (1, 0)\,. & \text{(Integrable case)} \end{cases}$$

To properly recover their characteristic level statistics, it is important to **unfold the spectrum** (account for local density of states) and take into account any **symmetries** that the Hamiltonian may have.

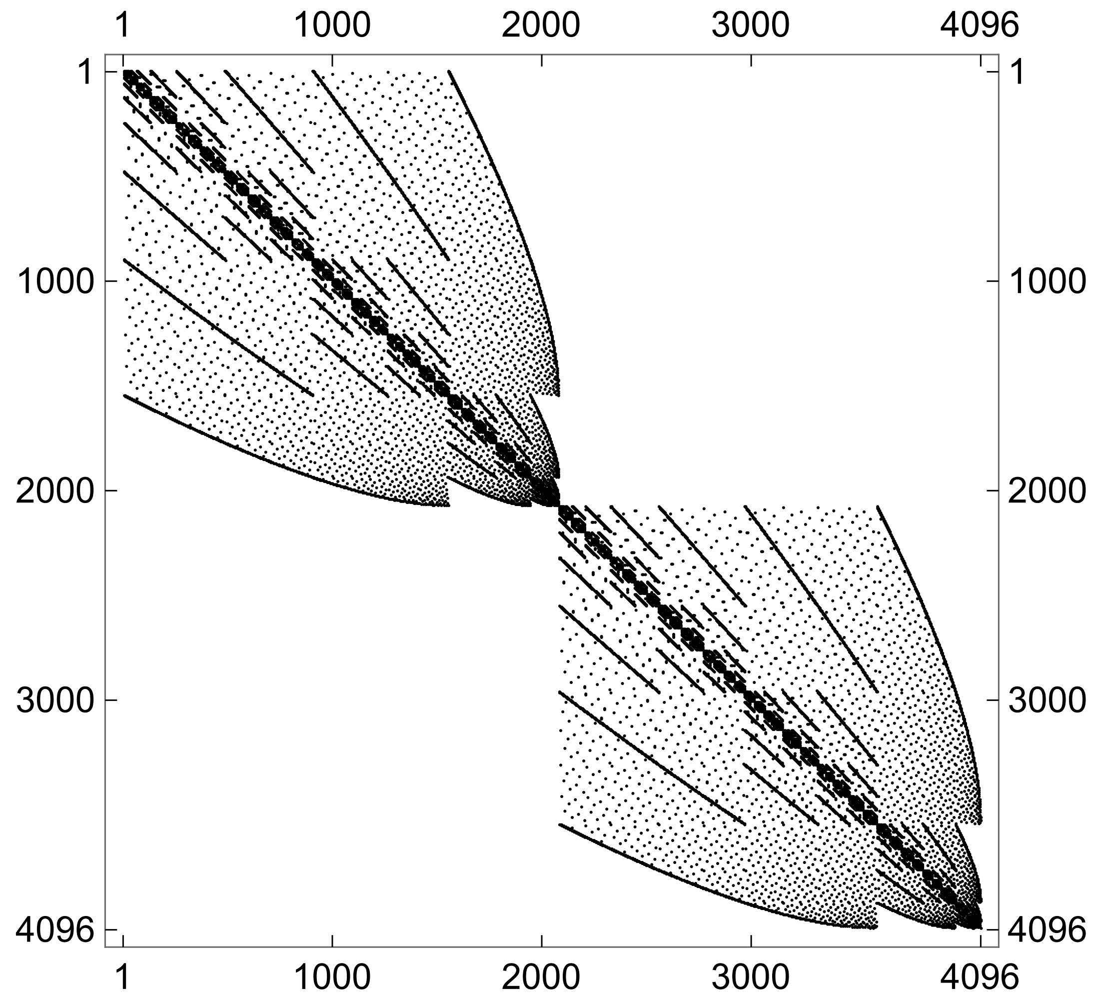


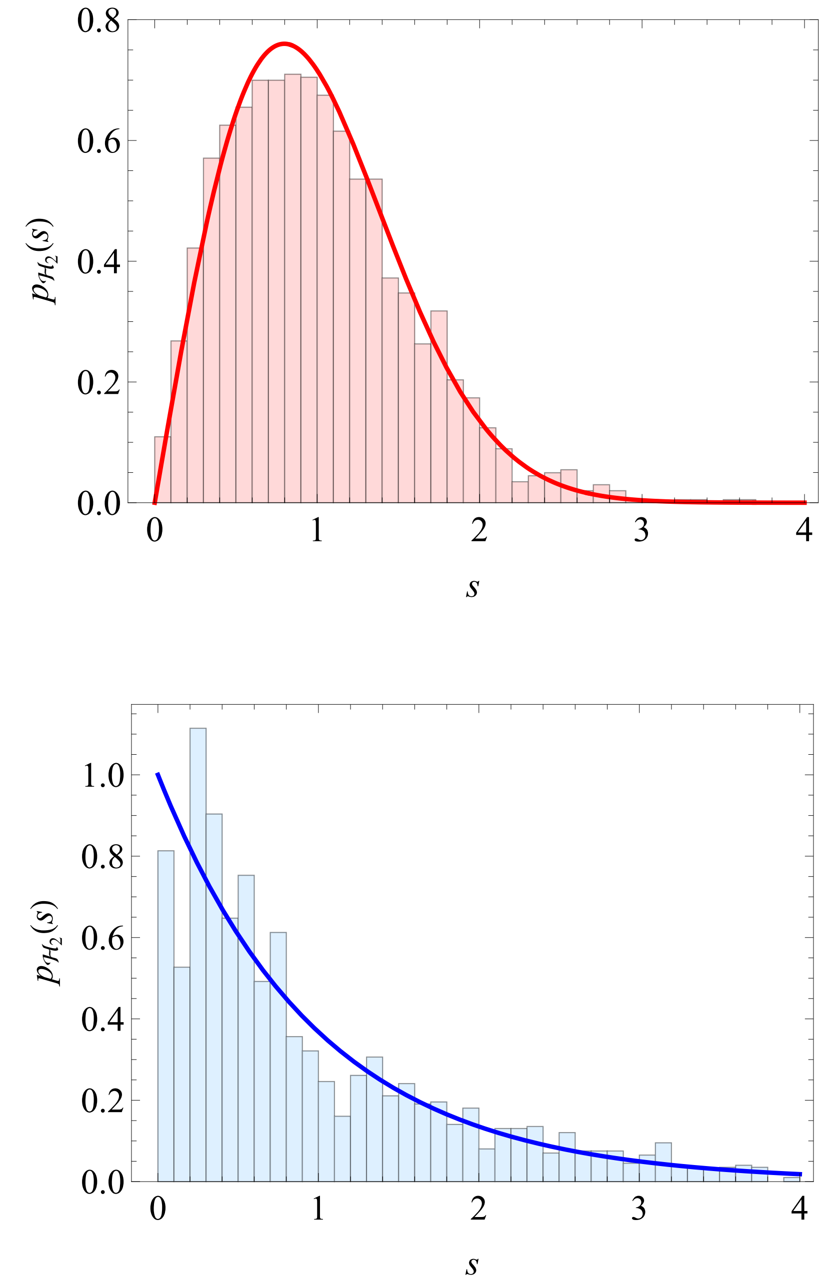

# Characteristic Features



- TFD state at $\beta \to 0$

- NNN deformation of XXZ

($N = 15$ sites , even parity sector and $M_z = -5/2$)

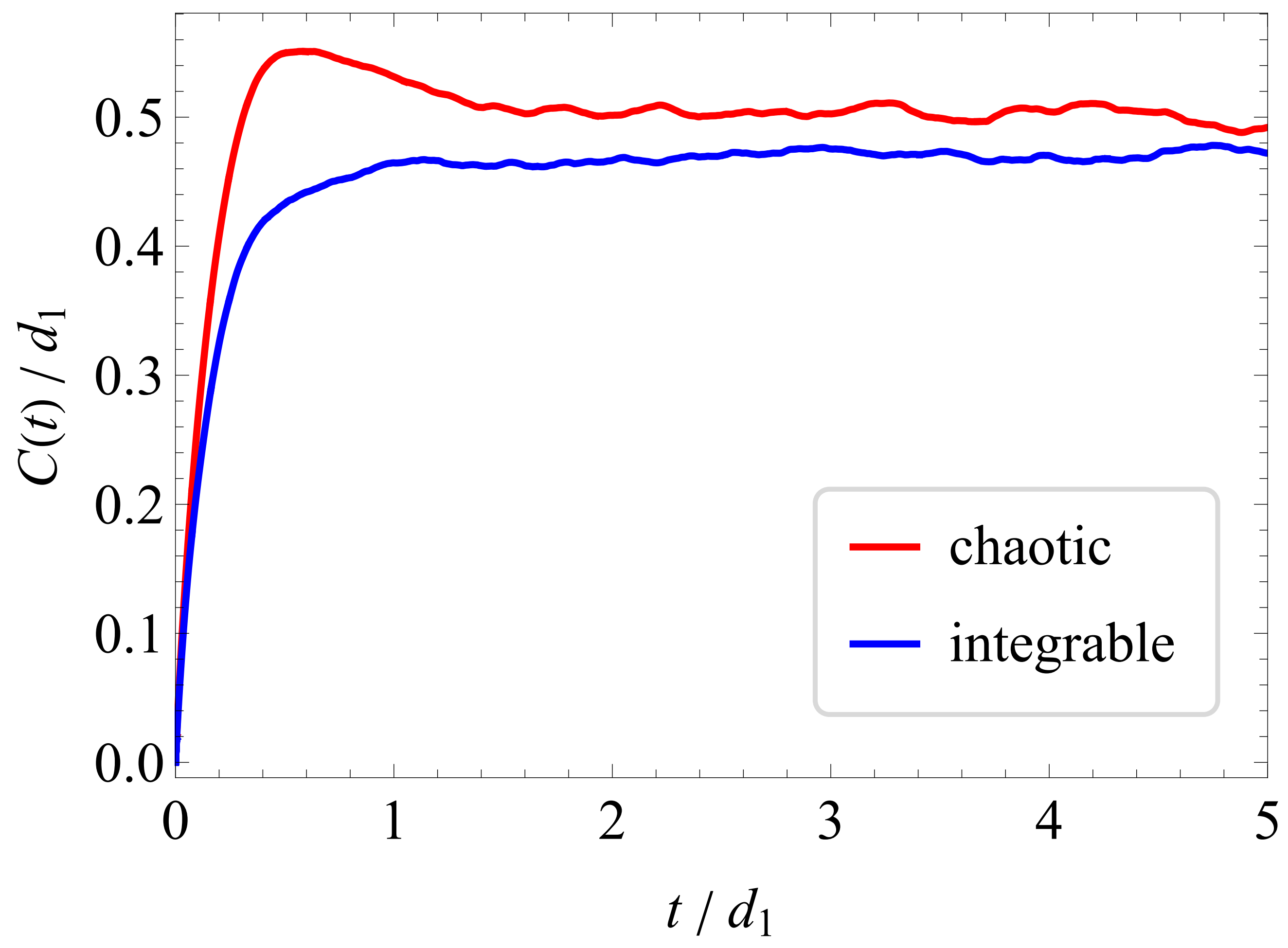


- MFI

($N = 12$ sites, even parity sector)

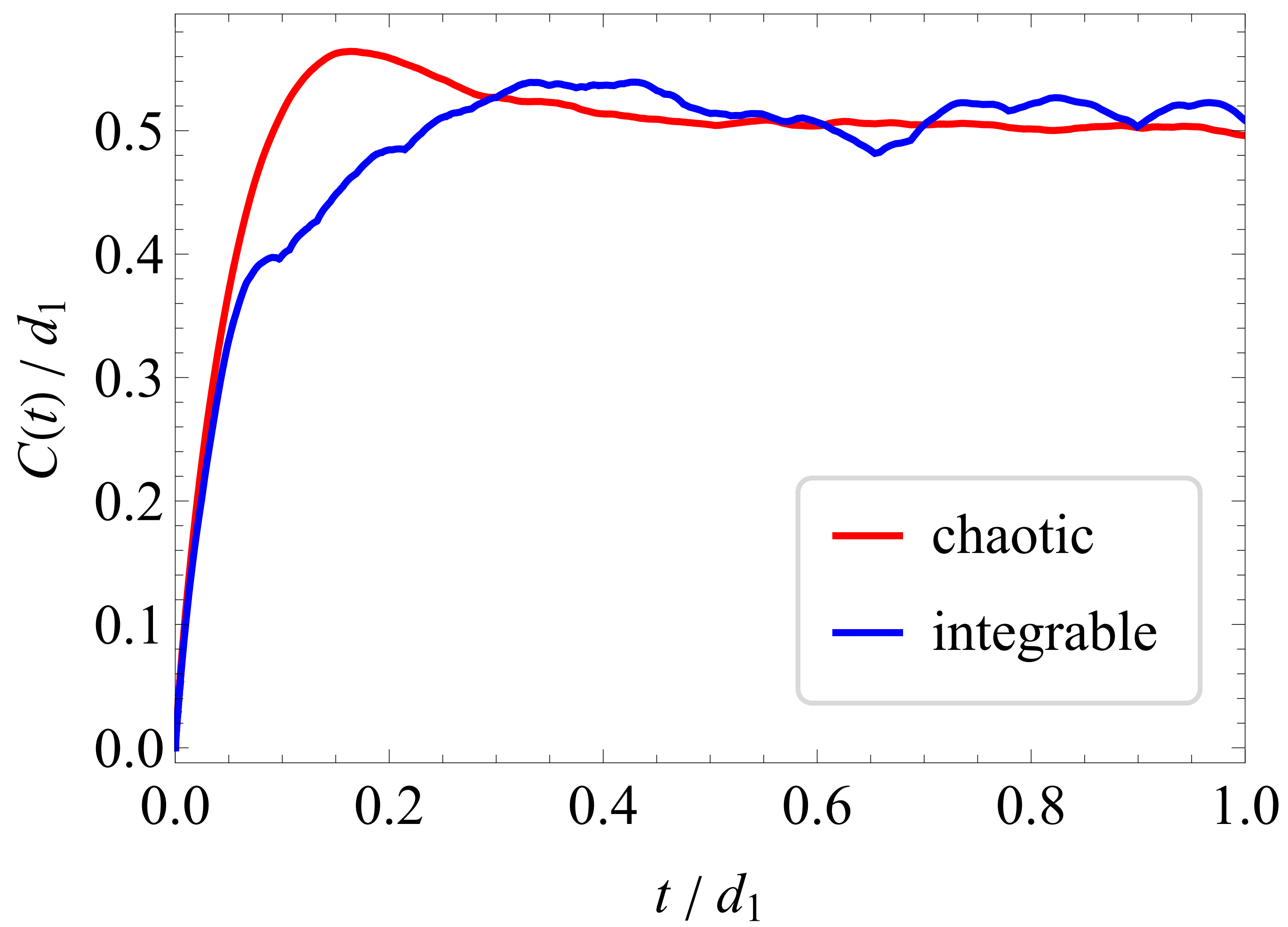


- TFD state for MFI in its chaotic phase

($N = 12$ sites, even parity sector)

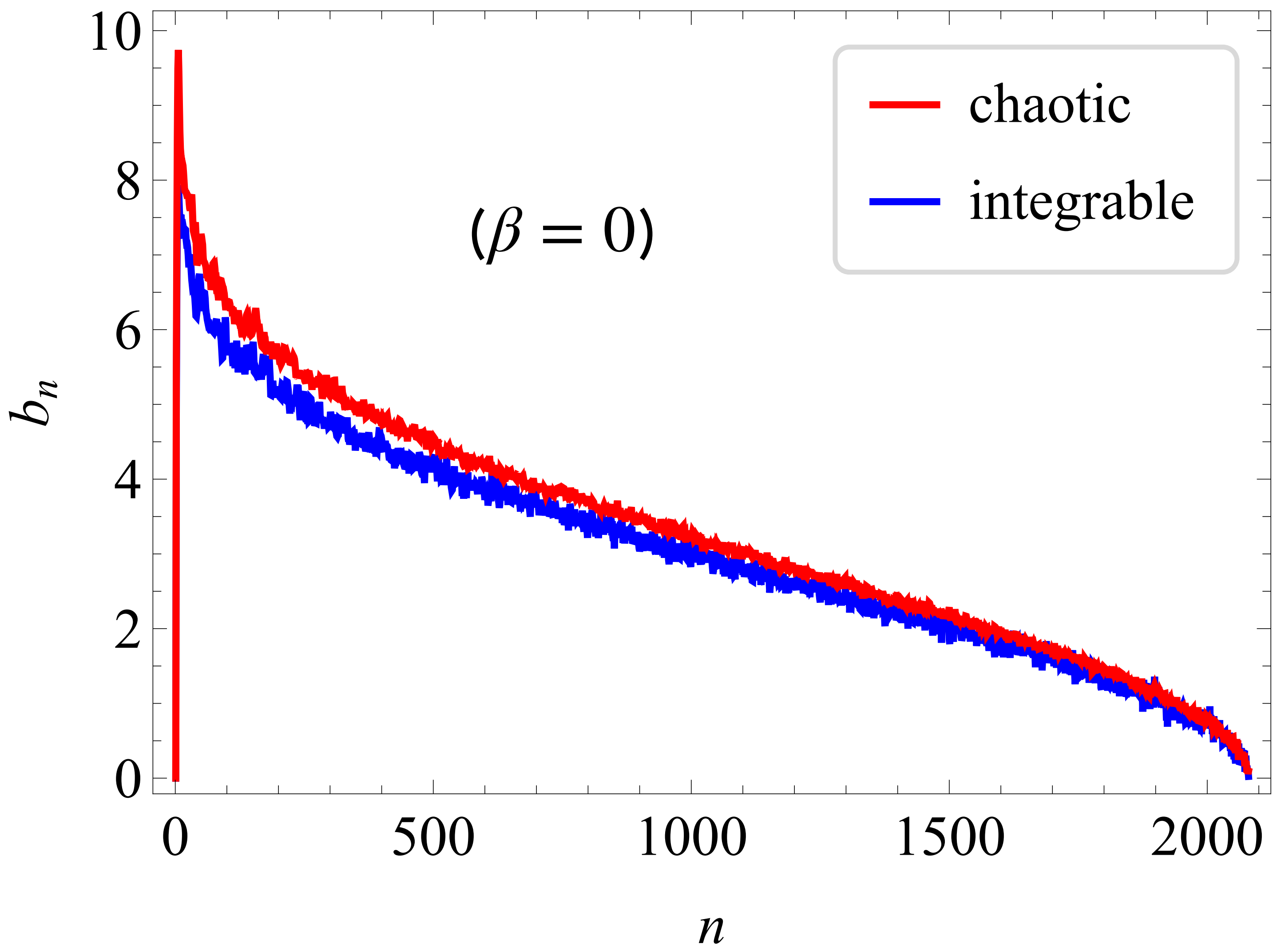


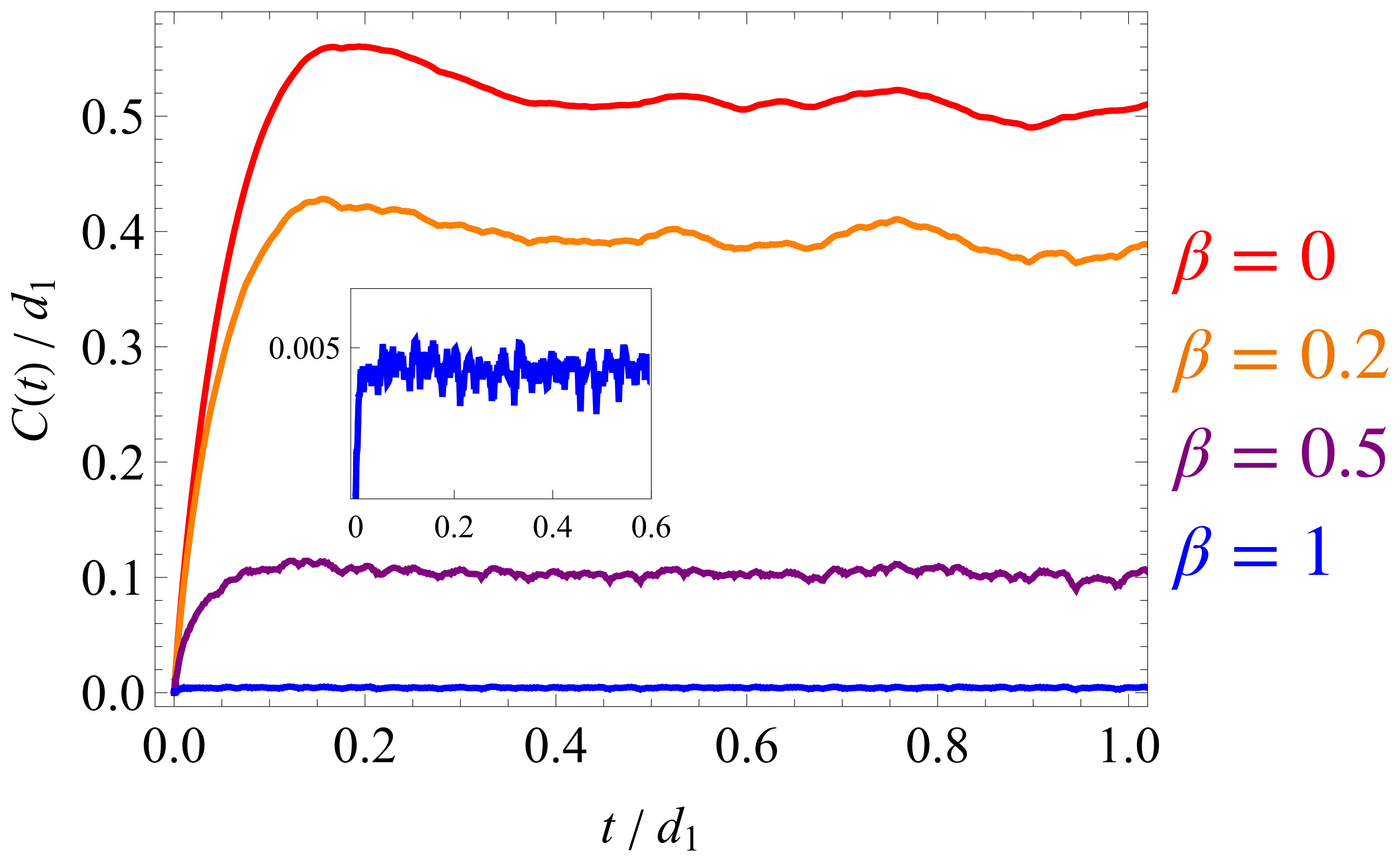

# Comparing Timescales



The physics behind the dynamical behavior of spectral complexity can be understood by comparing it with the typical timescales in the SFF. The following are log-log plots for the even sector of the mixed-field Ising in the **chaotic regime** for $N = 12$ and $\beta = 0$:

# Comparing Timescales



The physics behind the dynamical behavior of spectral complexity can be understood by comparing it with the typical timescales in the SFF. The following are log-log plots for the even sector of the mixed-field Ising in the **chaotic regime** for $N = 12$ and $\beta = 0$:

Spread

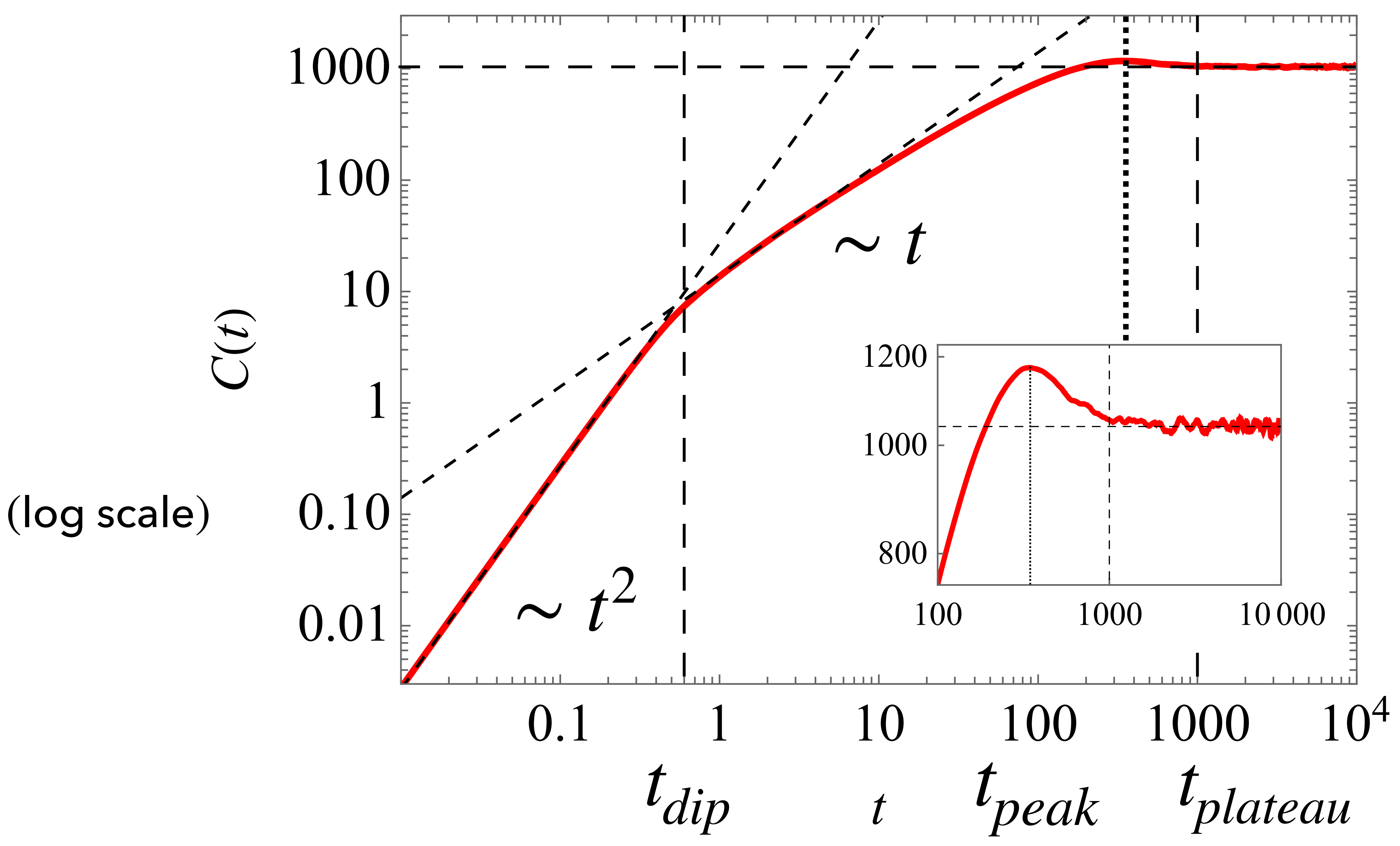


SFF

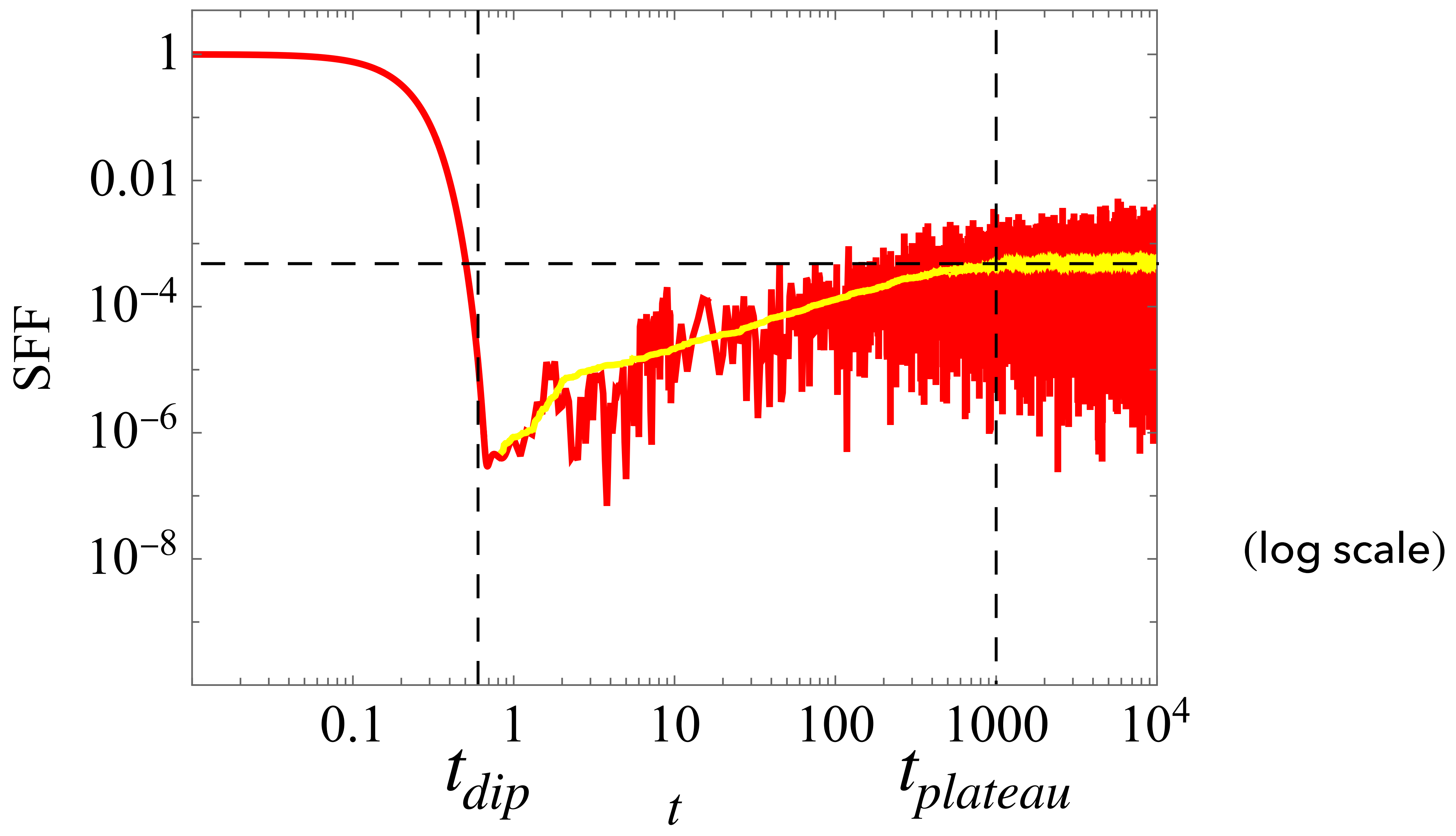


where: $t_{dip} \sim \mathcal{O}(1)$ , $t_{plateau} \sim d$ , and $\boxed{t_{dip} < t_{peak} \lesssim t_{plateau}}$ (c.f. RMTs where $t_{dip} \sim \sqrt{d}$ ).

The physics that gives rise to the peak in spread complexity might also responsible for the ramp in the SFF: **spectral rigidity** ([Balasubramanian , et al. (2022)]).

# Comparing Timescales



The following are log-log plots of spread complexity and the SFF for the even sector of the mixed-field Ising in the **integrable regime** for $N = 12$ and $\beta = 0$:

# Comparing Timescales



The following are log-log plots of spread complexity and the SFF for the even sector of the mixed-field Ising in the **integrable regime** for $N = 12$ and $\beta = 0$:

Spread

(log scale)

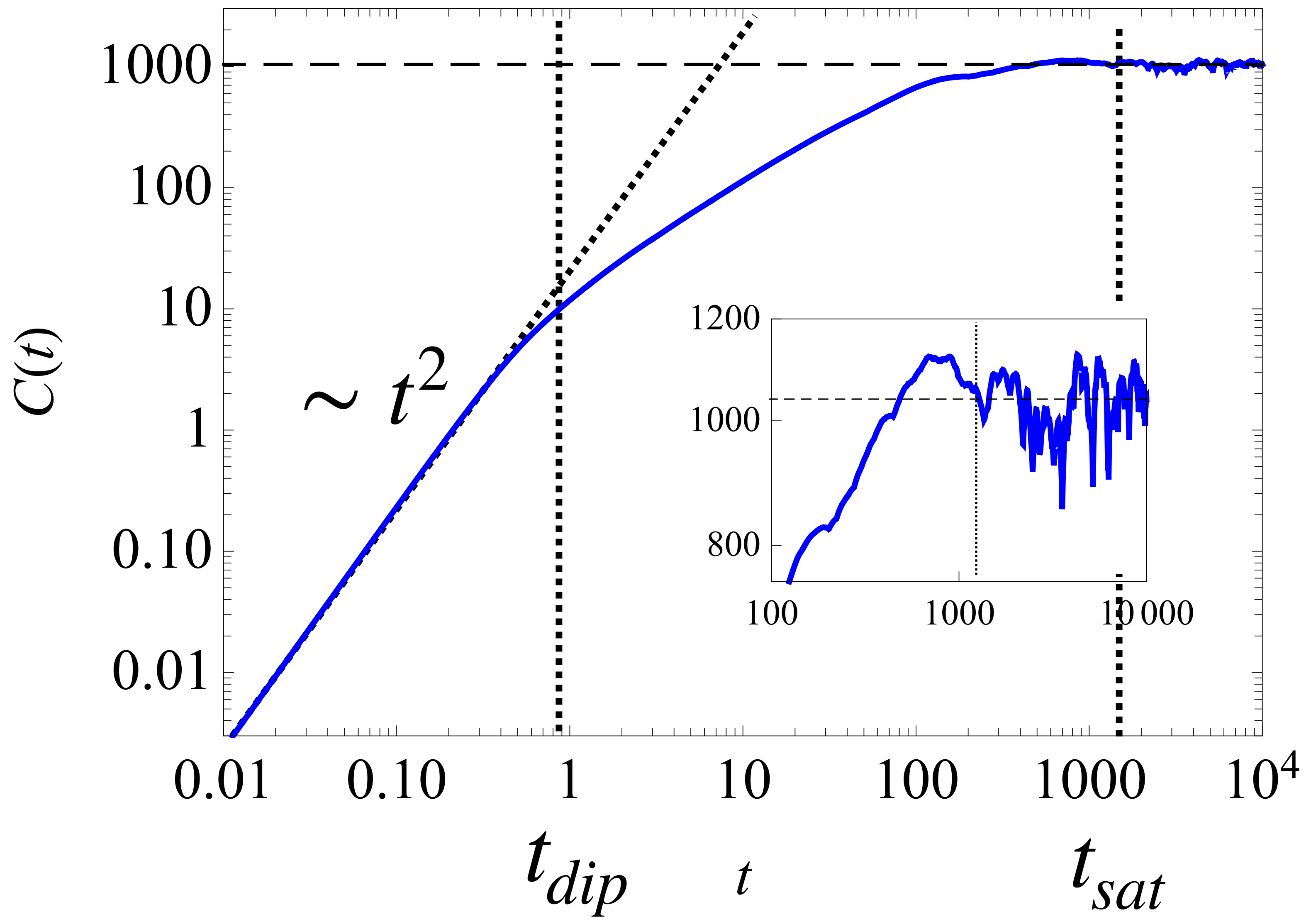


SFF

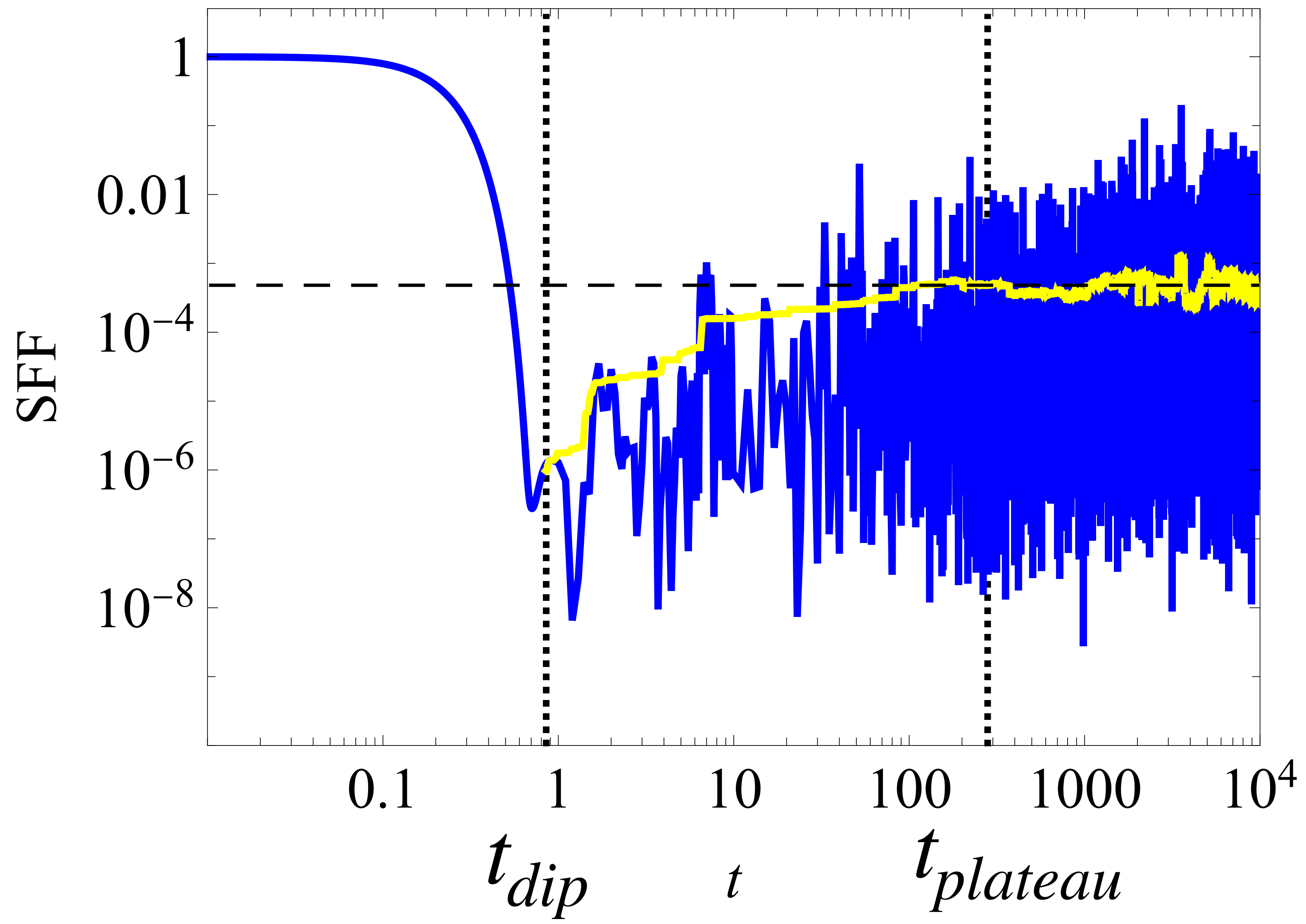


(log scale)

where: $t_{dip} \sim \mathcal{O}(1)$ and $t_{plateau} \sim \mathcal{O}(d)$ .

# III. Generalizations of Spread Complexity and Random Matrix Quenches

# Generalized Spreading Operator



Generalizations of spread complexity of the form

$$C_\psi^{(m)}(t) = \sum_{n\geq 0} n^m |\langle K_n|\psi(t)\rangle|^2 = \sum_{n\geq 0} n^m |\phi_n(t)|^2$$

with $m = 1,2,3,\ldots$, can be seen as as arising from the expectation value of the generalized spreading operator $\hat{n}_\psi^{(m)} = \sum_{n\geq 0} n^m |K_n\rangle\langle K_n|$ in the time-evolved state $|\psi(t)\rangle$

$$\langle \hat{n}_\psi^{(m)}\rangle_t := \langle\psi(t)|\hat{n}_\psi^{(m)}|\psi(t)\rangle = \langle\psi_0|\hat{n}_\psi^{(m)}(t)|\psi_0\rangle = C_\psi^{(m)}(t)$$

# Generalized Spreading Operator



Generalizations of spread complexity of the form

$$C_\psi^{(m)}(t) = \sum_{n\geq 0} n^m |\langle K_n | \psi(t)\rangle|^2 = \sum_{n\geq 0} n^m |\phi_n(t)|^2$$

with $m = 1,2,3,\ldots$, can be seen as as arising from the expectation value of the generalized spreading operator $\hat{n}_\psi^{(m)} = \sum_{n\geq 0} n^m |K_n\rangle\langle K_n|$ in the time-evolved state $|\psi(t)\rangle$

$$\langle \hat{n}_\psi^{(m)}\rangle_t := \langle \psi(t)|\hat{n}_\psi^{(m)}|\psi(t)\rangle = \langle \psi_0|\hat{n}_\psi^{(m)}(t)|\psi_0\rangle = C_\psi^{(m)}(t)$$

These were introduced in the context of the statistics of measurements in quantum mechanics [Fu, Pal, Pal & Kim (2024)], related to the moments of the characteristic function describing the probability distribution of measurements of the spreading operator.

Since the average position of the particle on the Krylov chain characterizes the dynamics of the system, it is natural to study higher moments, $\langle \hat{n}^{(2)}\rangle_t, \langle \hat{n}^{(3)}\rangle_t$. All these higher-order quantities are also measures of '**complexity**' in the sense that they are 'minimized' for a finite time in the Krylov basis.

# Generalized Spread Complexity



One question is whether these generalized spreads complexities show more sensitivity as probes of quantum than the usual one. One setting where they can be contrasted is in RMTs. For example, for a single realization of a GOE matrix and for $N = 1000$:

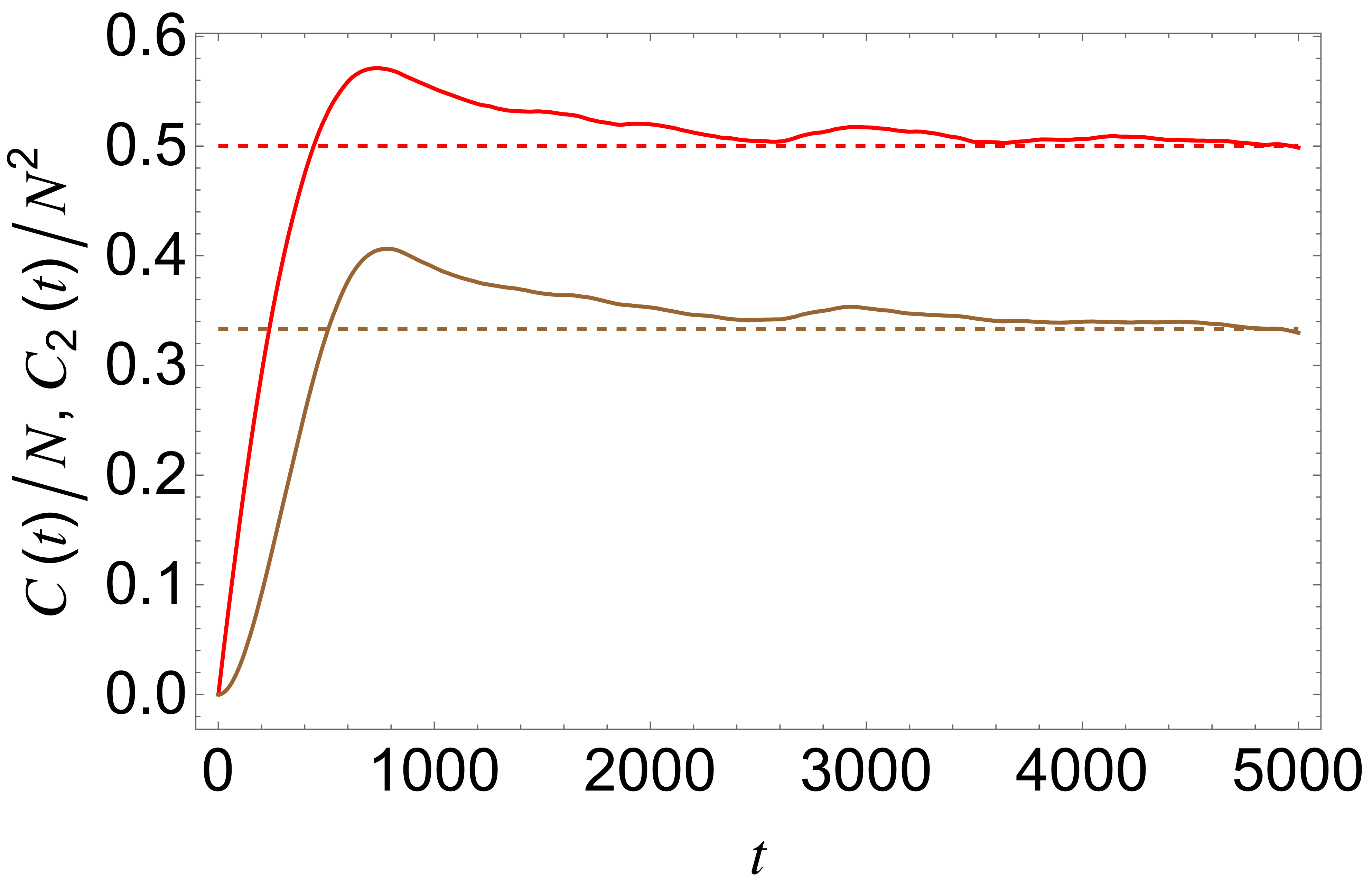


The peak (a signature of quantum chaos in spread complexity) becomes more visible in higher order spread complexities.

Generically, the generalized complexities have an early-time quadratic growth: $C_m(t) \approx b_1^2 t^2 \sum_n n^m \delta_{n,1} + O(t^3)$ .

# Random Matrix Quenches



Quantum quenches provide a framework for investigating the non-equilibrium dynamics of closed, interacting quantum systems following a change in one or more of the system's parameters.

Consider a sudden quench protocol involving two random $N \times N$ matrices from a one parameter class of random matrices ($H_r(h)$) of the form ([Brandino, De Luca, Konik & Mussardo (2012)])

$$H_r(h) = \begin{pmatrix} A & hB \\ hB^\dagger & C \end{pmatrix}$$

# Random Matrix Quenches



Quantum quenches provide a framework for investigating the non-equilibrium dynamics of closed, interacting quantum systems following a change in one or more of the system's parameters.

Consider a sudden quench protocol involving two random $N \times N$ matrices from a one parameter class of random matrices ($H_r(h)$) of the form ([Brandino, De Luca, Konik & Mussardo (2012)])

$$H_r(h) = \begin{pmatrix} A & hB \\ hB^\dagger & C \end{pmatrix}$$

$(H_r(h) \sim H_d + hV)$

($h$ breaks $\mathbb{Z}_2$ symm. of $H_d$)

e.g. Ising with transverse magnetic field

- Here, the matrices $A$ , $C$ are $(N/2) \times (N/2)$ symmetric matrices sampled from a normalized random matrix ensemble with measure

$$\mu(M) = \exp\left(-\frac{\tilde{\beta}N}{4}\mathrm{tr}\left(M^2\right)\right) \qquad \begin{cases} \tilde{\beta} = 1 \text{ (GOE)} \\ \tilde{\beta} = 2 \text{ (GUE)} \end{cases}$$

- In the GOE case, the $B_{ij}$ are real numbers drawn from a normal distribution with zero mean and variance $1/N$.
- In the GUE case, the $B_{ij}$ are complex numbers $x_{ij} + iy_{ij}$ , where both $x_{ij}$ and $y_{ij}$ are independently drawn from a normal distribution with zero mean and variance $1/(2N)$.

# Random Matrix Quenches



This quench protocol provides a way to study the evolution of states that are not directly constructed from the eigenstates of the evolving Hamiltonian. Time evolution is implemented by the **post-quench** Hamiltonian $H$

$H_0|n_0\rangle = E_n^0|n_0\rangle$ Pre-quench $t<0$ $t=0$ $t>0$ Post-quench $t$ $H|n\rangle = E_n|n\rangle$

$$\left.\begin{matrix}\text{GOE } (\tilde\beta = 1)\\ \text{GUE } (\tilde\beta = 2)\end{matrix}\right\} \ni H_0 := H_r(-1) = \begin{pmatrix} A & -B \\ -B^T & C \end{pmatrix}$$

Sudden quench

$$H := H_r(1) = \begin{pmatrix} A & B \\ B^T & C \end{pmatrix} \in \left\{\begin{matrix}\text{GOE } (\tilde\beta = 1)\\ \text{GUE } (\tilde\beta = 2)\end{matrix}\right.$$

# Random Matrix Quenches



This quench protocol provides a way to study the evolution of states that are not directly constructed from the eigenstates of the evolving Hamiltonian. Time evolution is implemented by the **post-quench** Hamiltonian $H$

$H_0 | n_0 \rangle = E_n^0 | n_0 \rangle$ Pre-quench $t < 0$ $t = 0$ $t > 0$ Post-quench $H | n \rangle = E_n | n \rangle$ $t$

$$\left.\begin{matrix} \text{GOE } (\tilde{\beta} = 1) \\ \text{GUE } (\tilde{\beta} = 2) \end{matrix}\right\} \ni H_0 := H_r(-1) = \begin{pmatrix} A & -B \\ -B^T & C \end{pmatrix} \quad \boxed{\text{Sudden quench}} \quad H := H_r(1) = \begin{pmatrix} A & B \\ B^T & C \end{pmatrix} \in \left\{\begin{matrix} \text{GOE } (\tilde{\beta} = 1) \\ \text{GUE } (\tilde{\beta} = 2) \end{matrix}\right.$$

The eigenstates of the pre-and post-quench Hamiltonians are completely random with respect to each other, as can be verified by computing the inverse participation ratio IPR($|n\rangle$),

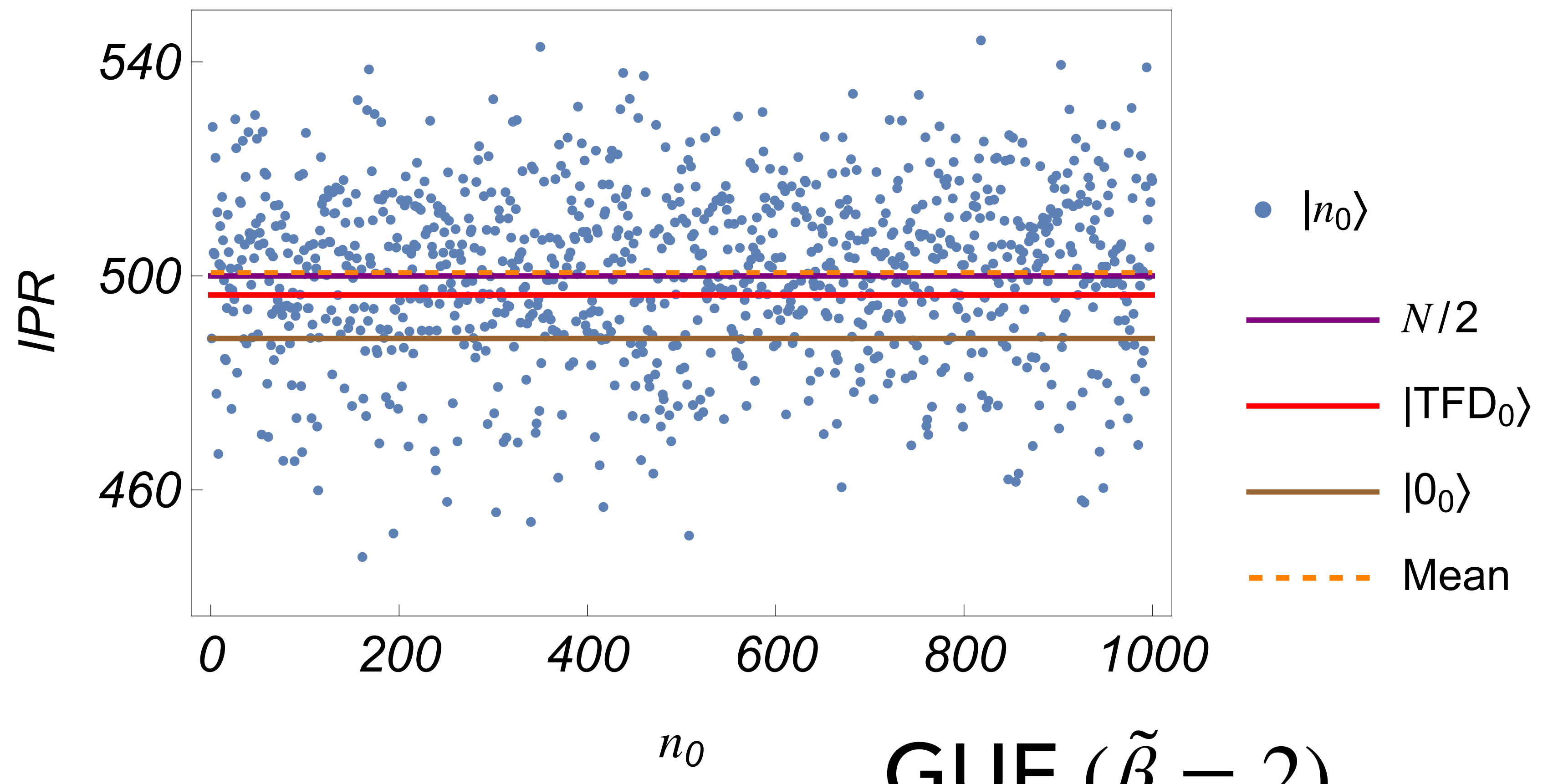


GUE ($\tilde{\beta} = 2$)

$$\text{IPR}(|\psi_0\rangle) := \frac{1}{\sum_{n \geq 0} |\langle n | \psi_0 \rangle|^4}$$

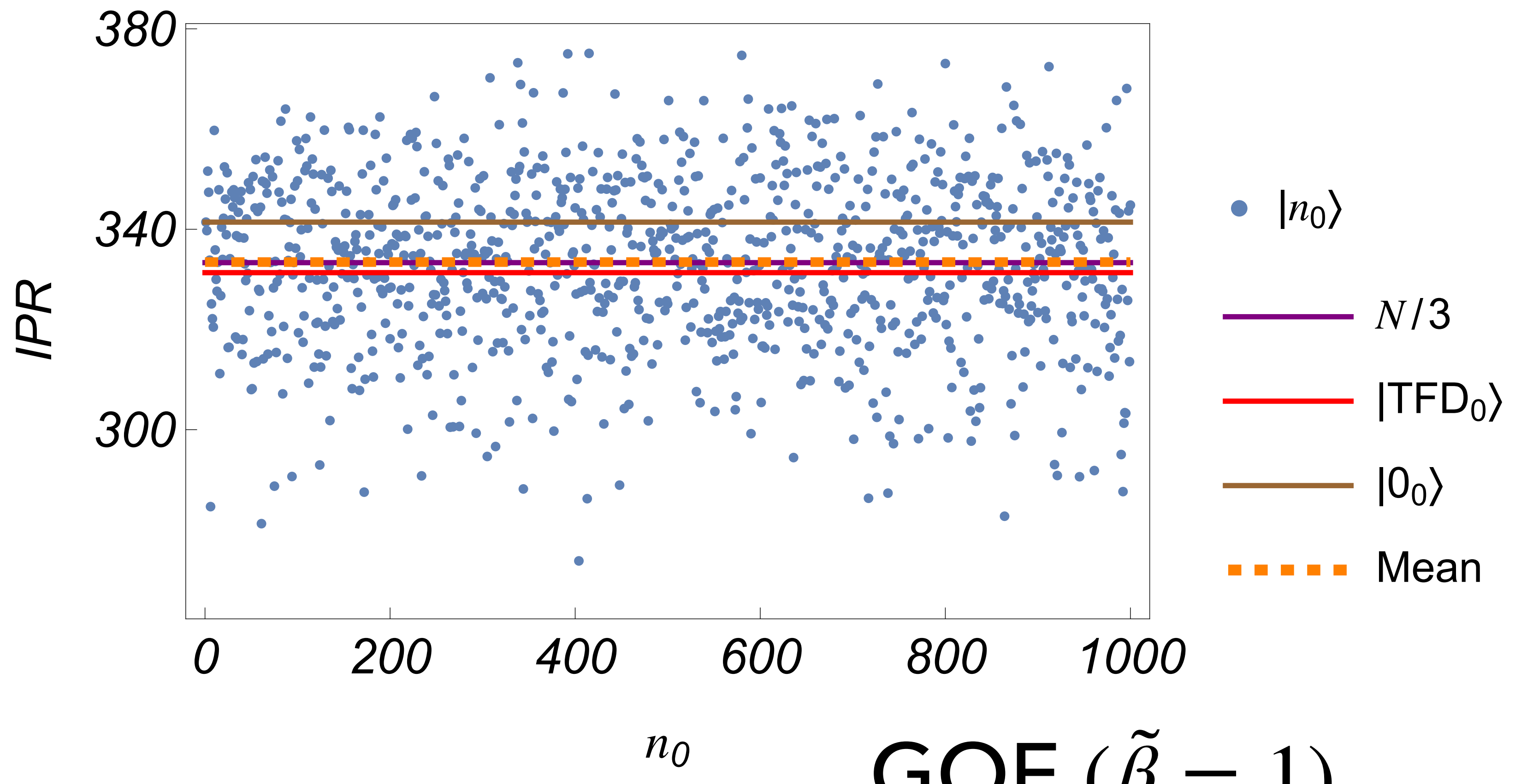


GOE ($\tilde{\beta} = 1$)

# GOE Random Matrix Quenches



Our goal is to study the evolution of the generalized spread complexities in such a protocol for different choices of the initial state: pre-quench $|\mathrm{TFD}_0\rangle$, pre-quench ground state $|0_0\rangle$ and post-quench $|\mathrm{TFD}\rangle$.

$|\mathrm{TFD}\rangle$

$|\mathrm{TFD}_0\rangle$

$|0_0\rangle$

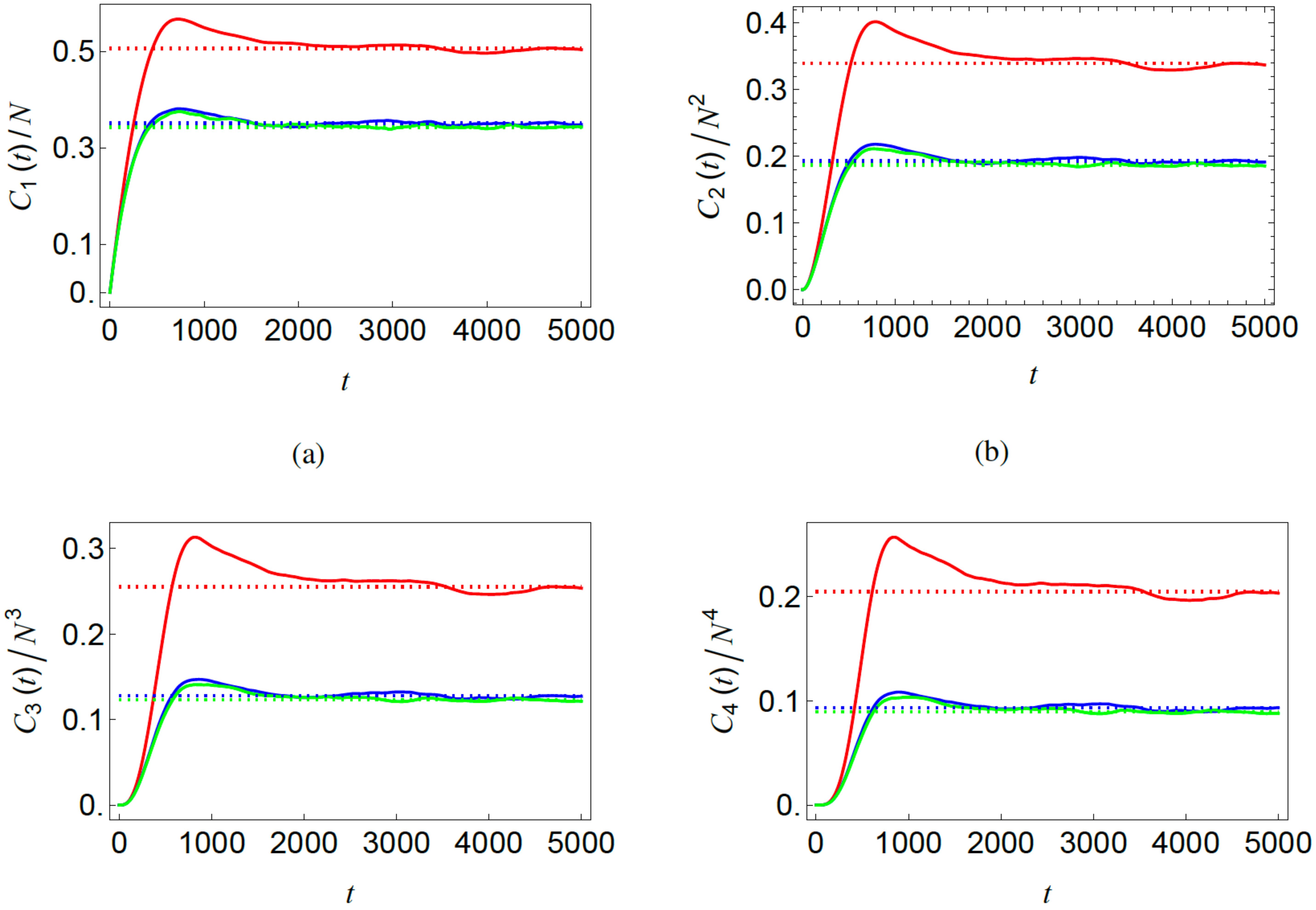


(Average over 4 realizations of $H_r(\pm 1)$ with $\tilde{\beta} = 1$ and $N = 1000$)

# GUE Random Matrix Quenches



Same situation for GUE:

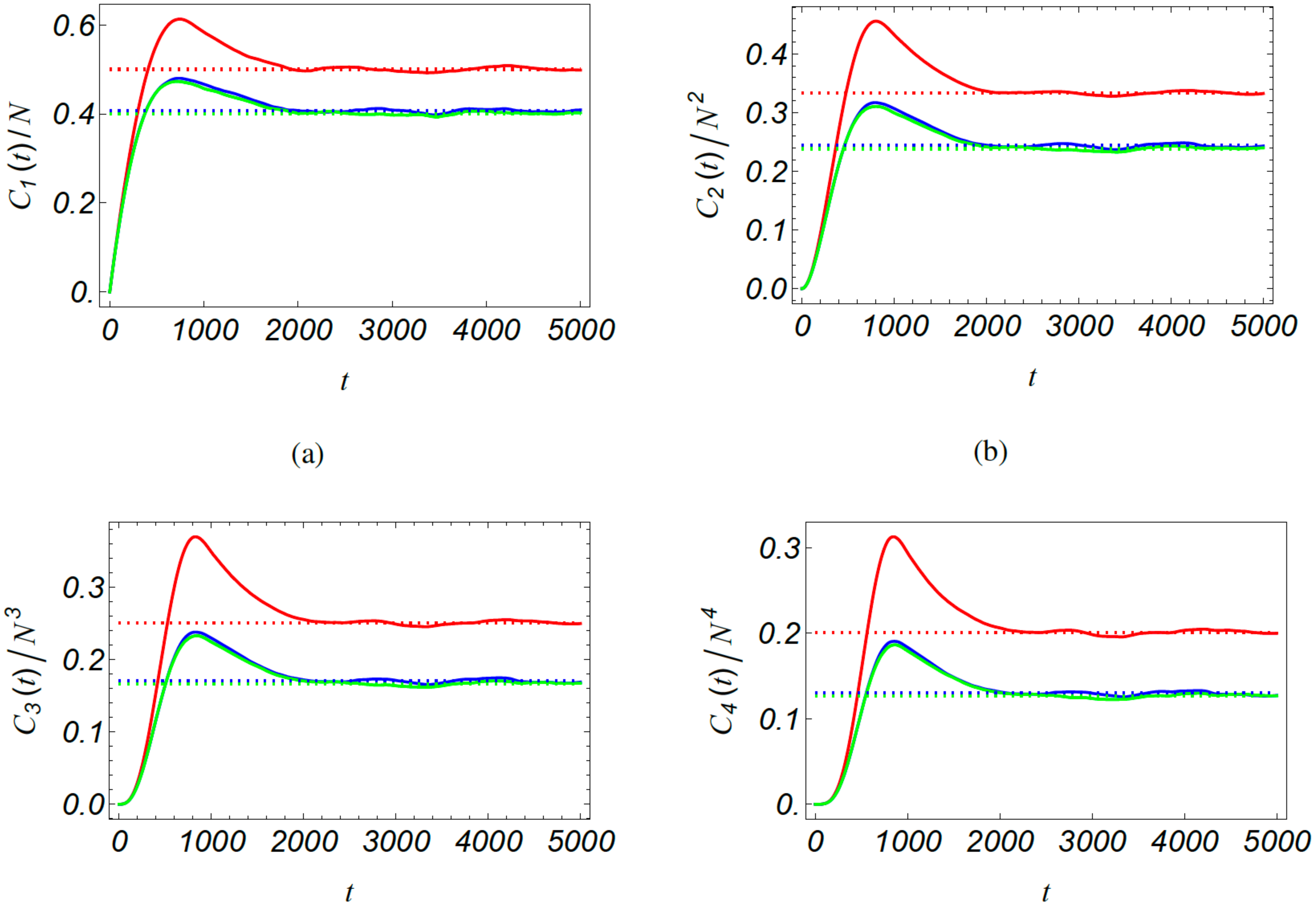


$|\text{TFD}\rangle$
$|\text{TFD}_0\rangle$
$|0_0\rangle$

(Average over 4 realizations of $H_r(\pm 1)$ with $\tilde{\beta} = 2$ and $N = 1000$)

# Summary

- Chaotic quantum many-body systems have Lanczos sequences with asymptotic linear growth. The converse is not true: $\boxed{b_n \sim \alpha n \not\Rightarrow \text{Chaos}}$ . Linear growth in QFTs is expected from poles of $\Pi^W(t)$. IR cutoffs in the power spectrum generate staggering in the Lanczos sequence. This also leaves an imprint in the behavior of Krylov complexity, with subleading effects in its late-time asymptotic growth rate. **The generalized chaos bound is satisfied:** $\boxed{\lambda_K \leq 2\pi/\beta}$.

- In chaotic quantum billiards, the growth rate of the Lanczos coefficients $\alpha$ is bounded by $\pi/\beta$ and this inequality is **saturated** at small temperatures. At the same time, the Lanczos coefficients for integrable billiards show a larger variance compared to its chaotic counterparts. Example of variance of $b_n$ as a probe of chaotic behavior. ([Hashimoto, Murata, Tanahashi, Watanabe (2023)], [Balasubramanian, Nath Das, Ermdenger Xian (2024)])

- Spread complexity has a characteristic feature in spin chains at their chaotic point: a *clear* **peak** occurring slightly before the plateau time of the SFF: $\boxed{t_{peak} \lesssim t_{plateau}}$. The peak seems to arise from **spectral rigidity**.

- Generalized spread complexities are complexity measures that arise naturally from higher-moments in the operator statistics of the spreading operator. These are more **sensitive** to features in chaotic systems such as the **peak** before the saturation.

# Open Questions and Future Directions

- Recent efforts have **matched** the wormhole (Einstein-Rosen bridge) length in Jackiw-Teitelboim (JT) gravity, with the spread complexity of chord states in the triple-scaling limit of the double-scaled Sachdev-Ye-Kitaev (DSSYK) model ([Rabinovici et al. (2023)]). Very recently (03.12.24) [Balasubramanian et al. (2024)], the late-time saturation of spread complexity was studied in this same context. Do other holographic complexity proposals correspond to different generalizations of spread complexity?

- Another defining feature of holographic (and computational) complexity is the switchback effect. Are Krylov/ spread complexity sensitive to this phenomenon?

# Open Questions and Future Directions

- Recent efforts have **matched** the wormhole (Einstein-Rosen bridge) length in Jackiw-Teitelboim (JT) gravity, with the spread complexity of chord states in the triple-scaling limit of the double-scaled Sachdev-Ye-Kitaev (DSSYK) model ([Rabinovici et al. (2023)]). Very recently (03.12.24) [Balasubramanian et al. (2024)], the late-time saturation of spread complexity was studied in this same context. Do other holographic complexity proposals correspond to different generalizations of spread complexity?

- Another defining feature of holographic (and computational) complexity is the switchback effect. Are Krylov/spread complexity sensitive to this phenomenon?

- "Krylov/spread complexity is not a measure of distance between operators/states" [Aguilar-Gutierrez, Rolph (2023)]. Yet, the time average of spread complexity is related to an upper bound on Nielsen complexity [Craps, Evnin, Pascuzzi (2023)]. What is the precise connection between spread complexity and other measures of quantum complexity?

- To better understand thermalization and its avoidance (e.g. MBL) in isolated quantum systems we may need to refine our working definition of quantum chaos. "Scrambling is necessary but not sufficient for chaos" [Dowling, Kos, Modi (2023)]. What about the initial state/operator dependence? An interplay of quantum versions of ergodic hierarchies [Gesteau (2023), Ouseph et al. (2023)], free probability theory [Voiculescu (1985)] and Krylov subspace methods could open the way to understand these questions.

Thank you!

# Additional Slides

# Smooth UV Cutoffs in free QFTs

Another way of modifying the UV physics of the theory is by introducing a “smooth cutoff” in the power spectrum by hand. As an example, consider the conformal limit $m \to 0$ in $d = 4$

$$f^W(\omega) = N(\beta, \Lambda, \delta) \left| \frac{\omega}{\sinh(\beta\omega/2)} \right| e^{-|\omega/\Lambda|^{1/\delta}} \Theta(\Lambda - |\omega|)$$

$\beta b_n$ $\quad (\beta = 1, \beta\Lambda = 40)$

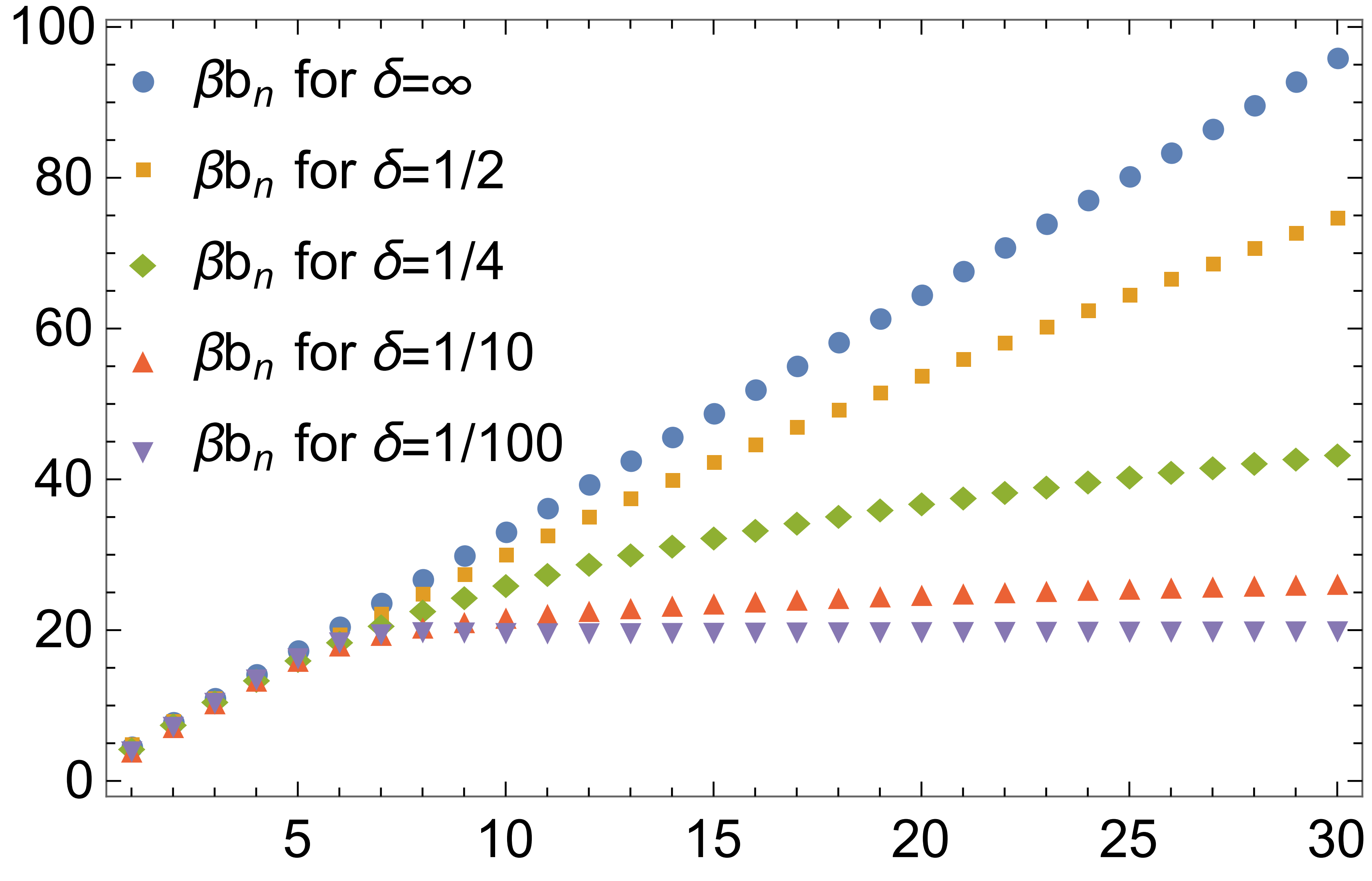

$n$

$$\delta = \begin{cases} \infty & \text{(Wightman power spectrum)} \\ 0 & \text{("Hard" UV cutoff)} \end{cases}$$

- The high-frequency tail of the power spectrum determines the asymptotic behavior of Lanczos coefficients.
- The only way to significantly alter the high-frequency tail of the power spectrum is with an exponential correction.

# Spectral Complexity

Spectral Complexity is a spectral quantity (associated with the holographic complexity of the thermofield double (TFD) state) introduced in [Iliesiu, Mezei, Sárosi (2021)]. For quantum systems with a discrete spectrum:

$$\boxed{C_S(t) := \frac{1}{d\,Z(2\beta)} \sum_{\substack{n,m \\ E_n \neq E_m}} \left( \frac{\sin(t(E_n - E_m)/2)}{(E_n - E_m)/2} \right)^2 e^{-\beta(E_n+E_m)}}$$

where $H|n\rangle = E_n|n\rangle$ and $d = \dim(\mathscr{H})$. Spectral complexity is directly related to the Spectral Form Factor (SFF):

$$\frac{\mathrm{d}^2}{\mathrm{d}t^2} C_S(t) = \frac{2Z(\beta)^2}{d\,Z(2\beta)} \mathrm{SFF}(t) - \frac{2}{d}$$

where:

$$\mathrm{SFF}(t) := \frac{|Z(\beta+it)|^2}{|Z(\beta)|^2} = \frac{1}{|Z(\beta)|^2} \sum_{n,m} e^{-\beta(E_n+E_m)} e^{it(E_n-E_m)}$$

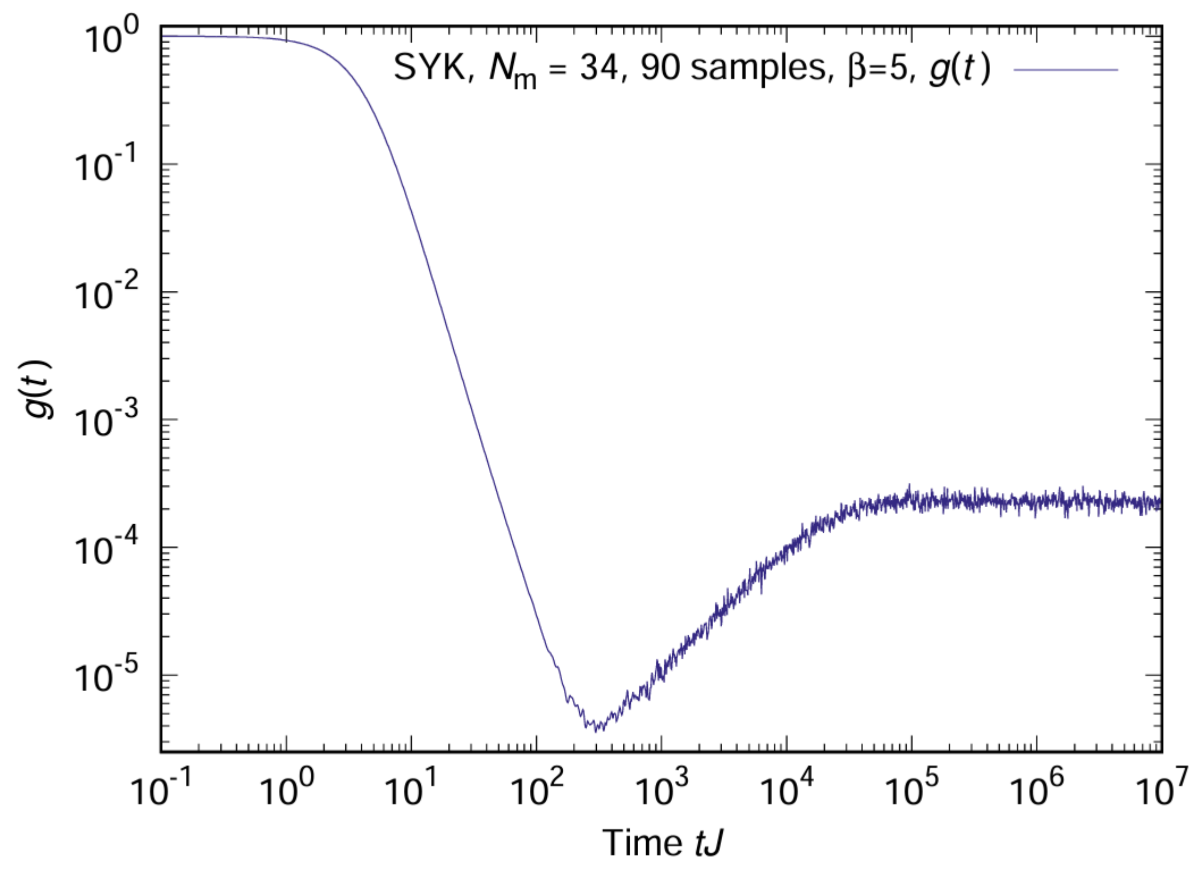


This is easy to see if one notes that $\mathrm{SFF}(t) = \left|\langle \mathrm{TFD}|e^{-i(H\otimes\mathbb{I})t}|\mathrm{TFD}\rangle\right|^2$, where $|\mathrm{TFD}\rangle = \frac{1}{\sqrt{Z(\beta)}} \sum_n e^{-\frac{\beta}{2}E_n}|n\rangle \otimes |n\rangle$.

- Spectral complexity depends only on the spectrum $\{E_n\}$ of the theory.

# Spread and Spectral Complexity in Holography

- Spread Complexity. A measure of *state complexity* introduced in [Balasubramanian et al. (2022)] which was recently shown to **match** the wormhole (Einstein-Rosen bridge) length in Jackiw-Teitelboim (JT) gravity, when computed for chord states in the triple-scaling limit of the double-scaled Sachdev-Ye-Kitaev (DSSYK) model ([Rabinovici et al. (2023)]).

$$\boxed{\lambda \tilde{C}(t) = \frac{\tilde{\ell}(t)}{L_{AdS}}} = 2\log\left(\cosh\left(t\sqrt{\frac{E}{2L_{AdS}\,\phi_b}}\right)\right) - \log\left(\frac{L_{AdS}E\,\phi_b}{2}\right)$$

- Spectral Complexity. Introduced in [Iliesiu, Mezei, Sárosi (2021)] as the holographic dual of the quantum-corrected length of the wormhole in JT gravity. It accounts for its linear growth (for $t \ll e^{S_0}$) and **late-time** ($t \gg e^{S_0}$) **saturation**.

$$\langle \ell(t) \rangle = \begin{cases} C_1 t + \dots & t \ll e^{S_0} \\ \boxed{C_0 - \dots \qquad t \gg e^{S_0}} \end{cases}$$

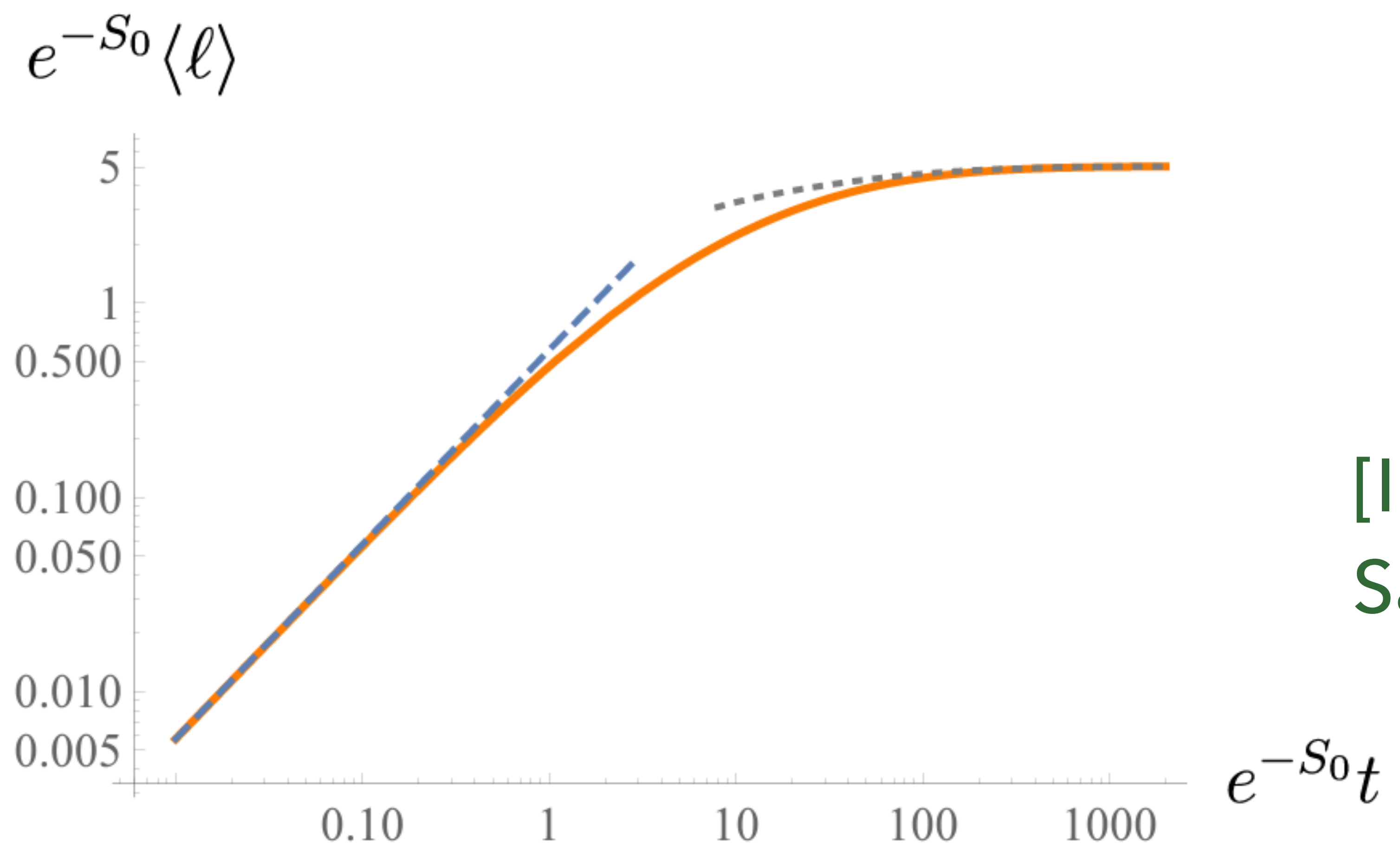


[Iliesiu, Mezei, Sárosi (2021)]

# Models and Characteristic Features

We consider two paradigmatic spin chains: next-to-nearest-neighbour (NNN) deformation of the Heisenberg (XXZ) chain and the mixed-field Ising model:

$$H = H_{XXZ} + H_{NNN} \qquad (J, J_{zz}, J_c) = \begin{cases} (1, 0.5, 1)\,, & \text{(Chaotic case)},\\ (1, 0.5, 0)\,, & \text{(Integrable case)}\,. \end{cases}$$

$$\begin{cases} H_{XXZ} = \displaystyle\sum_{i=1}^{N-1} J\,(S_i^x S_{i+1}^x + S_i^y S_{i+1}^y) + J_{zz} S_i^z S_{i+1}^z \\ H_{NNN} = \displaystyle\sum_{i=1}^{N-2} J_c S_i^z S_{i+2}^z \end{cases}$$

$$H_I = \sum_{i=1}^{N-1} S_i^z S_{i+1}^z + \sum_{i=1}^{N} \left(h_x S_i^x + h_z S_i^z\right)$$

$$(h_x, h_z) = \begin{cases} (1.05, -0.5)\,, & \text{(Chaotic case)}\\ (1, 0)\,. & \text{(Integrable case)} \end{cases}$$

- Spread Complexity (TFD state)
- Spectral Complexity

- mixed-field Ising

($N = 12$ sites, $\beta = 0$, for the even parity sector)

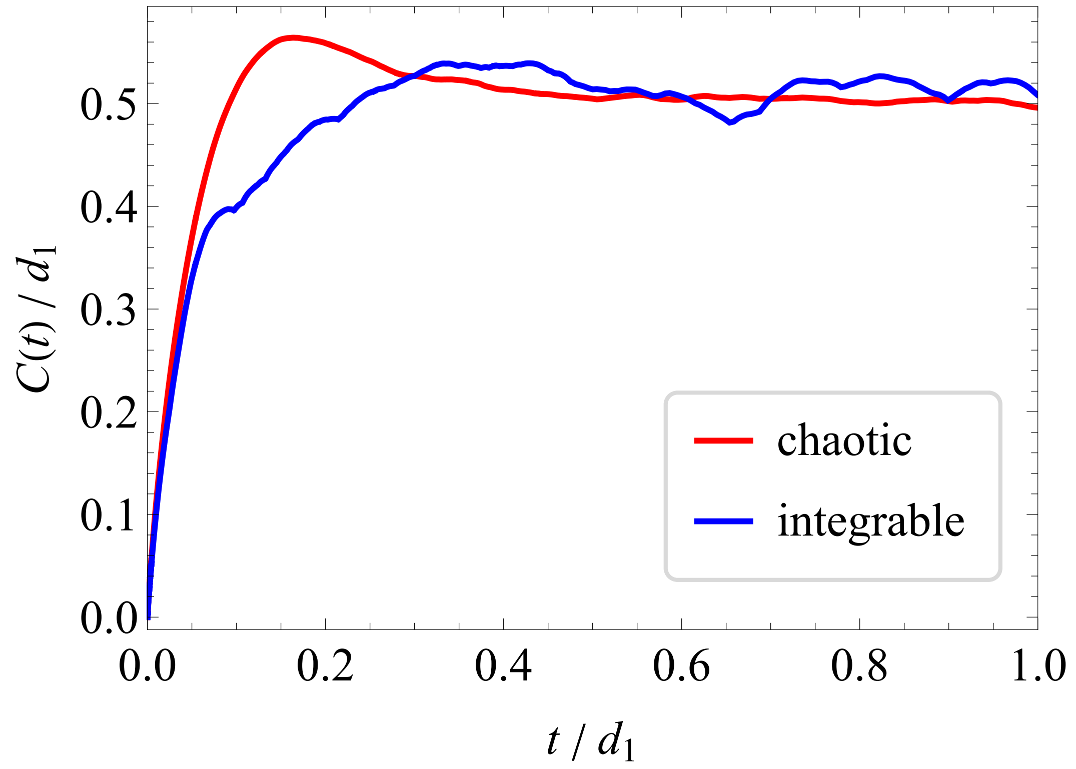


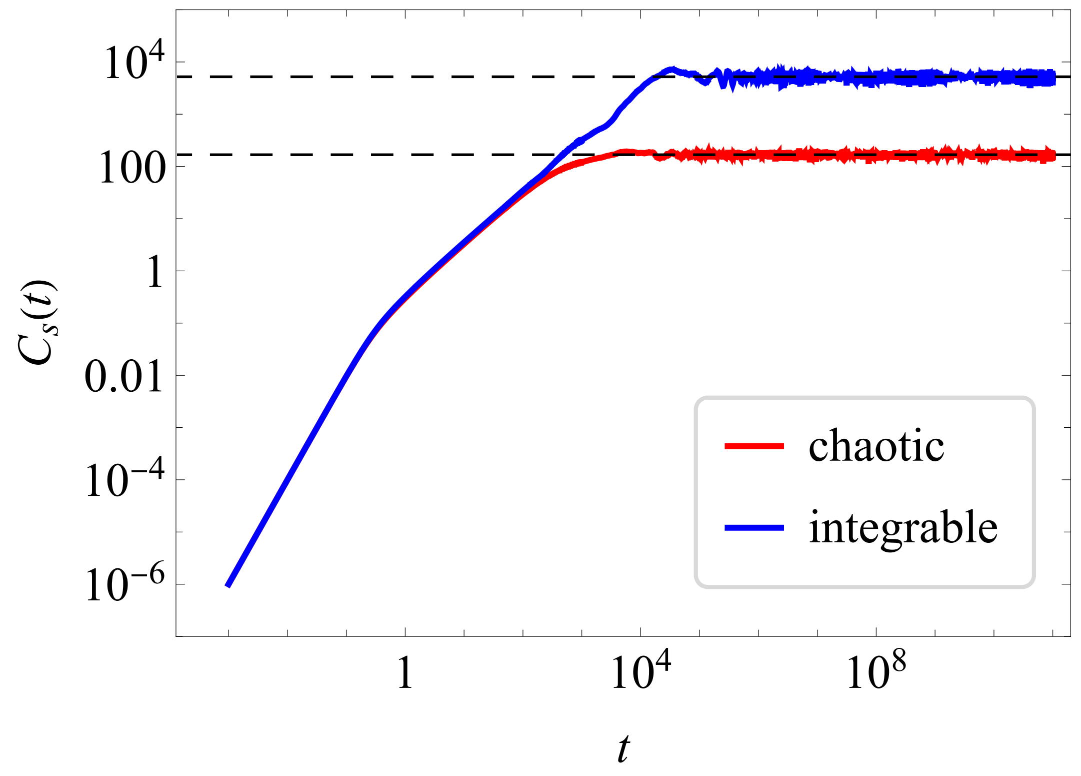


- NNN deformation of XXZ

($N = 15$ sites, $\beta = 0$ , for the even parity sector and total spin in the z-direction

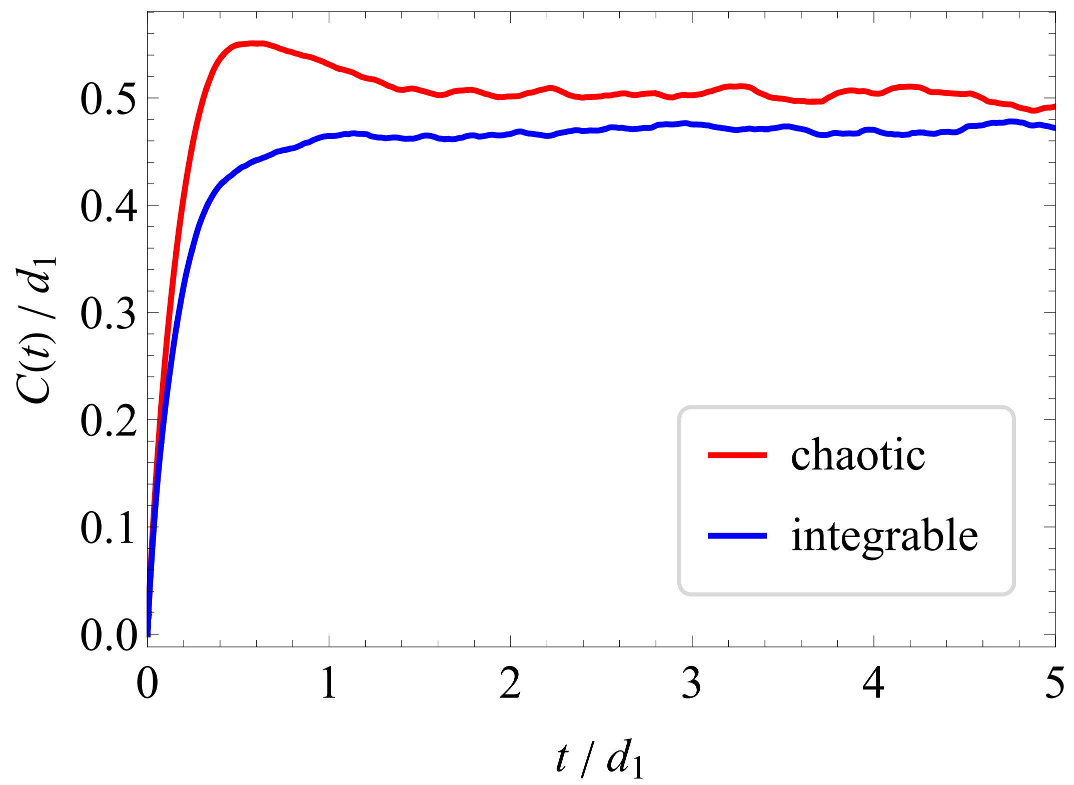


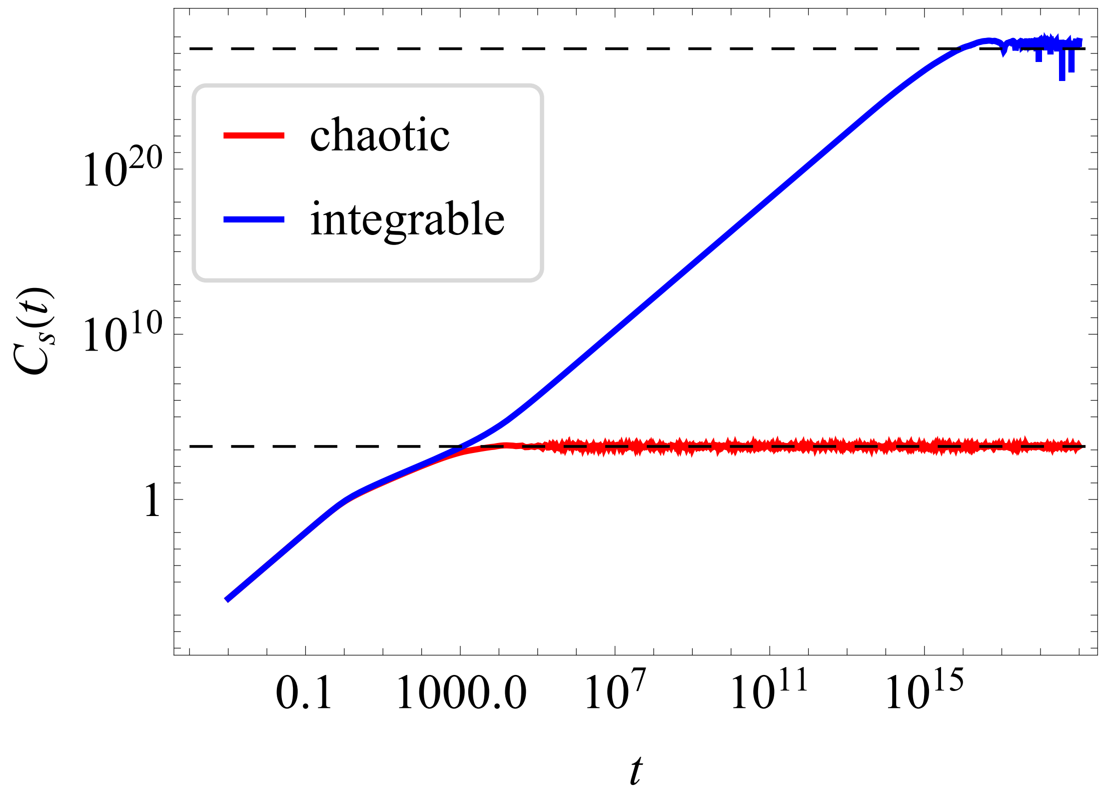

# Comparing Timescales

The physics behind the dynamical behavior of spread and spectral complexity can be understood by comparing them with the typical timescales in the SFF. The following are log-scale plots for the even-parity sector of the mixed-field Ising in the **chaotic phase** for $N = 12$ and $\beta = 0$:

Spread

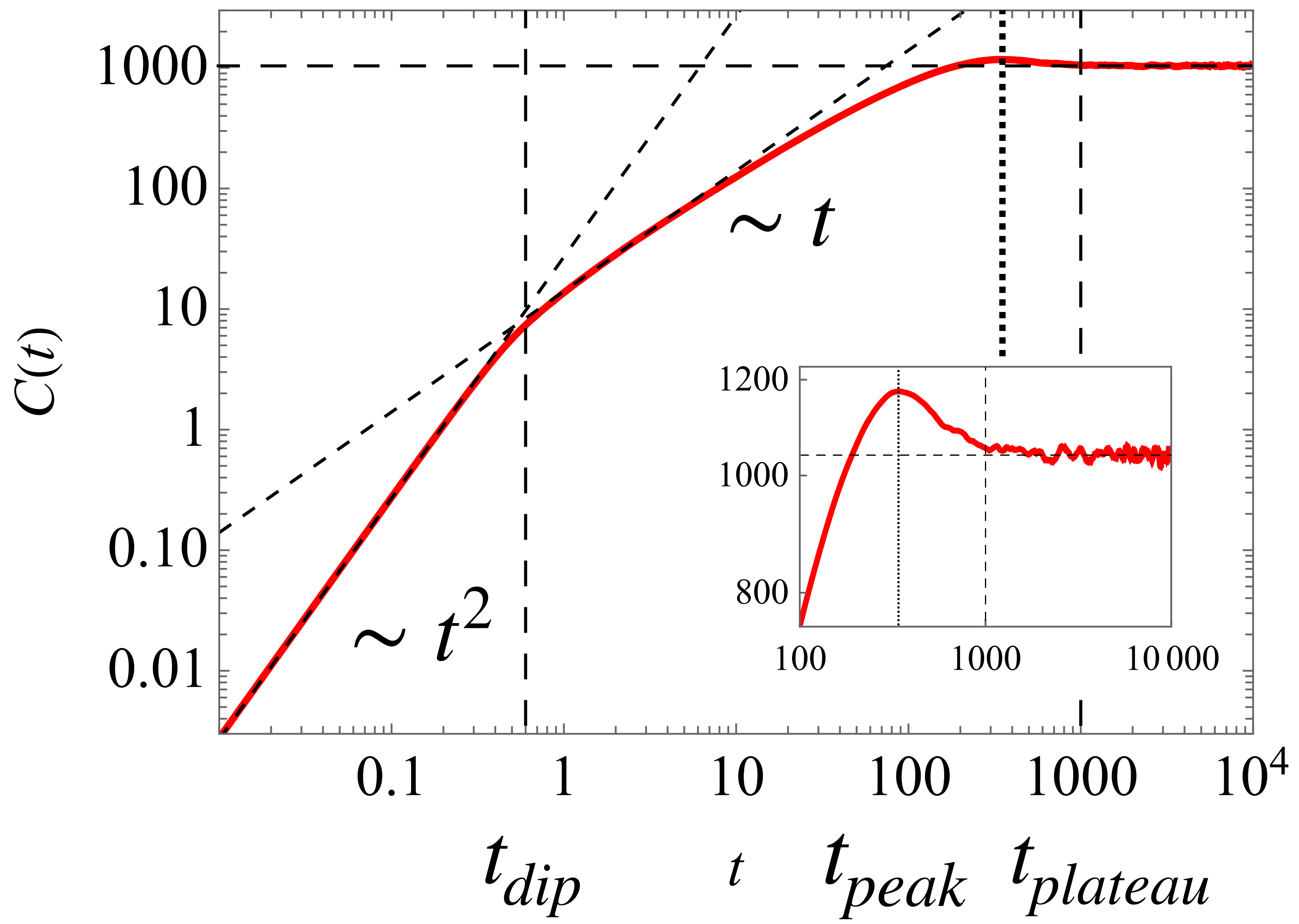


SFF

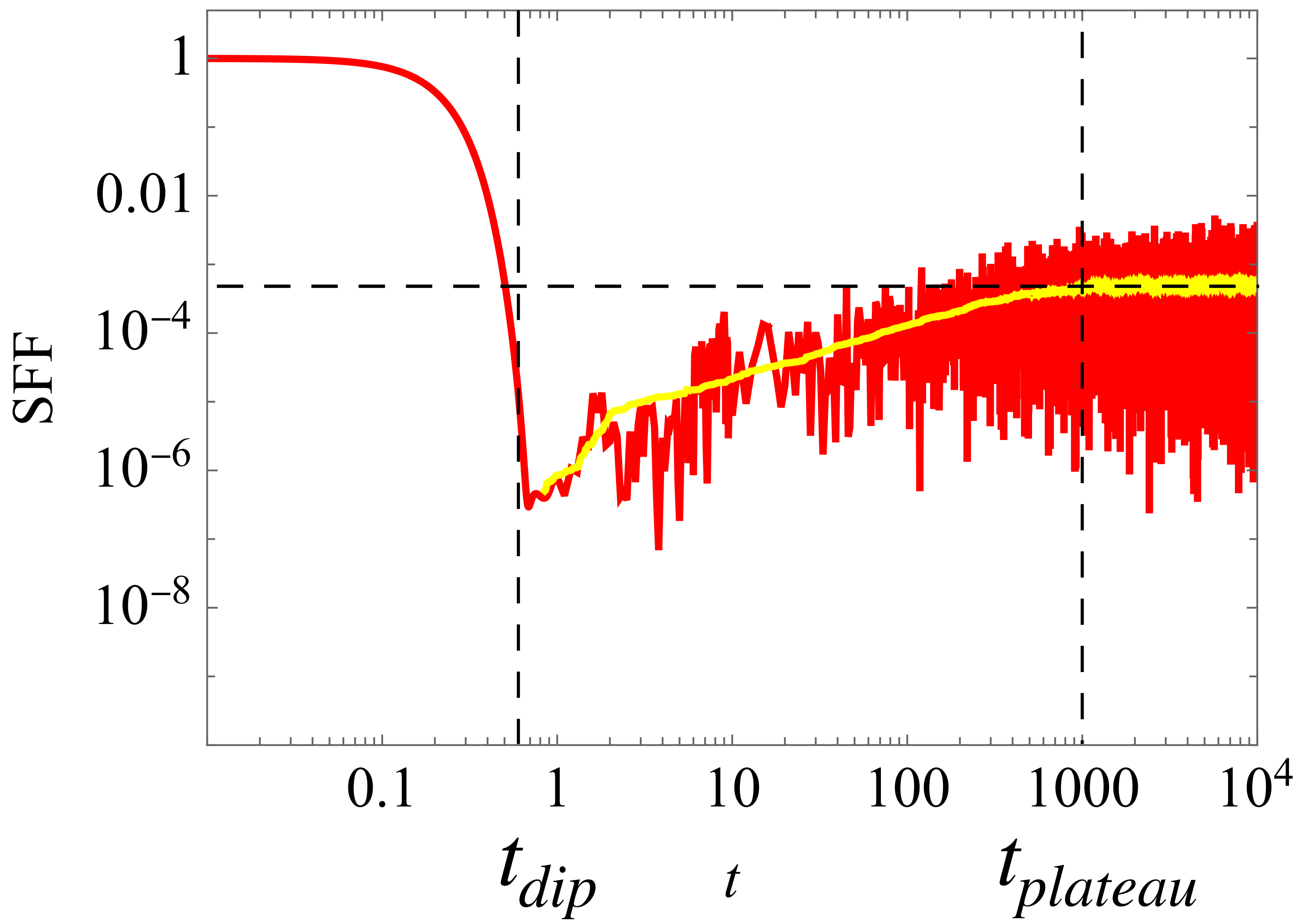


Spectral

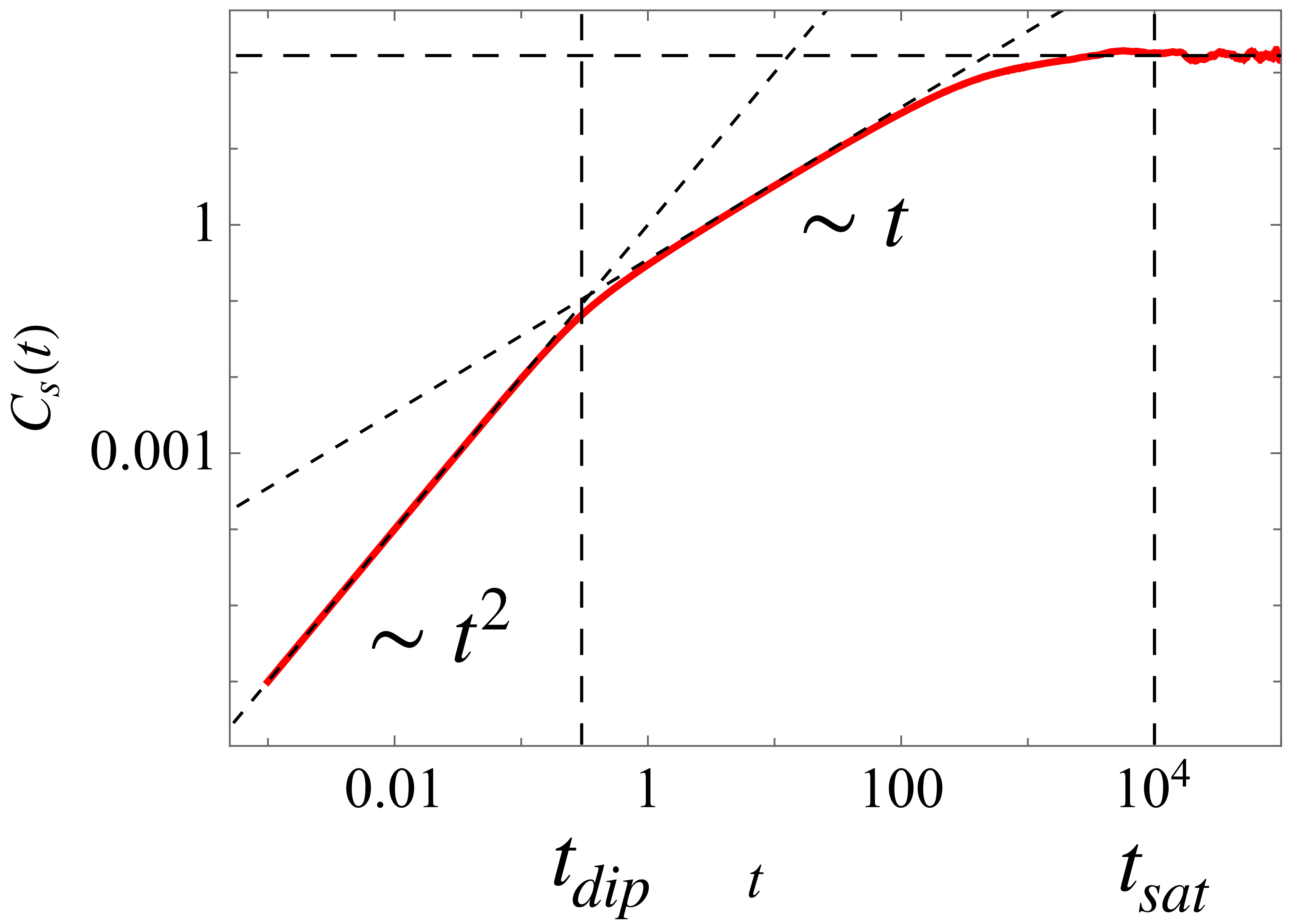


where: $t_{dip} \sim \mathcal{O}(1)$ , $t_{plateau} \sim \mathcal{O}(d)$ , $t_{sat} \sim \mathcal{O}(d^b)$ $(1 < b < 2)$ and $\boxed{t_{dip} < t_{peak} \lesssim t_{plateau} < t_{sat}}$ .

(c.f. RMTs where $t_{dip} \sim \mathcal{O}(\sqrt{d})$ )

# Saturation of Spectral Complexity: Lessons from RMTs

The long-time average of spectral complexity contains contributions from $(E_n - E_m)^{-2}$, so the term with the smallest energy difference contributes dominantly to its saturation value.

To understand the better understand the saturation timescale of spectral complexity, we consider the (average of the) **minimum energy difference** $\overline{\Delta E_{min}}$ in RMTs as a function of the matrix size $d$:

$$\overline{\Delta E_{min}} = \frac{1}{\mathcal{N}} \sum_{i=1}^{\mathcal{N}} \Delta E_{min}^{(i)}$$

Generating $\mathcal{N}$ sets of $d$ energy eigenvalues, $\Delta E_{min}^{(i)}$ is the minimum energy difference in the $i$-th set.

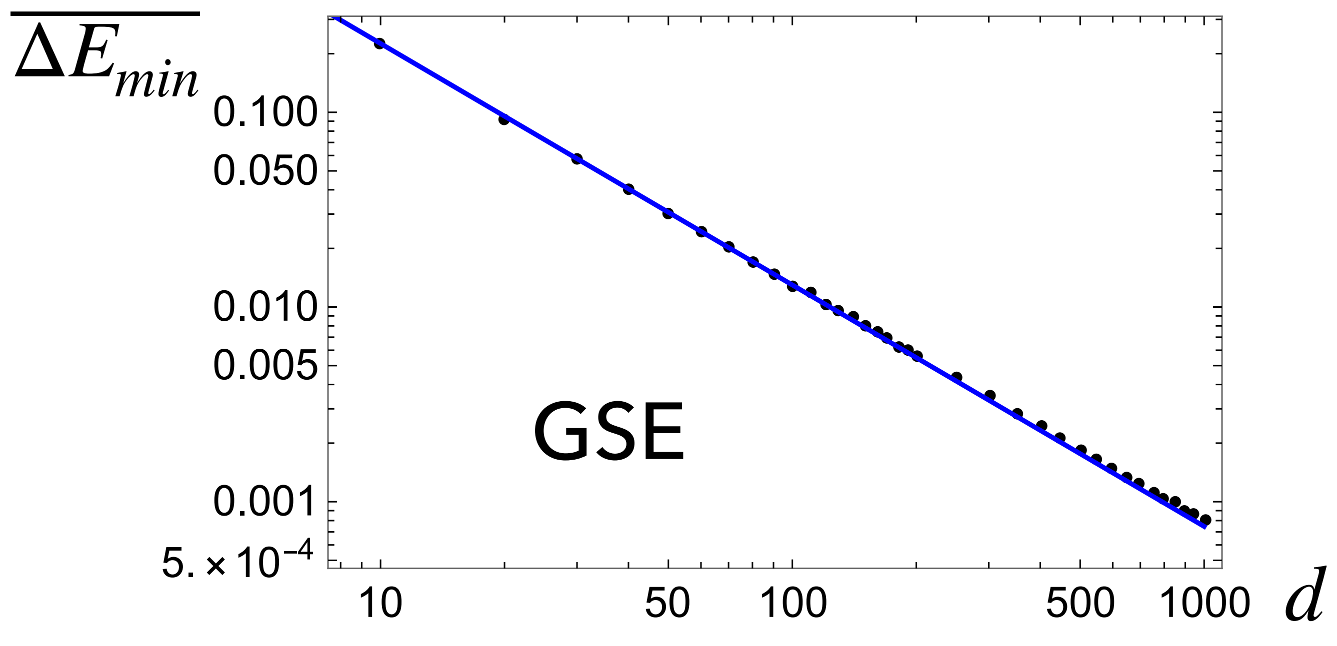


$\overline{\Delta E_{min}} = 3.92\, d^{-1.24}$ (GSE)

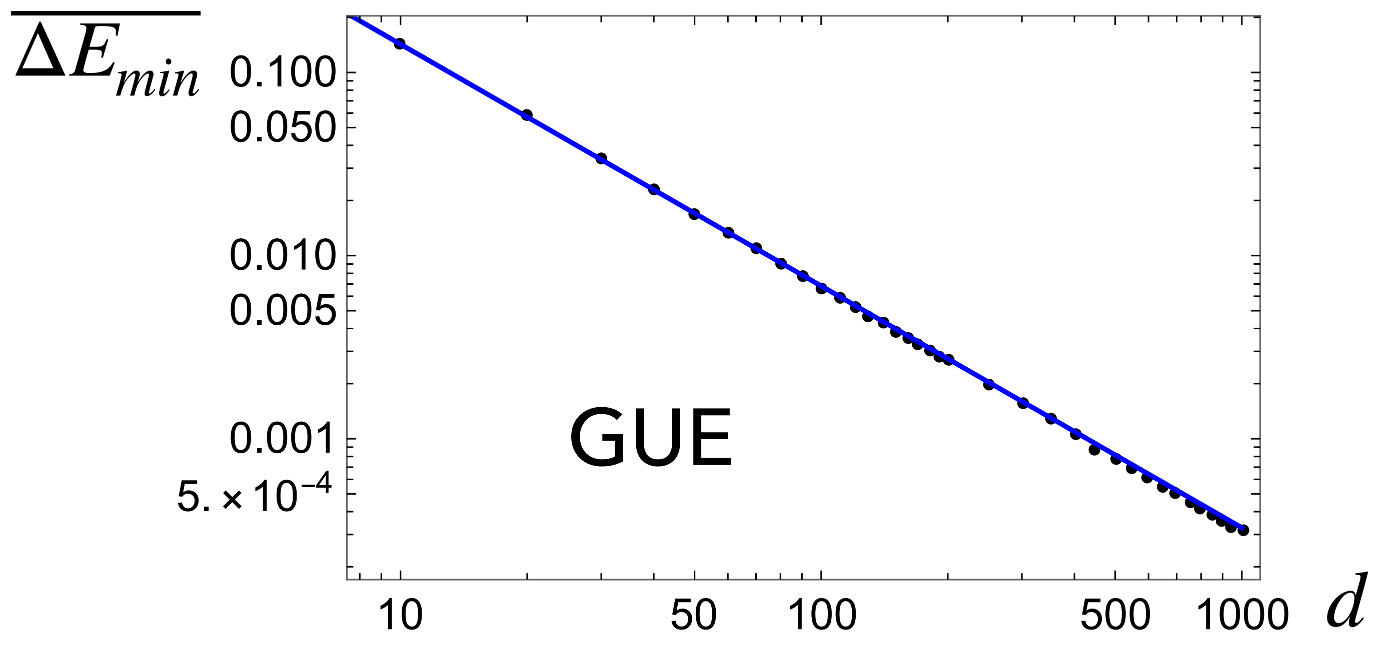


$\overline{\Delta E_{min}} = 2.98\, d^{-1.32}$ (GUE)

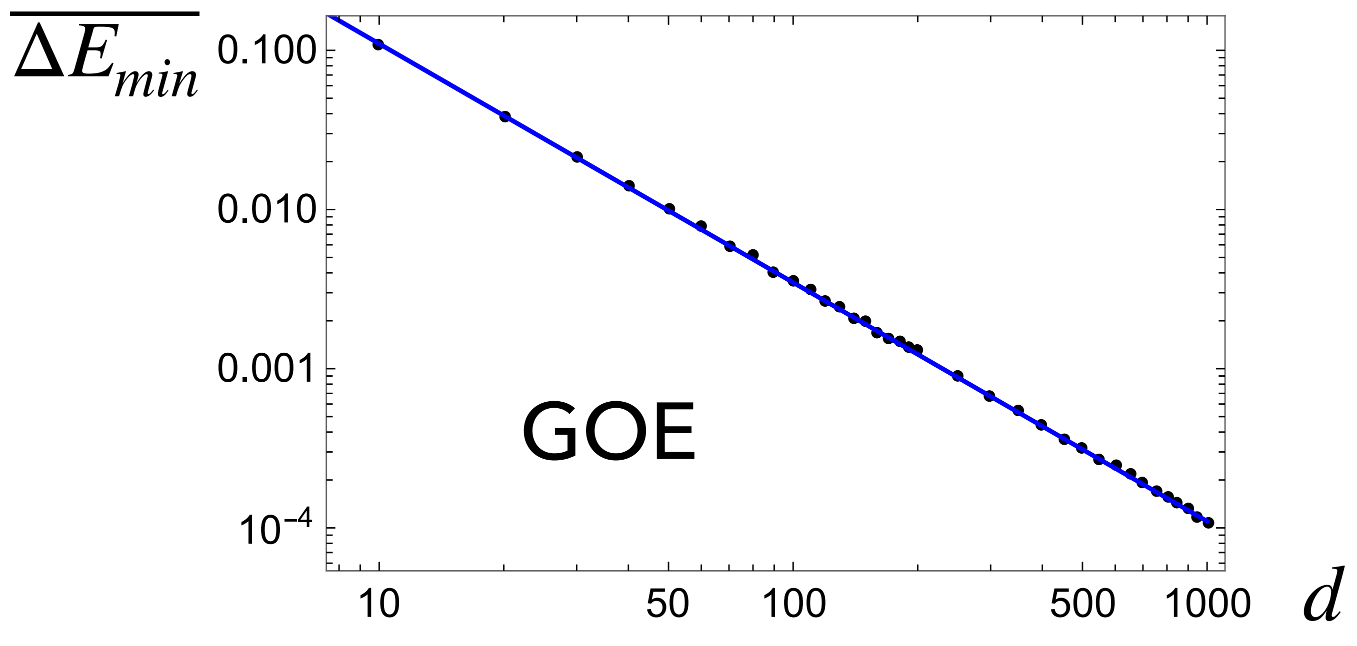


$\overline{\Delta E_{min}} = 3.48\, d^{-1.50}$ (GOE)

In the mixed-field Ising we find a similar power-law behavior of the minimum energy difference as a function of the matrix size with $\Delta E_{min} = 0.65\, d^{-1.40}$ (even parity sector) and $\Delta E_{min} = 1.78\, d^{-1.57}$ (odd parity sector).

# Spectral complexity in Quantum Billiards

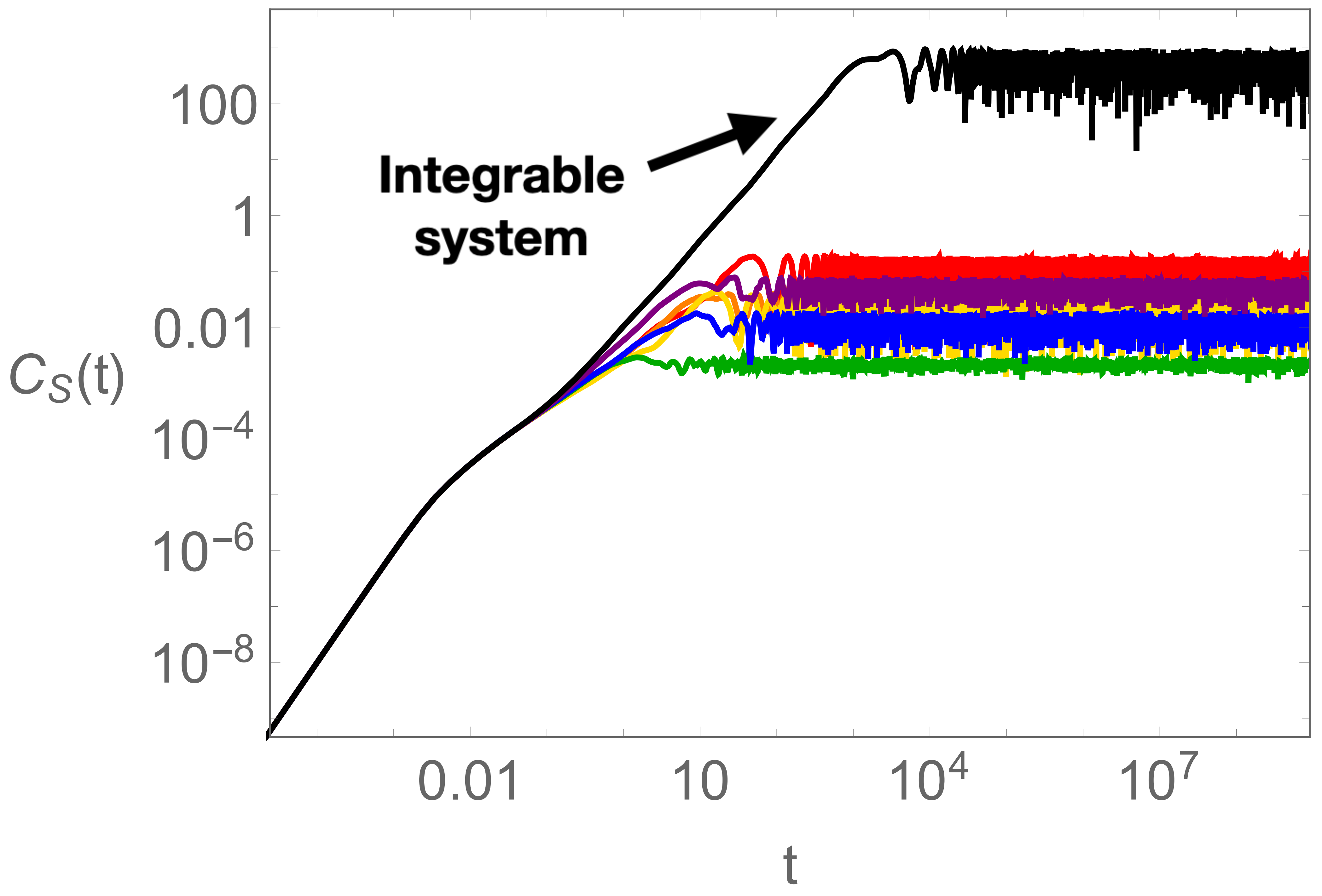


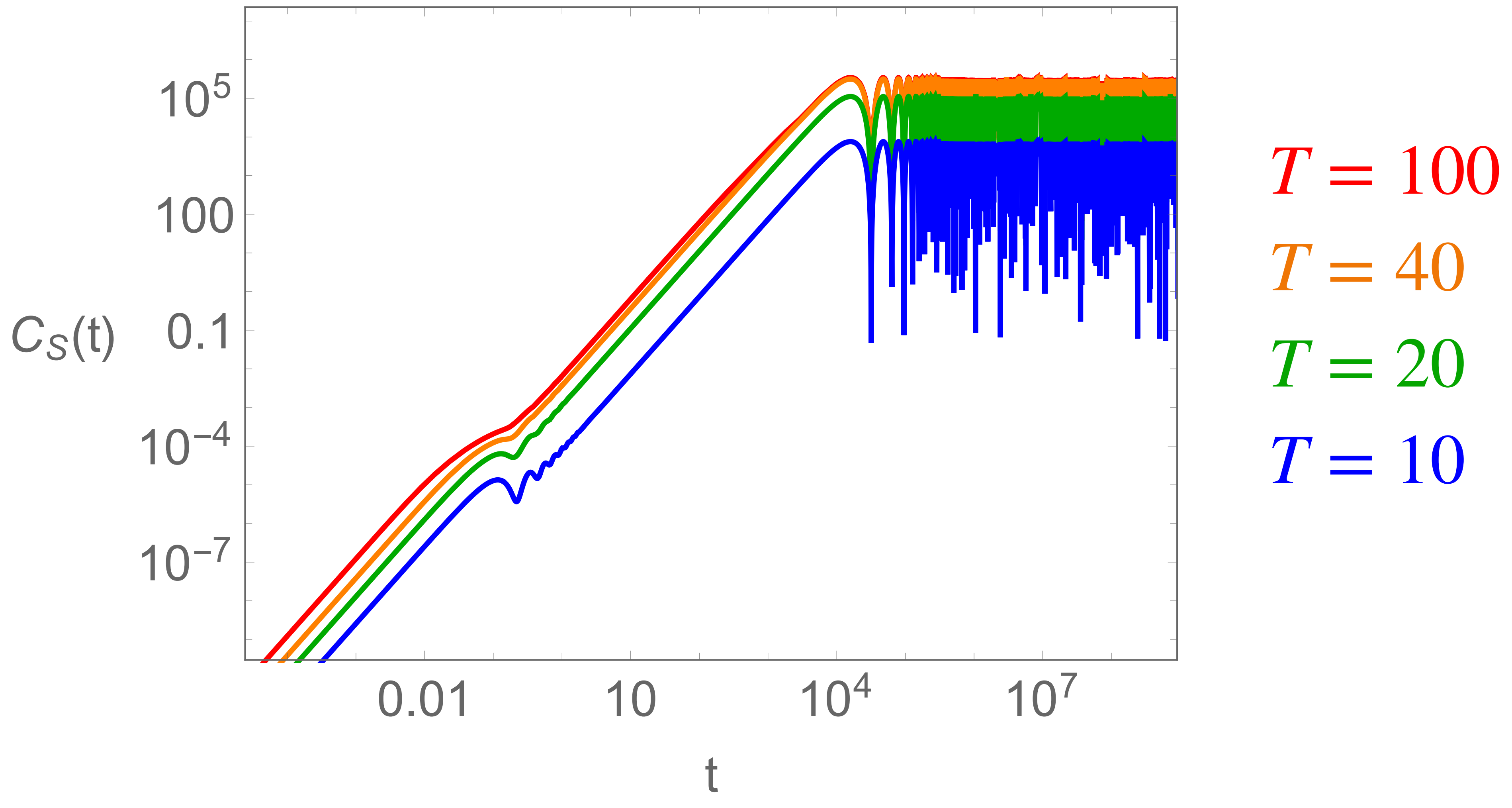


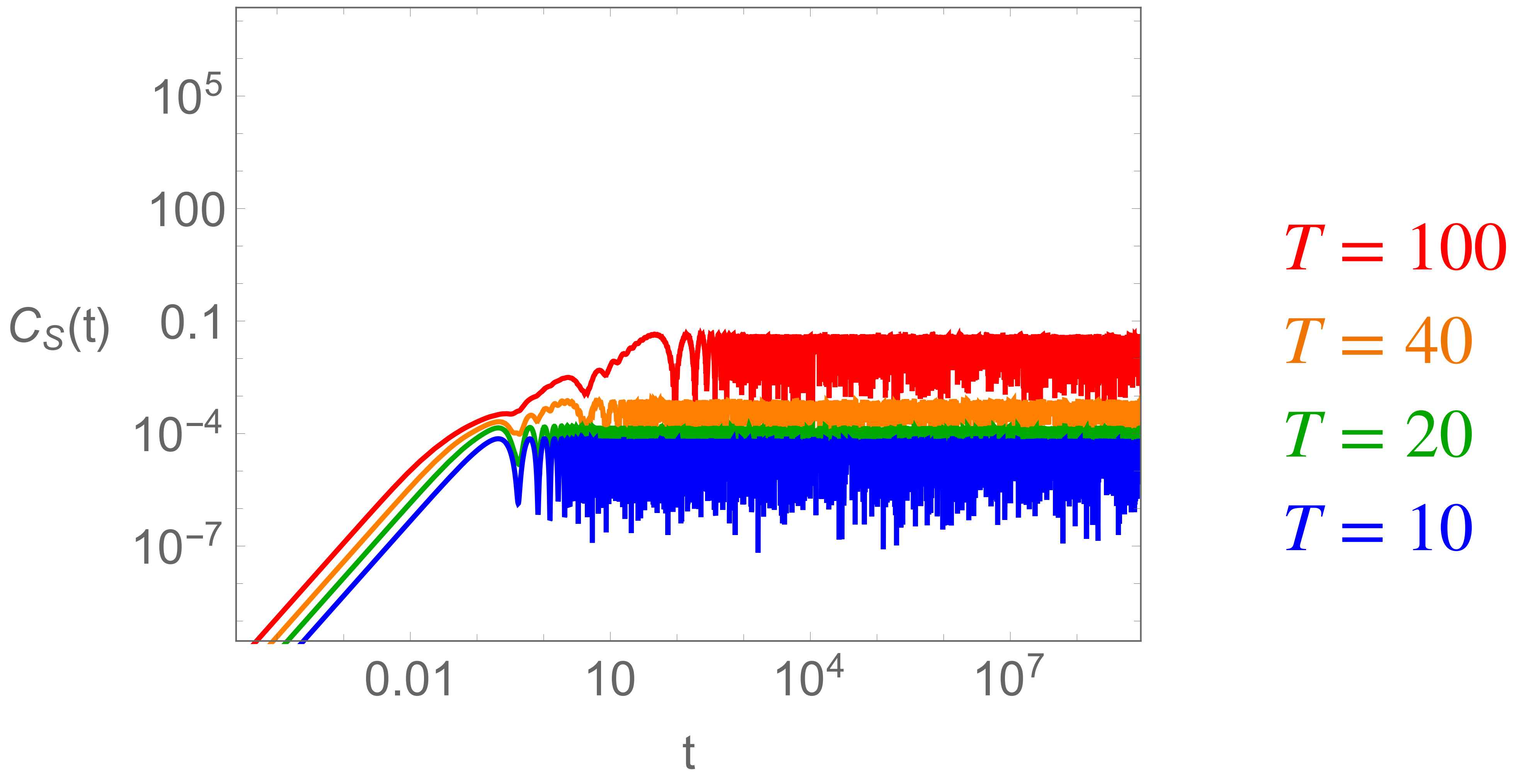

# Summary of Comparison



- Spread and spectral complexity have characteristic features in chaotic quantum many-body systems: a *clear* **peak** in spread complexity and a **saturation** timescale of spectral complexity governed by $\Delta E_{min}$ .

- The early time behavior of both spread and spectral complexity is quadratic ( $\sim t^2$) and they are connected by a form of the Ehrenfest theorem in Krylov space [Erdmenger, Jian, Xian (2023)], but differ at later timescales. In particular, they **saturate** at different timescales.

- The peak in spread complexity occurs slightly before the plateau time of the SFF. It appears to be governed by similar physics as the ramp in the SFF.

- The saturation value and timescale of spread complexity do not seem to be a good indicator of quantum chaos, since these are comparable with their integrable counterparts. (c.f. Krylov operator complexity).

- The saturation value and timescale of spectral complexity are determined by energy level-repulsion.

- The dip time in our SFF differs form the one for RMTs. A possible explanation is the difference in density of states between RMTs (Wigner semi-circle) and spin chains (Gaussian-like).

# Spread and spectral complexity in Chains

Consider the previously-mentioned **spin chains** that have a well-studied transition from integrability to chaos according to their energy-level statistics.

In the chaotic regime, such characteristic features are:

1) A *clear* **peak** in spread complexity occurring at a timescale $d^{1/2} < t_{\text{peak}} \lesssim d$ , where $d = \dim(\mathscr{H})$.

2) A **saturation** of spectral complexity occurring at a timescale of $t_{\text{sat}} \sim d^b$ governed by the minimum energy difference in the theory's spectrum, where $2 > b > 1$ is a number. (Note that $t_{\text{sat}} \sim e^{bS}$ if we identity $S = \log(d)$.)

# Is it important to take symmetry into account?

The following are plots for the energy-level statistics for the mixed-field Ising for $N = 12$ and $\beta = 0$, in the without block-diagonalizing the Hamiltonian by parity (even vs odd sectors):

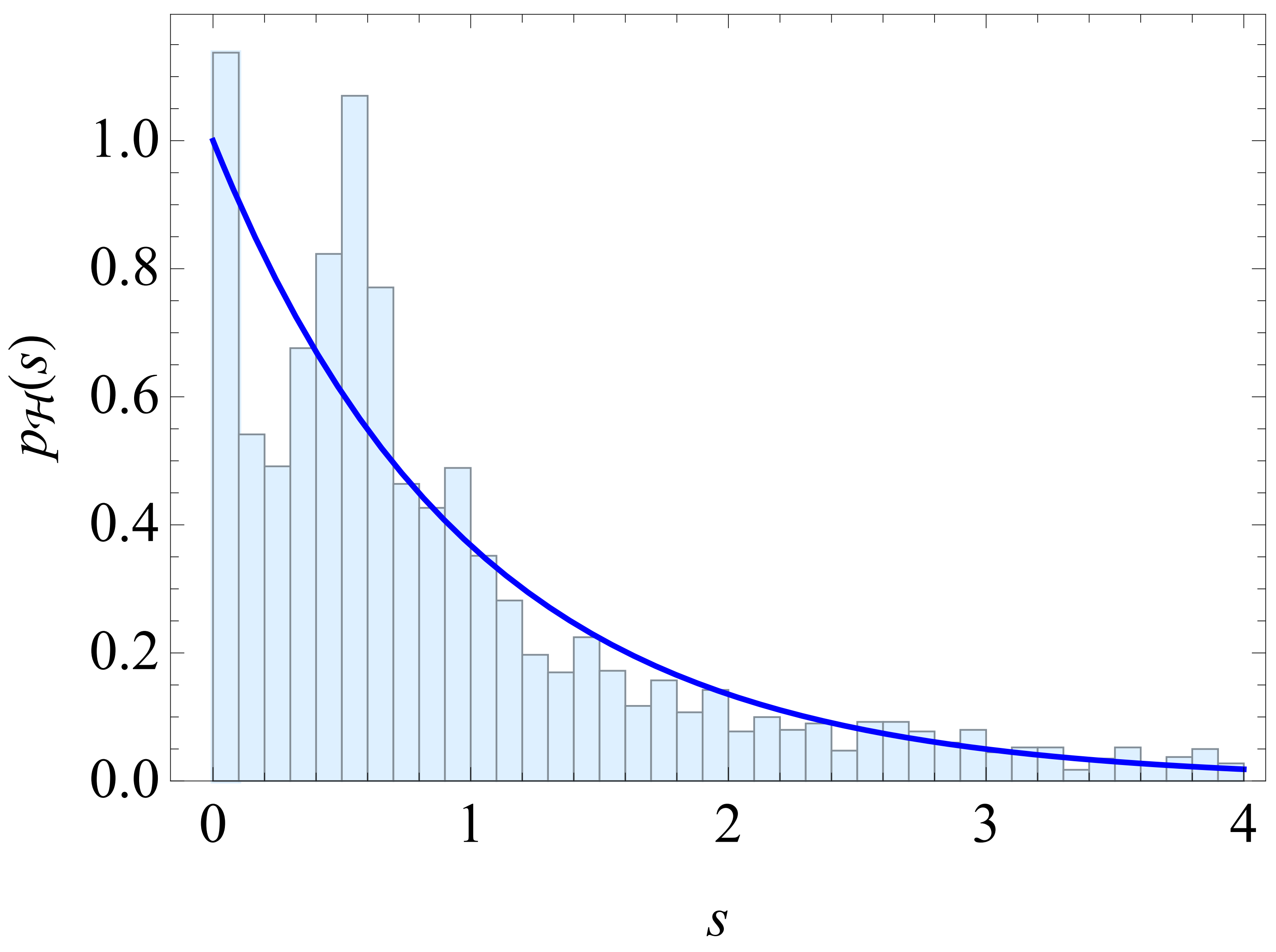


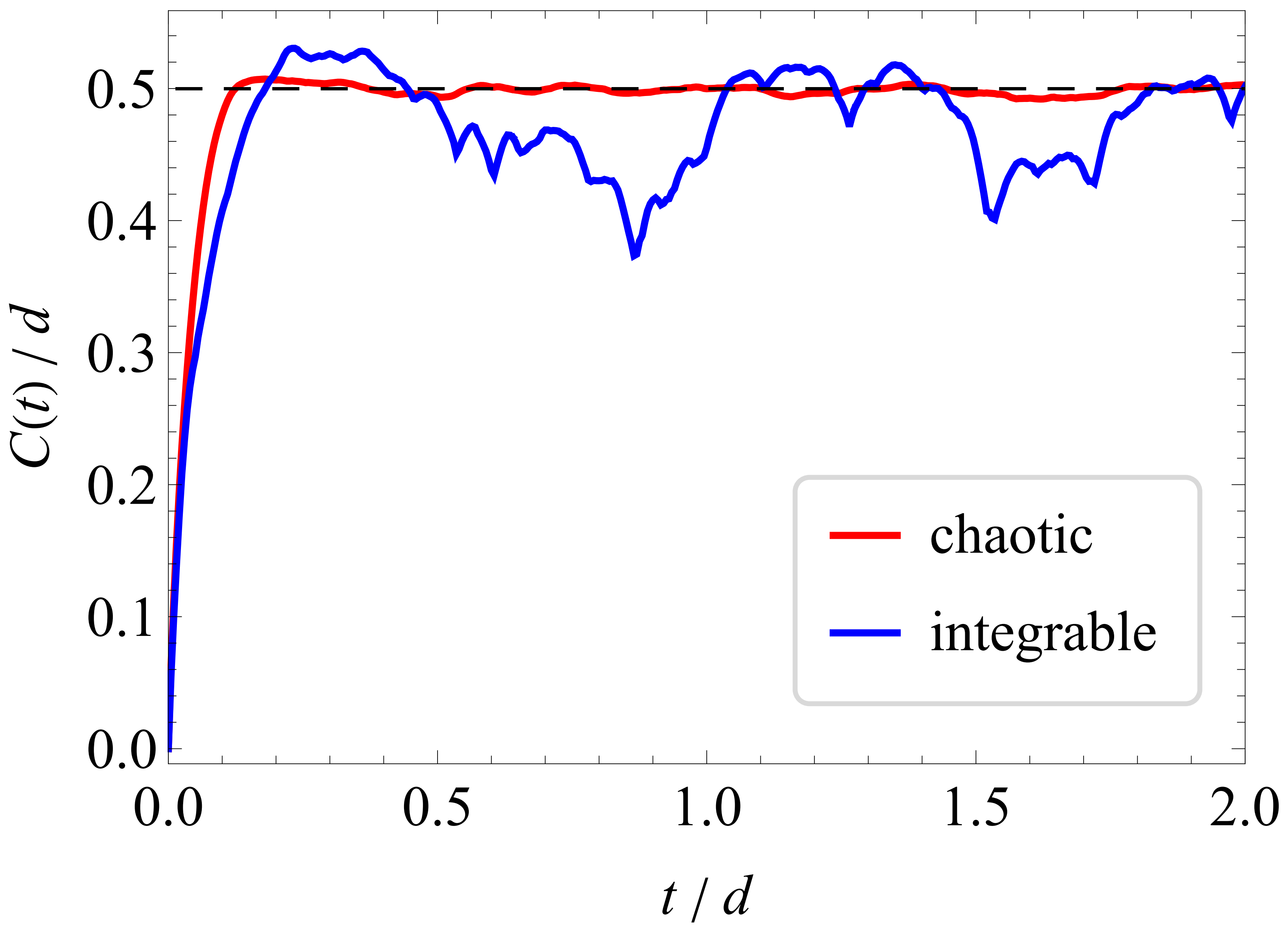


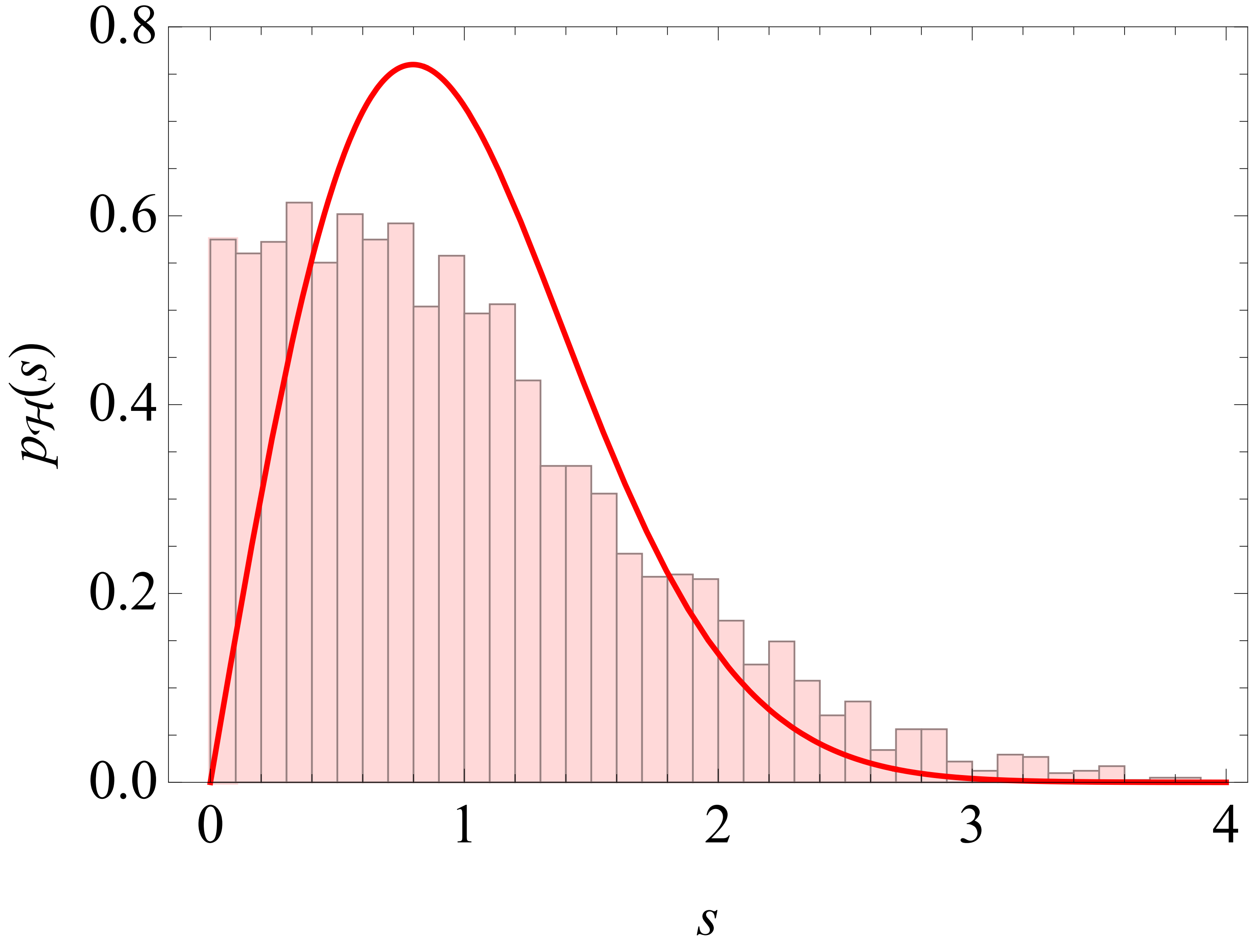

# What is the Parity Symmetry?

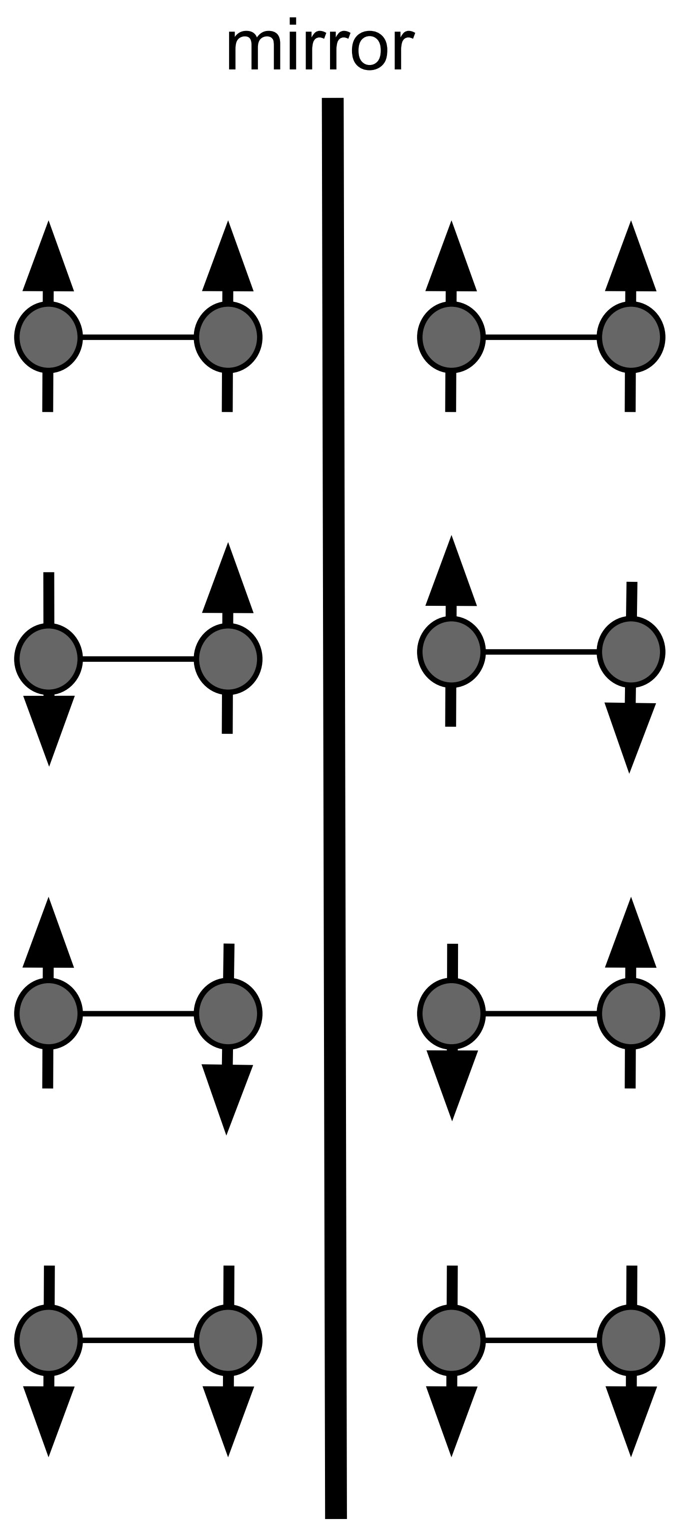


basis

$|\uparrow\uparrow\rangle$

$|\uparrow\downarrow\rangle$

$|\downarrow\uparrow\rangle$

$|\downarrow\downarrow\rangle$

mixed-field Ising model

$$H = -\sum_{i=1}^{N-1} S_i^z S_{i+1}^z - \sum_{i=1}^{N} (h_x S_i^x + h_z S_i^z)$$

E.g. for N=2 sites

$$H = \begin{pmatrix} -2\,hz - J & -hx & -hx & 0 \\ -hx & J & 0 & -hx \\ -hx & 0 & J & -hx \\ 0 & -hx & -hx & 2\,hz - J \end{pmatrix}$$

$$\hat{P}|\uparrow\uparrow\rangle = |\uparrow\uparrow\rangle$$

$$\hat{P}|\downarrow\downarrow\rangle = |\downarrow\downarrow\rangle$$

$$\hat{P}|\uparrow\downarrow\rangle = |\downarrow\uparrow\rangle$$

$$\hat{P}|\psi_\pm\rangle = \pm|\psi_\pm\rangle$$

$$|\psi_\pm\rangle = \frac{|\uparrow\downarrow\rangle \pm |\downarrow\uparrow\rangle}{\sqrt{2}}$$

new basis: $v_1 = |\uparrow\uparrow\rangle,\ v_2 = |\psi_+\rangle,\ v_3 = |\downarrow\downarrow\rangle,\ v_4 = |\psi_-\rangle$

$$H = \begin{pmatrix} -2\,HZ - JJ & -\sqrt{2}\,HX & 0 & 0 \\ -\sqrt{2}\,HX & JJ & -\sqrt{2}\,HX & 0 \\ 0 & -\sqrt{2}\,HX & 2\,HZ - JJ & 0 \\ 0 & 0 & 0 & JJ \end{pmatrix}$$